A comprehensive study of urban gaseous and particulate air pollution in Houston, TX: Source apportionment and the emissions inventory assessment

Thesis by

Birnur Buzcu Guven

In Partial Fulfillment of the Requirements
for the Degree of
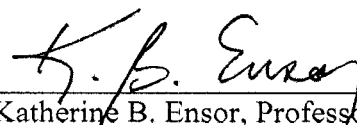
Doctor of Philosophy

APPROVED, THESIS COMMITTEE:

Matthew P. Fraser, Assistant Professor, Chair
Civil and Environmental Engineering

Philip B. Bedient, Herman Brown Professor of
Engineering
Civil and Environmental Engineering

Katherine B. Ensor, Professor of Statistics
Statistics

Rice University, Houston, TX
April, 2006

RICE

UMI Number: 3216678

INFORMATION TO USERS

The quality of this reproduction is dependent upon the quality of the copy submitted. Broken or indistinct print, colored or poor quality illustrations and photographs, print bleed-through, substandard margins, and improper alignment can adversely affect reproduction.

In the unlikely event that the author did not send a complete manuscript and there are missing pages, these will be noted. Also, if unauthorized copyright material had to be removed, a note will indicate the deletion.

UMI®

UMI Microform 3216678

ABSTRACT

A comprehensive study of urban gaseous and particulate air pollution in Houston, TX:
Source apportionment and the emissions inventory assessment

by

Birnur Buzcu Guven

Ground-level ozone is of a growing concern in many areas of the United States. Ozone is a significant health concern, particularly for people with asthma and other respiratory diseases. Ozone is rarely emitted directly into the air but is formed by the reaction of volatile organic compounds (VOCs) and nitrogen oxides (NOx) in the presence of sunlight. VOCs are emitted from a variety of sources, including motor vehicles, chemical plants, refineries, factories, consumer and commercial products, other industrial sources, and biogenic sources. NOx is emitted from motor vehicles, power plants, and other combustion sources. Ozone and ozone precursors also can be transported into an area from pollution sources found hundreds of miles away.

In accordance with the 1990 Clean Air Act Amendments, EPA has required more extensive monitoring of ozone and its precursors in areas with persistently high ozone levels. In these areas, the States have established ambient air monitoring networks consisting of CAMS (continuous air monitoring system) sites, which collect and report detailed data for volatile organic compounds, nitrogen oxides, ozone and meteorological parameters. Analyses of these data help the regulatory agencies to better understand the underlying causes of ozone pollution, to devise effective remedies and to measure air quality trends. This thesis focuses on how to integrate these measurements of VOCs with the receptor modeling techniques in order to identify the sources of VOCs and to attribute

ambient VOC concentrations to their original sources. The measurements taken from three CAMS stations in Houston, TX serve as the basis of this research.

After presenting the source attribution of volatile organic compounds, where the contribution from different sources to ambient VOC levels are determined, the methods to identify the source regions associated with elevated VOC levels are described. The quantitatively reconstructed emissions from a recently prepared VOC emissions inventory are compared with the receptor model calculations of ambient VOC measurements.

Finally, a separate growing concern in the US, the particulate matter pollution, is addressed. The impacts of regional wild fires in Texas on the secondary particulate matter formation are examined. The results of the laboratory investigations on the formation of the secondary sulfate particles through heterogeneous surface reactions are presented.

Acknowledgements

I would like to forward my thanks and appreciations to Dr. Matthew Fraser for always being supportive and helpful whenever I needed guidance during my studies. He is actively involved in the work of all his students, and clearly always has their best interest in mind. I could not have imagined having a better advisor and mentor.

I would also like to express my sincere gratitude to my committee members Dr. Phillip Bedient and Dr. Kathy Ensor for spending their time for my thesis and giving me valuable advices.

Special thanks to my officemates, Zhiwei Yue, Shagun Bhat, and Yuling Jia and also to Pranav Kulkarni at University of Houston. They have been a great source of practical information and great help in the lab.

Finally, I would like to thank those closest to me, whose presence helped make my graduate work, possible. My husband Oguzhan's patience, encouragement, love guidance and help were essential for my smooth-sailing through the Ph.D. program. Finally, I would like to thank my beloved parents for their absolute confidence in me.

Contents

List of Tables

List of Figures

CHAPTER 1

Introduction

1.1 Motivation

Volatile organic compounds are of concern for air quality regulators for a number of reasons including that some of the VOCs are considered air toxics or hazardous air pollutants. Another reason, which this study mainly focuses on, is that VOCs are precursors of a number of secondary air pollutants such as peroxyacyl nitrates (PAN), secondary organic aerosols, and ground-level ozone. VOCs, together with nitrogen oxides (NOx) in the presence of sunlight lead to the photochemical production of tropospheric ozone.

Exceedance of ozone standards in urban areas is the most widespread air quality problem in the USA. Houston, having the largest number of petrochemical facilities in the nation and unique weather patterns, experiences much higher ozone production rates than the other major US cities (*Ryerson et al.*, 2003). Ozone is the only criteria pollutant for which Houston currently fails to meet the National Air Quality Standard (NAAQS) of 120 ppb over a one-hour averaging period. Prior research suggests that high ozone production rates in Houston are strongly associated with high anthropogenic VOC reactivity in emissions from industrial sources (*Ryerson et al.*, 2003).

Emission inventories are widely used as an input to comprehensive photochemical air quality models and the development of effective air pollution control strategies is influenced by the accuracy of the emission inventories. In general, uncertainties in

emission inventories are greater for volatile organic compounds than for the criteria pollutants (*Scheff and Wadden*, 1993) since hydrocarbon emissions come from a much broader range of emission sources, both anthropogenic and biogenic, as well as combustion and non-combustion processes. Recently, emission inventories for VOCs prepared by Texas Commission on Environmental Quality (TCEQ) have been found to be insufficient and not accurately representing the sources and the amounts of the highly reactive VOCs from industrial point sources. Since these factors might influence the effectiveness of air quality improvement plans that rely on these emission inventories, there is a strong need for reliable source reconciliation methods for the evaluation and the validation of emission inventories. Therefore, site-specific source profiles are required to accurately represent the VOC mix and VOC reactivity in ozone production mechanism.

Several efforts have been made to evaluate the accuracy of regional emission inventories in order to improve future inventory development (*Fujita et al.*, 1992, *Scheff and Wadden*, 1993). *Fujita et al.* (1994) used chemical mass balance receptor model to compare emission inventory with ambient data close to the emission sources in Southern California. There have been several studies of mobile source emission estimates based on ambient pollutant ratios (*Fujita et al.*, 1992; *Harley et al.*, 1997). *Cardelino et al.* (1995), *Vivanco and Andrade* (2006) and *Chinkin et al.* (1995) compared emission inventory and ambient concentration ratios of non-methane organic carbon (NMOC), NOx and CO as well as NMOC compositions for selected species. *Jiang et al.* (1997) presented a detailed comparison of the NMOC composition of the emission inventory and that of ambient air in Lower Fraser Valley in Canada.

One way to evaluate emission inventories is to perform a bottom-up inventory assessment that begins with the assessment of pollutant sources in a region and then make emission estimates based on source activity (*Haste et. al.*, 1998). The source activity estimates are then compared to the emission inventory. Top-down evaluations compare emission estimates to ambient air quality data or use ambient data to estimate emission profiles. Top-down evaluations are based on the principal that ambient concentrations of pollutants are primarily influenced by fresh emissions emitted in the vicinity of the monitor; however, transport of pollutants, and atmospheric chemical reactions might also affect ambient concentrations. The influence of these effects can be minimized by selecting monitoring sites located in areas with high emission rates and by studying data collected in early morning hours, when photochemical reactivity, wind speed and mixing height are low.

Receptor modeling techniques are another way of comparing ambient concentration data to the emission inventories. Receptor modeling techniques for source attribution are based on the interpretation of measured ambient concentrations of species to determine their sources and to quantify the contributions of these sources to the ambient concentrations. The results of the receptor models can provide important and independent evaluations of inventories.

Traditional univariate receptor modeling requires site-specific source profiles to accurately determine the contribution of different sources. Positive Matrix Factorization (PMF) is an advanced multivariate receptor modeling technique, which calculates site-specific source profiles together with time variations of these sources based on correlations imbedded in ambient data. PMF has been successfully applied to particulate

matter data in several studies (*Begum et al.*, 2004; *Kim and Hopke,* 2004; *Kim et al.*, 2003; *Ramadan et al.*, 2000; *Buzcu et al.*, 2003). The success of the method for particulate matter problems has led to its consideration for VOCs, although there have been only a few extensive applications (*Brown and Hafner*, 2003, *Zhao et al.*, 2004). Previous source apportionment efforts of VOCs have used Chemical Mass Balance (CMB) model (*Schauer et al., 2002, Fujita et al.*, 2003). *Anderson et al.* (2001) and *Miller et al.* (2002) evaluated four different receptor-oriented source apportionment models (CMB, Principal Component Analysis, PMF, and UNMIX) by applying them to simulated personal exposure data for select (VOCs). *Henry et al.* (1997) applied SAFER model on source apportionment for the summer 1993 VOC data.

As pointed out earlier, unlike many areas of the US, Houston has large point sources contributing to the elevated VOC levels. The speciation profiles that are typically used for point sources in urban and regional modeling analyses are typically old and based on outdated measurement techniques. Therefore, many of the existing VOC speciation profiles do not accurately represent the VOC mix in the Houston area. As a result, there is a strong need for an extensive study that develops valid speciation profiles of VOC sources and that helps us understand ozone precursors in the Houston area. There is also a need for an independent, objective estimate of industrial source compositions and contributions to VOC pollution, and evidence that regulatory agencies and photochemical models are making predictions based on accurate emissions inventories.

1.2 Background and Literature Review

1.2.1 Ozone And Volatile Organic Compounds As Ozone Precursors

Although strict emission controls have been enforced for decades, approximately one-third of the population of the U.S. is exposed to ground level ozone concentrations which exceed the health based National Ambient Air Quality Standard (NAAQS) of 120ppb (*US EPA*, 2000). Highest concentrations of ozone mostly occur in major metropolitan areas. The greater Houston metropolitan area experiences the highest ozone concentrations in the U.S. having exceeded hourly averaged ozone concentrations with 200 ppb during severe episodes.

Ozone production in the lower troposphere occurs by reaction of NOx (NO + NO₂) and VOC (volatile organic compounds, consisting mainly of hydrocarbons) in the presence of sunlight. Control of ozone is accomplished by identifying the sources of NOx and VOC, quantifying their contribution to ozone production and then reducing emissions of either NOx or VOC or both. Ozone precursors are ubiquitous in urban areas, the major source categories being mobile sources, power plants, and solvent use (*US EPA*, 2000). Houston, being distinguished by the largest concentration of petrochemical industrial facilities in the U.S., is also exposed to emissions from refineries and nearby petrochemical plants. In Houston, highly elevated concentrations of NOx and reactive VOCs from collocated sources lead to rapid formation of high levels of ozone. A large electric utility power plant plus numerous petrochemical plants are major NOx sources. In the case of petrochemical plants and refineries, these NOx emissions are co-located with large emissions of reactive VOCs, including ethylene and propylene. Therefore, optimum conditions for ozone formation are routinely found in the NOx- and VOC-rich

plumes from the petrochemical industrial facilities (*Ryerson et al.* 2003). *Kleinman et al.* (2002) compared Houston and other four urban areas including Nashville, TN, Phoenix, AZ, New York, NY and Philadelphia, PA and found very high concentrations of VOCs, specifically reactive olefins, together with high concentrations of NOx in the industrial Houston Ship Channel region. They also found that a large portion of Houston atmosphere is similar to other urban areas in terms of concentration of ozone precursors and ozone production rate. However, Houston Ship Channel region has a distinctive chemistry and unique weather patterns, with elevated concentrations of anthropogenic hydrocarbons causing ozone production rates to be several-fold greater than other cities (*Kleinman et al.*, 2002). The abundance of bays and estuaries in Houston affects the photochemistry in this area providing a source of moisture and also drives a complex circulation pattern that allows air parcels to make multiple passes over industrial facilities emitting reactive alkenes and alkanes (*Berkowitz et al.*, 2004). These conditions lead to an increase in the concentrations of VOCs in air parcels that can pass over the greater Houston area. Therefore, air parcels with high ozone concentrations can be transported across the urban area producing rapid local increases in ozone and frequently resulting in ozone levels in excess of the 120 ppb NAAQS (*Berkowitz et al.*, 2004).

Ryerson et al. (2003) studied the contribution of urban sources to the highly reactive VOCs around the Ship Channel region and found that on-road tailpipe emissions were insignificant contributors to the observed alkene concentrations, and thus to the bulk of VOC reactivity determining ozone formation. They concluded that the resulting rapid ozone formation is primarily ascribed to emissions of ethylene and propylene from local

petrochemical industrial sources, with relatively minor contributions from other VOC sources.

VOCs can be emitted via continuous emissions from stacks, episodic emissions specific to individual processes, and fugitive leaks from pipes and valving. Episodic emissions are non-routine emissions, which are related to upset events, unscheduled maintenance, and startup and shutdown activities.

A study performed by *Allen et al.* (2004) characterized the nature of the variability in reactive VOCs emissions in the Houston/Galveston area (HGA) and assessed the impact of variability on ozone formation processes in the region. According to the reported emission events in 2003 in HGA, the mass of VOCs in emission events was relatively low when considered on an annual time-scale and over a broad geographic area. The mass of VOCs emitted as events, relative to annual VOC emissions, is less then 4%; for highly reactive VOCs, event emissions constitute about 12% of the total annual emissions. However, events are extremely limited in time and space and thus event emissions have the potential to be extremely concentrated. This characteristic is critical to development of an accurate HGA emissions inventory and consequently to understanding and modeling the formation of ground level ozone. *Allen et al.* (2004) determined that only a small fraction of instances where emissions increase substantially above annual averages would lead to changes in the peak ozone concentrations in Houston. They stated that in order for emission events to influence peak ozone concentrations, they must occur during times that are favorable to ozone formation and at locations that provide sufficient sources of NOx emissions that will lead to significant reactions of the emissions.

1.2.2 Emission Inventories

Emission inventories have become a primary tool for developing air quality strategies in recent years. Since they provide information on emission rates of pollutants associated with specific sources and time periods, inventories are important data to air quality models used to simulate the formation of ozone and determine the most effective control strategy. Current emission inventories have significant weaknesses, which lead to uncertainties in the modeling efforts and in developing appropriate air quality strategies. For example, in Houston, photochemical models based on existing emissions inventories are not able to accurately reproduce the high ozone levels observed in several sites because of the underestimation of reactive alkene emissions from the petrochemical facilities.

There are several techniques used to evaluate emissions data, including bottom-up evaluations that begin with source activity data and estimate emissions accordingly; and top-down evaluations that compare emission estimates to ambient air quality data. Top-down analyses of emissions data with surface data are commonly called "emissions reconciliation". One approach to emissions reconciliation is a selective, quantitative comparison of inventory- and ambient-derived molar pollutant ratios (e.g. VOC:NOx) and VOC speciation profiles (*Brown et al.* 2004). Findings often point toward weaknesses or omissions in the emission inventory, which can be iteratively remedied until the inventory data and ambient data reconcile with one another (*Haste et al.*, 1998; *Korc et al.*, 1995; *Fujita et al.*, 1992).

In order to validate the emission inventories, several researchers have calculated the ratios of different airborne compounds measured at one or more monitors, and

compared these to the same ratios from nearby emissions sources (*Fujita et al.*, 1992; *Korc et al.*, 1995; *Stoeckenius et al.*, 2000). The emissions used in these studies were spatially allocated in a two-dimensional Cartesian grid; ratios were calculated for different combinations of grid cells, including cells immediately surrounding the monitor, the single cell in which the monitor is located, and cells located in the upwind quadrant. Although there are many uncertainties associated with such a comparison, this methodology is based on the assumption that if the emission inventory is approximately accurate, the measured pollutant ratios and the inventoried pollutant ratios should be equivalent.

In the heavily industrialized area in Houston, there are numerous facilities that emit large amounts of VOC, NOx, and other pollutants. These sources are geographically distributed in an irregular manner along the Houston Ship Channel; the use of a standard emissions grid for comparison with ambient measurements may be too coarse to capture the significant emissions variability that can occur over a very short distance in the area (*Jolly et al.*, 2004). In a study that assessed the accuracy of emissions estimates of several very reactive VOCs in the area (*Estes et al.*, 2002), researchers grouped ambient data at the study monitors by wind direction, using a resolution of 10 degrees to separate bins. Ratios of the different reactive VOCs to NOx measured at each bin were compared to those from upwind point emission sources.

Jolly et al. (2004) also followed the same approach but used ambient and emissions VOC:NOx ratios to estimate the relative accuracy of the VOC emission inventory. This allowed an independent assessment of a host of different VOC species by grouping them into 13 different VOC classes. This study also compared pollutant ratios

when air passed over areas concentrated in point sources to ratios when air traveled over areas lacking point sources in order to assess the relative accuracies of the non-point source and point source VOC inventories. They found that for most VOCs, some components of the emission inventory were approximately accurate while other components underestimated VOC emissions by up to a factor of 9. In sum total, the non-point VOC emissions inventory is underestimated by about an amount equal to approximately half the amount the point source inventory is underestimated.

Brown et al. (2004) focused on top-down evaluation methods using surface and aloft (via aircraft) ambient data available for Houston/Galveston area and showed that non-methane organic carbon and NOx point source emission inventory appeared to be underestimated and should be evaluated and corrected. They determined that propylene, n-butane and ethane were underestimated and benzene and pentanes were over-represented in the emission inventory.

Receptor modeling techniques were used as another way of comparing ambient concentration data to the emission inventories. Receptor modeling techniques for source attribution are based on the interpretation of measured ambient concentrations of species to determine their sources and to quantify the contributions of these sources to the ambient concentrations. The results of the receptor models can provide important, independent evaluation of emissions inventories. *Fujita et al.* (1995) compared source contributions non-methane organic gas (NMOG) concentrations calculated by Chemical Mass Balance (CMB) model, which is a univariate receptor model, with the corresponding emission inventory estimates and found some discrepancies in the emission inventories for Southeast Texas.

Scheff and Wadden (1993) also used CMB model to identify the important source categories contributing to total Non-Methane Organic Carbon (NMOC) mass, and used this information to evaluate emissions inventories. Average source contribution estimates agreed well with the inventories except for refineries, which were significantly underestimated in the inventories. They also supported their conclusions by comparing CMB results with wind trajectories and the locations of petroleum refineries in the study area.

Traditional univariate receptor modeling requires site-specific source profiles to accurately determine the contribution of different sources. Positive Matrix Factorization (PMF) is an advanced multivariate receptor modeling technique, which calculates site-specific source profiles together with time variations of these sources based on correlations imbedded in ambient data. With emissions profiles constantly changing as a result of emissions controls, process modifications and non-routine emissions, PMF offers an advantage over univariate modeling approaches.

1.2.3 Receptor Modeling

Receptor modeling techniques are mathematical procedures for identifying and quantifying the sources of pollutants at a receptor, primarily on the basis of ambient concentration measurements at that receptor. Univariate receptor modeling techniques assume that both the ambient concentrations of chemical species and the composition of all sources of these species are known for environmental data. This then allows the contribution of these sources to pollutant levels at the receptor locations to be calculated.

Chemical Mass Balance (CMB) Model

Chemical mass balance (CMB) model is a univariate receptor model that originated the theory of all other receptor models. CMB consists of a least squares solution to a set of equations where the concentrations of chemical species at each receptor are expressed as a sum of products of source profiles (the mass fraction of the species in the emissions from each source type) and source contributions (the contribution of each source to the mass at a receptor). CMB model has a number of assumptions, which are to be met before fitting ambient and source chemical profiles, including: (1) that the composition of source emissions is constant over the period of sampling, (2) that chemical species are conserved in transport from source to receptor, (3) that the number of sources is less than or equal to the number of chemical species, (4) that the source composition profiles are linearly independent of each other, (5) that the measurement uncertainties are random, uncorrelated and normally distributed, and (6) that all sources with potential for significantly contributing to the receptor have been identified and have had their emissions characterized.

The concentration (x_{ij}) of chemical species i in sample j, is given by

$$x_{ij} = \sum_{k=1}^{p} f_{ik} g_{kj} + e_{ij} \qquad [1]$$

where f_{ik} is the concentration of species i in the emissions from source k, g_{kj} is the mass contribution of source k to sample j, and e_{ij} is the difference between the measured and calculated species concentration (*Watson et al,*. 1990). The sum is performed over all sources k=1,...,p.

The source profiles and the measurements of the concentrations at each receptor together with the uncertainty estimates are the inputs of the CMB model. The model calculates the contribution of each source to the mass concentration at the receptors, and determines the uncertainties of these values. The uncertainties of source profiles and receptor concentrations are included in the model calculations to weight the importance of these values and to calculate the uncertainties of the output values.

Equation 1 can be solved using effective variance weighted least-squares method by minimizing the weighted sums of the squares of the differences (χ_j^2) between the measured and calculated concentration values (*Watson*, 1984).

$$\chi_j^2 = \frac{1}{(m-p)} \sum_{i=1}^{m} \left[\frac{(x_{ij} - \sum_{k=1}^{p} f_{ik} g_{kj})^2}{V_{ij}} \right] \qquad [2]$$

where

$$V_{ij} = \sigma_{x_{ij}}^2 + \sum_{k=1}^{p} (g_{kj})^2 \sigma_{f_{ik}}^2 \qquad [3]$$

where σ_{xij} is the standard deviation of the measured concentration of species i in sample j and σ_{fik} is the standard deviation of the fraction of species i in emissions from source k. Source contribution estimates, g_{kj}, are calculated by an iterative procedure based on the value of g_{kj} estimated from the previous iteration. The effective variance, V_{ij}, is adjusted at each iteration step as new values of g_{kj} are calculated (*Miller et al,*. 2002). In effective variance weighted least-squares method, the compounds having higher precisions are given more weight than the compounds with lower precisions.

CMB model provides several goodness of fit parameters of the model results

(*Watson et al.*, 1998). These parameters and their optimum values are:

- t-statistics (source contribution estimate / uncertainty of source contribution estimate) > 2,

- Chi-square < 4,

- R^2 > 0.80,

- Percentage mass explained by the sources must be between 80 and 120%.

- C/M ratio (ratio of calculated to measured concentration of chemical species) must be close to one.

- Absolute value of R/U ratio (ratio of residual to uncertainty) < 2.

CMB model performance is examined generally by statistical tests such as colinearity and influence diagnostics (*Henry*, 1992) and Monte Carlo simulations with synthetic data sets (*Javitz et al.*, 1988) to determine the viability of using source profiles to resolve source contributions by CMB (*Watson et al.*, 2001).

CMB models have some limitations associated with the lack or incompleteness of source profile data. Without reliable source profiles for a certain region, it is difficult to determine which sources should be included in the model calculations. Even if the emission inventories can be used to determine the source types, existing source profiles may not represent the characteristics of the sources in that particular region. Another limitation of CMB model is that CMB cannot resolve similar or collinear sources; colinearity leads to very large uncertainties of the source contribution estimates in CMB calculations. CMB also has a limitation in explicitly treating profiles that change between source and receptor.

Wiens et al. (2000) modified CMB model and developed estimation methods including a robustness option to make model predictions less susceptible to outlying data. *Wiens et al.* (2000) suggested that adding robustness to the estimation methods could reduce the risk of incorrect results when the assumptions of CMB model cannot be totally met.

Positive Matrix Factorization

For the locations where the sources are unknown or the source compositions have not been measured, it is necessary to determine the number of sources, the chemical composition of emissions from these sources, and the contribution of these sources to particle mass. These calculations are generally performed using multivariate receptor models, or more specifically factor analysis (FA) or principal component analysis (PCA) methods.

The PCA method is expressed in matrix form as

$$X=FG \tag{4}$$

where X is the data matrix of measured concentrations of species at receptor locations, F is the *n by p* matrix of factor loadings, and G is the *p by m* matrix of factor scores.

The principal component solution of data matrix X can be obtained from the *singular value decomposition* of X.

$$X=USV^T \tag{5}$$

U and V are calculated from eigenvalue-eigenvector analyses of XX^T and X^TX matrices, respectively. F and G in Equation 2 can be determined as $F=US$ and $G=V^T$. In PCA, it is

usual to continue the analysis after the factors of X have been calculated. Using a suitable

non-singular matrix T, X can be represented as

$$X = GTT^{-1}F \qquad [6]$$

creating new factors GT and $T^{-1}F$. T is called as "transformation" or "rotation" matrix,

which generates physically more meaningful and clearer results.

Since singular value decomposition of a matrix is varied with scale changes of

columns or rows of X, various scaled forms of X such as row- and column-scaling have

been used in PCA (*Paatero and Tapper*, 1993). *Paatero and Tapper* (1993) showed that

these scalings were not proper for physical and chemical applications, because they did

not make use of the known experimental uncertainties. They further showed that the

scalings were limited to dealing with whole columns and/or rows; point-by-point scaling

of matrix elements was not possible in PCA formulation. For this reason, they formulated

an alternative application of PCA called "Positive Matrix Factorization".

Positive Matrix Factorization (PMF) incorporates error estimates of the data to

solve matrix factorization of the linear model as a constrained, weighted least squares

problem (*Paatero and Tapper*, 1994). PMF solves the equation

$$x_{ij} = \sum_{k=1}^{p} f_{ik} g_{kj} + e_{ij} \qquad [7]$$

or

$$X = FG + E \qquad [8]$$

in matrix form where e_{ij} are defined as the elements of the residual matrix E. In PMF, the

sources are restricted by the physically meaningful limitations to have non-negative

species concentration and non-negative contributions to the samples. The error estimates

for each measured data point are used as point-by-point weights. Thus PMF is better

suited for physical and environmental sciences than PCA models (*Paatero and Tapper*,

1994). The number of sources, p, is chosen by the user. Given p, PMF solves Equation 7

by minimizing the weighted sum of squares

$$Q = \left\| \frac{X - FG}{s} \right\|^2_{F,G} = \sum_i \sum_j \left(\frac{e_{ij}}{s_{ij}} \right)^2 \qquad [9]$$

where

$$e_{ij} = x_{ij} - \sum_{k=1}^{p} f_{ik} g_{kj} \qquad [10]$$

and $f_{ik} \geq 0$, $g_{kj} \geq 0$ for $i=1,...,n$, $j=1,...,m$, and $k=1,...,p$, and s_{ij} is an estimate of the

uncertainty in the ith variable measured in the jth sample. PMF uses these error estimates

of the data to give less weight to the observations with greater sampling errors, data

below detection limits, or outlying or missing data. Commonly, missing values are

replaced by the mean value of the variable and large standard deviations are assigned for

these values (*Antilla et al.*, 1995). The problem is solved by a unique iterative algorithm

defined by *Paatero* (1997) simultaneously varying the elements of F and G at each

iteration step and minimizing ||E|| in the equation

$$(G_o + \Delta G)(F_o + \Delta F) = X + E \qquad [11]$$

where the second order term $\Delta G \Delta F$ can be ignored (G_o and F_o are matrices G and F at the

first iteration step).

In PMF, the error estimates, s_{ij}, for each ambient concentration data point, x_{ij} can be calculated heuristically based on the data value and the uncertainty of the data measured, σ_{ij}. The general equation is

$$s_{ij} = C_1 + C_2\sqrt{|x_{ij}|} + C_3|x_{ij}| \qquad [12]$$

where $C_1 = \sigma_{ij}$, $C_2 = 0$, and $C_3 = $ a dimensionless user-specified value between 0.1 and 0.5.

PMF can handle extreme and outlying data values, which can have a significant effect on the solution by offering a "robust" mode. In the robust mode the objective function becomes

$$Q = \sum_{i=1}^{m}\sum_{j=1}^{n}\left(\frac{e_{ij}}{h_{ij}s_{ij}}\right)^2 \qquad [13]$$

where

$$h_{ij}^2 = \begin{cases} 1 & if\left|e_{ij}/s_{ij}\right| < \alpha \\ \left|e_{ij}/s_{ij}\right|/\alpha & otherwise \end{cases} \qquad [14]$$

and $\alpha = $ the outlier distance. Recent work has suggested appropriate values of α to be 2.0, 4.0, or 8.0 (*Paatero*, 2000).

In order to determine minimum the number of factors required to obtain a good fit between model parameters and observed data, the value of the sum of the squares of the weighted residuals, Q, determined in Equation 9, should be approximately equal to the total number of data points in the data matrix, X. The value of Q should not be changed significantly after an appropriate number of factors are included in the model application.

There is rotational ambiguity in the results of all factor analysis methods, including PMF. There is no unique solution to factor analysis problem even though there is a global minimum fitting process. The inclusion of constraints can reduce the rotational ambiguity in the solution, but this will still not provide a unique solution. Rotational freedom can be decreased by searching for zero values in either G or F matrices and forcing the solution to these values. Rotations can be controlled by the peaking parameter, FPEAK. A positive value of FPEAK forces the routine to subtract F factors from each other (the corresponding G factors are added to each other), and a negative value of FPEAK causes G factors to be subtracted from each other (F factors to be added to each other). If there are zero values in the F or G matrices, they will restrict subtractions because of the non-negativity constraint and will reduce the number of possible rotations. FPEAK values are chosen by trial and error: there is no theoretical background for selecting a value of FPEAK. Since the rotations are part of the optimization process, the value of Q depends on FPEAK. If increasing values of FPEAK cause Q to deviate significantly from the theoretical Q value, then the FPEAK value should be decreased.

The ability of PMF in extracting the source profiles that most closely represent the major sources used to generate the ambient concentration data has been tested and the results of PMF analysis compared with results from other multivariate receptor models (*Miller et al.*, 2002; *Poirot et al.*, 2001). Although *Miller et al.* (2002) determined that PMF model was best able to extract the important sources, these studies determined that using multiple receptor models produces more robust results and helps improving the understanding of source-receptor relationships for fine particles.

PMF has been successfully applied to particulate matter data in several studies (*Buzcu et al.*, 2003). The success of the method for particulate matter problems has led to its consideration for VOC, although there have been only a few extensive applications (*Buzcu and Fraser*, 2006).

Conditional Probability Function (CPF)

Receptor modeling techniques provide the main sources of pollutants that can be identified, but do not provide information on either their local or regional origin nor on their geographical location. Geographical interpretation of air quality data requires information on the origin of an air mass arriving at the sampling site, related to the meteorological and atmospheric dynamics conditions, from local to larger scales (*Salvador et al.*, 2004).

Air mass back trajectories are computed by meteorological models and can be analyzed jointly with pollutant concentrations. The simplest and most frequently used analysis involves mapping single trajectories for days of interest, considering that they establish a direct link between a source region and a receptor location. In addition to the uncertainties associated to trajectory models, it must be assumed that a trajectory is just an estimation of the general pathway of an infinitesimally small air parcel (*Kahl*, 1993). In view of this, statistical methods that employ large trajectory ensembles are more suitable (*Stohl*, 1998). Some statistical techniques have been developed for identifying pollutant source regions combining air back trajectories information and concentrations of any element measured at the sampling site. One of these, known as potential source contribution function (PSCF), calculates the probability that an air parcel with a given

level of pollutant concentration or higher arrives at a receptor site after having been passed through specific geographic area (*Gao et al.*, 1993).

Conditional probability function (CPF) (*Ashbaugh et al.*, 1985) is another technique, which analyzes point source impacts from various wind directions using either ambient concentration data or source contribution estimates calculated by receptor models coupled with wind direction values measured on site. The CPF is the fraction of total samples within wind sector, $\Delta\theta$, having a source contribution estimate higher than a predetermined threshold criterion value to the total number of occurrences from the same wind sector for that specific factor. CPF is defined as;

$$CPF_{\Delta\theta} = (m_{\Delta\theta} / n_{\Delta\theta}) * W(n_{\Delta\theta}) \qquad [15]$$

$$W(n_{\Delta\theta}) = 0.1 * n_{\Delta\theta} \quad \text{when } 0 < n_{\Delta\theta} \leq 9$$

$$W(n_{\Delta\theta}) = 1 \qquad \text{when } n_{\Delta\theta} \geq 10$$

where $m_{\Delta\theta}$ is the number of occurrences from wind sector $\Delta\theta$ that exceeded the criterion value, $n_{\Delta\theta}$ is the total number of data from the same wind sector and $W(n_{\Delta\theta})$ is the weight function. Since small values of $n_{\Delta\theta}$ produce high CPF values with high uncertainties, CPF values were down-weighted using a weight function, $W(n_{\Delta\theta})$ when $n_{\Delta\theta}$ is less than 10. This weighting is important because if the wind never came from a given direction, there would be no VOC observations from that direction. On the other hand, a high frequency of winds from a given sector would enhance the confidence of the CPF associated with that sector.

1.2.4 Secondary Sulfate Aerosol Formation

Particulate matter is a ubiquitous air pollutant and its composition and effect on the environment has been studied by many researchers. Recently, secondary formation of particulate matter has been shown to be a major source of ambient fine particles (*Buzcu et al.*, 2006). In particular, it has been shown that the sum of secondary organic mass and secondary sulfate mass could exceed the mass of primary particles during regional haze episodes. *Buzcu et al.* (2006) have shown that existing routes of secondary sulfate formation from the oxidation of gaseous SO_2 cannot explain observed ambient secondary sulfate levels during severe wood smoke episodes and demonstrated that heterogeneous reactions can explain the observed sulfate enhancements during the wood smoke episodes.

Gas-phase sulfur dioxide can react with mineral aerosol to form particulate sulfate. Atmospheric modeling studies have shown that mineral aerosol has a potentially important role in the chemistry of troposphere, by interacting with trace atmospheric gases such as SO_2 (*Dentener et al.*, 1996; *Luria and Sievering*, 1991). Several studies have quantified the heterogeneous chemistry on mineral aerosol to further understand the impact that these reactions may have on the chemistry of the atmosphere (*Goodman et al.*, 2000; *Goodman et al.*, 2001; *Underwood et al.*, 2001). Some researchers detailed the chemistry of the heterogeneous oxidation of SO_2 on mineral surfaces, including mineral dusts (*Ullerstam et al.*, 2002; *Ullerstam et al.*, 2003), calcium carbonate (*Lei et al.*, 2004) and fly ash material (*Mamane and Pueschel*, 1979). SO_2 can be oxidized to sulfate in aqueous aerosol by ozone and hydrogen peroxide (*Seinfeld and Pandis*, 1998, *Krischke et al.*, 2000; *Keene et al.*, 1998). *Jang et al.* (2003) found that indigenous sulfuric acid

produced from combustion of fossil fuels could initiate the acid-catalyzed heterogeneous

reactions on the particle phase.

Reaction of SO_2 on mineral aerosols is complicated because the mechanism for

SO_2 oxidation on mineral particles to form sulfate is uncertain (*Dertener et al.*, 1996). In

the troposphere, gas-phase SO_2 reacts to produce sulfur trioxide, which is then rapidly

converted to sulfuric acid in the presence of water vapor according to reactions 1 and 2.

$$SO_2 + OH + O_2 \rightarrow SO_3 + HO_2 \tag{1}$$

$$SO_3 + H_2O \rightarrow H_2SO_4 \tag{2}$$
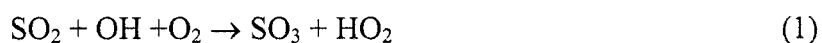
The capacity limited heterogeneous oxidation of SO_2 on mineral particle surfaces

at room temperature may be regarded to consist of the following sequence of steps: **1.**

Chemisorption of oxygen onto the surface sites, **2.** Diffusion of SO_2 to the surface, **3.**

Reaction between SO_2 and chemisorbed oxygen to form SO_3, **4.** Hydration of SO_3 to

H_2SO_4, and **5.** Partial dissolution of minerals by H_2SO_4.

The results of previous studies, which investigated the sulfate formation on fly

ash and crustal material, indicated that the formation of sulfates strongly depends on

relative humidity and the make-up of the crustal material. The reaction capacities

reported differed by more than two orders of magnitude. These differences could be

attributed in part to differences in the experimental set-up and procedures (*Mamane and*

Gottlieb, 1989).

The characteristics of particulate matter collected from urban environment as well

as from stacks were studied in terms of SO_2 adsorption and oxidation at ambient

temperature (*Liberti*, 1978). Urban atmospheric dust desorbed SO_2 with an almost

quantitative yield (100%), whereas in most dusts collected from stacks no desorption occurred. A stack emission particulate can be defined as a fresh system, which is going to equilibrate in the atmosphere, whereas atmospheric particulate matter is an aged system where equilibrium with air components has been reached (*Liberti*, 1978). Dust sampled from a stack does not show the presence of SO_2, which was always found in aged systems (*Liberti*, 1978). Both dusts might be reactive but reactions in a fresh system proceed faster and much more extensive. In all dusts where the adsorbed SO_2 is 100% desorbed by heating at 175°C, no chemisorption occurs and no sulfate formation is observed. On the other hand, in dust samples where SO_2 adsorbed is not released at 175°C, such as alkaline dust sampled in a cement factory stack, no free SO_2 was detected and the sulfate weight increase corresponded to the amount of SO_2 adsorbed (*Liberti*, 1978).

Karge and Dalla Lana (1984) determined that interaction of SO_2 with basic sites on the surface leads to the formation of chemisorbed SO_2 while adsorption at acid sites leads to physisorbed SO_2. Weakly adsorbed SO_2 forms on acidic sites and surface coordinated sulfite forms when SO_2 interacts with basic oxide anions or hydroxides on the aluminum and magnesium oxide surfaces (*Goodman et al.*, 2001). The conversion of chemisorbed sulfite to sulfate has been reported in the literature for high-temperature reactions between SO_2 and oxide surfaces in the presence of oxygen (*Chang*, 1978; *Martin et al.*, 1987).

Usher et al. (2002) have investigated the heterogeneous uptake and oxidation of SO_2 on particles representative of mineral dust found in the troposphere. They have found that SO_2 irreversibly adsorbs as sulfite (SO_3^{2-}) and /or bisulfite (HSO_3^-) on all particle

surfaces with the exception of SiO_2. The adsorbed species can be oxidized to sulfate (SO_4^{2-}) and/or bisulfate (HSO_4^-) upon exposure to ozone. In the surface-catalyzed oxidation of SO_2 the rate-limiting step is the surface reaction, not the adsorption of the SO_2 (*Baldwin*, 1982). After the adsorption of SO_2 on a surface site, the SO_2 is eventually oxidized and remains on the site, preventing further reaction.

At ambient temperatures, the heterogeneous oxidation of SO_2 on surfaces of non-hygroscopic metal oxide particles is not a true catalytic reaction (*Chun and Quon*, 1973). The active sites on the surfaces of the particles become occupied by the products of reaction during the course of the reaction. These active sites are not available subsequently for further reaction, as would be the case in a true catalytic reaction. Hence, the oxidation of SO_2 on the surfaces of Fe_2O_3 particles is expected to form a finite quantity of acid; the quantity being proportional to the number of active sites originally available for reaction (*Chun and Quon*, 1973).

Judeikis et al. (1978) investigated SO_2 reactivity with fly ash materials and encountered with very low SO_2 removal rates, indicating the possibility of the exposure of these materials to near saturation levels of SO_2 either before or during collection. The analysis of the fly ash indicated a strong sulfate signal. Therefore, they washed the fly ash material with distilled water to remove soluble sulfates, and observed substantial increases in the fly ash reactivity against SO_2.

Judeikis et al. (1978) also pointed out the possible effects of organics on rates and capacities for SO_2 removal. Urban aerosols contain an organic fraction that may be less reactive toward SO_2 removal (*Friedlander*, 1973).

The relative humidity is an important factor in sulfate formation. *Cheng et al.*
(1971) showed that SO_2 oxidation may proceed at all humidities, but the rate was much
smaller at low humidity levels than at saturation. They carried out most experiments at
relative humidity above 80%. They calculated SO_2 removal capacities ranging from ~1 to
~200 mg SO_2 per g of solid for a variety of materials. They suggested that the
atmospheric catalytic oxidation of SO_2 involves both water and dissolved oxygen, and
require the presence of a catalyst. Known catalysts for the reaction include a number of
metal salts, such as the oxides of magnesium and aluminum, which may exist in ambient
air as suspended particulate material (*Cheng et al.*, 1971).

1.3 Research Objectives

The primary objective of this thesis is to identify the sources of volatile organic
compounds and evaluate the VOC emission inventories. Within the extent of this
objective are the attribution of ambient VOCs to the original sources, the identification of
the potential source regions, the evaluation of the composition and locations of reported
emissions with the major sources as derived from the ambient data, the analysis of the
event emissions and the comparison of the ozone standard exceedances with the source
apportionment results.

Accomplishment of the primary objective will fill the gap of the inadequacy of
the existing speciation profiles of the VOC sources to accurately represent the VOC mix
and will make this research serve as an important contribution to understand ozone
precursors and their role in ozone production mechanism in the Houston area. The

comparisons of the reported emissions with the source apportionment results will contribute substantially to our understanding of the origin of the air pollutants.

The secondary objective is to evaluate of the impact of regional wildfires in East Texas on fine particulate matter concentration and composition using the Chemical Mass Balance (CMB) technique. The results of this objective may yield significant evidence of the secondary aerosol formation during a wood smoke episode. Within the scope of this objective is the investigation of the role of metal and mineral content of ambient $PM_{2.5}$ on the heterogeneous chemistry of secondary fine particle formations. These investigations will improve our understanding of the role of metals in heterogeneous sulfate formation, which can contribute to the formation of elevated $PM_{2.5}$ sulfate levels during regional haze episodes.

1.4 Approach

The following approach detailes the scientific process used to reach the objectives of this thesis, as outlined in Section 1.3.

Chapter 2 Source Attribution Using Positive Matrix Factorization

Historically, source attribution for ozone precursors in the Houston/Galveston area has relied on the development of emission inventories, where emissions from all sources are compiled together. As mentioned earlier, independent evaluation has found the emission inventories for VOC to be inaccurate in the Houston region. An alternative to using emission inventories for source attribution purposes is applying multivariate

receptor modeling techniques. Positive Matrix Factorization (PMF) is a receptor model, which performs statistical analysis of ambient air quality data that uses correlations between data in the concentration matrix to decouple the concentration matrix into two separate matrices, the source profile matrix describing the composition of each important source, and the source contribution matrix describing the contribution of each source to the ambient concentrations. The product of these two matrices yields the observed data matrix of the concentrations.

PMF will be performed on the hourly ambient concentrations of 54 different VOCs measured using automatic gas chromatographs (auto-GC) between June 2 and October 31, 2003 at three monitoring sites in Houston (Wallisville Road, HRM-3 Haden Road and Lynchburg Ferry). All three sites are located near the Houston Ship Channel, which is the center of industrial activity in Houston and where the highest concentrations of VOC and ozone production rates have been observed (*Ryerson et al.*, 2003). All these three sites are included in TCEQ's CAMS (continuous air monitoring system) network.

As opposed to the common practice of using long periods of hourly data, the source apportionment will be performed on hourly data separately for each week. Hourly concentrations of 54 VOC will be aggregated into weekly composites giving data matrices with 8316 entries (154 samples in each data set x 54 compounds) on average for each location studied. Using matrix factorization, the source profiles and source contributions (as a function of time within the one-week period) will be isolated for each important source, which contributes to ambient VOC levels. The chemical composition of each important source will be compared to literature reports of the composition of known sources of VOCs to relate each isolated source factor to a known source. The

advantage of this approach is the isolation of transient events, which are not observed in the analysis of longer time series. Another advantage of this method is to be able to observe the temporal variations in a larger time scale and study the daily variations in each source contribution.

PMF will also be performed on the isolated nighttime VOC data from July 2003. The data between the hours of 9pm and 6am local time will be used to minimize the effect of photochemical reactions on model results. This analysis will investigate the effect of photochemical loss of reactive VOC on source attribution of VOC mass.

Chapter 3 Evaluation of VOC Emission Inventory with Source Apportionment

1. Comparison of Source Attribution to Ozone Formation

An analysis will be performed on days when the ozone National Ambient Air Quality Standard (NAAQS) of 120ppb was exceeded at all sites between June and October 2003 to study the effects of high contributions of dominant sources of VOCs on ozone formation in Houston atmosphere. The source contributions calculated by PMF will be cross-correlated to the ozone concentrations measured at the same monitoring site to determine the relationship between the reactive olefin emissions and the ozone standard exceedances. It will also be investigated if the refining emissions, which are one of the major sources of VOCs in Houston Ship Channel area, can also lead to ozone violations as well as highly reactive compounds such as ethylene and propylene.

2. Identification of Source Regions

This study will identify the source regions associated with elevated hydrocarbon levels measured at three sites in Houston. The basis for the analysis is a set of conditional probability function (CPF) plots derived from the source contributions calculated by PMF and hourly measured wind directions at each site. A plot in polar coordinates with radial distance defined by the magnitude of CPF and the angle defined by the associated wind direction, visually illustrates the fraction of samples coming from a given direction that have high values and point to regions associated with these high values, which are considered as the potential source regions of VOCs.

CPF analysis will be performed both on hourly samples of all-day data and separately on nocturnal data to determine the effect of the changes in the mixing ratios of reactive VOC associated with photochemical oxidation.

3. Comparison of Source Attribution to Point Source Inventories

In many areas of United States where observed ozone concentrations exceed the NAAQS, the primary contribution to VOC levels is from mobile sources and dispersed area sources that are too small to track on an individual basis. Since point sources are not a major component of VOC in many areas, recent efforts at the national level to develop more accurate VOC speciation profiles have focused on area and mobile sources. In the Houston/Galveston area, however, the major contributions to VOC concentrations are from large point sources. The speciation profiles that are typically used for point sources in urban and regional modeling analyses are often outdated and not based on current measurement techniques. Therefore, many of the existing VOC speciation profiles that are routinely applied to point sources are not expected to accurately present the VOC mix

in the Houston/Galveston area, and thus, may not accurately represent the reactivity of VOC in ozone formation process.

VOC emissions from point sources in the eight-county Houston non-attainment area were estimated at about 28% of the total anthropogenic VOC inventory (*Jolly et al.*, 2004). These sources are concentrated in certain industrial areas and are sparse or nonexistent in other areas. Around all of the present study monitors are areas concentrated with point source emissions; therefore, this research will focus on the point sources located in the vicinity of the Houston Ship Channel, where the elevated VOC concentrations were monitored. Unlike other studies which have used ambient and emissions VOC:NOx ratios to estimate the relative accuracy of the VOC emission inventory (*Jolly et al.*, 2004), this study will compare the relative contributions of the important sources of VOCs calculated by PMF with the emissions of the same sources included in the corresponding emission inventory to see if the current point source emission inventories are consistent with the measurements. Finding the location of a nearby source is important in identification of the causes of high VOC concentrations in the region and in evaluating the emission inventories. CPF plots described in the previous section will be compared to the polar plots of the processed emissions from the inventory to see if they point to the same source regions. This provides a valuable independent review of existing emission inventories based on air quality measurements.

4. Evaluation of Source Attribution to Isolate Upset Emissions

Industrial facilities in Houston/Galveston area report their annual average VOC emission rates to TCEQ. Non-routine emissions are not included in these annual average emissions rates. These non-routine emissions are called "upset emissions" and associated

with plant startup, plant shutdown or an unplanned emission event with emissions greater than 5000 pounds (*Allen et al.*, 2004).

Upsets and maintenance activities can have significant emissions as compared to routine emission levels. These emissions may contribute to the ozone spikes observed in a heavily industrialized area such as Houston Ship Channel area.

VOC event emissions from non-routine operations are available in TCEQ's "Air Emission Event Report Database" starting from January 2003 (www.tceq.state.tx.us/compliance/field_ops/eer/index.html). As part of this research, these event emissions from petrochemical facilities will be compared to the extreme values observed in the temporal variations of petrochemical production source determined by PMF calculations. In this analysis, wind trajectory data and other atmospheric parameters will be used to perfom dispersion modeling calculations of the plume originating from the source of emissions using the three-dimensional Hybrid Single-Particle Lagrangian Integrated Trajectory (HYSPLIT) model. This will enable an evaluation of whether spikes in temporal variations observed in the ambient data can be confirmed in the emission inventory as event emissions. It will also determine if the monitoring network is able to detect these event emissions properly. In this analysis, we will focus only on the emissions from petrochemical facilities because ethylene and propylene, which are the dominant compounds emitted from these facilities are highly reactive and play a major role in ozone formation in the atmosphere.

Chapter 4 Secondary Sulfate Formation on Mineral Dust Surfaces

The secondary objective of this thesis is addressed in Chapter 4. To examine the role of fires on air quality in Texas, the impact of wildfires on fine particulate matter concentration and composition during an August-September, 2000 episode will be evaluated. The Chemical Mass Balance (CMB) approach will be used to estimate the contributions of primary and secondary sources to $PM_{2.5}$ levels. The goal is to determine whether the fires, in addition to being a significant source of carbonaceous aerosol, can lead to significant enhancements of particulate sulfate concentrations, and whether this excess sulfate can be accounted for if heterogeneous sulfate formation reactions are occurring on the wood smoke surfaces.

A series of laboratory investigations will be performed to quantify the impact of heterogeneous chemistry of the formation of sulfate aerosols on mineral surfaces. To investigate the role of different minerals in sulfate formation, road dust samples collected near sampling sites and samples of fly ash from a local coal-fired power plant will be resuspended on blank filters and these filters will be then exposed to known amounts of dilute SO_2 gas and analyzed for the sulfate formation. The results of the measurement of the formation of sulfate from the oxidation of gaseous SO_2 will be used to understand if the exposure of mineral materials to SO_2 in air leads to the formation of sulfate

Chapter 5 Conclusions

The major results of this research are summarized. Important accomplishments are highlighted and areas for future research are identified.

CHAPTER 2

Source Identification and Apportionment of Volatile Organic Compounds in Houston, TX

2.1. Introduction

Anthropogenic sources of VOCs include evaporation of solvents and gasoline, petrochemical manufacturing, petroleum refining and motor vehicle exhaust. In some regions, biogenic sources emit high amounts of VOCs to the atmosphere (*Kleinman et al.*, 2002). In this chapter, receptor modeling has been performed on ambient air quality data collected at three monitoring sites in Houston in order to further understand the emissions of VOCs in the Houston area and the role of specific sources. All three sites studied are located near the Houston Ship Channel, which is the center of industrial activity in Houston and the highest concentrations of VOCs and ozone production rates have been observed (*Ryerson et al.*, 2003).

Traditional univariate receptor modeling requires site-specific source profiles to accurately determine the contribution of different sources. Positive Matrix Factorization (PMF) is an advanced multivariate receptor modeling technique, which calculates site-specific source profiles together with time variations of these sources based on correlations imbedded in ambient data. PMF has been successfully applied to particulate matter data in several studies (*Begum et al.*, 2004; *Kim and Hopke*, 2004; *Kim et al.*, 2003; *Ramadan et al.*, 2000; *Buzcu et al.*, 2003). The success of the method for particulate matter problems has led to its consideration for VOCs, although there have

been only a few extensive applications (*Brown and Hafner*, 2003, *Zhao et al.*, 2004).
Previous source apportionment efforts of VOCs have used Chemical Mass Balance
(CMB) model (*Schauer et al.*, 1996, *Fujita et al.*, 2003). *Anderson et al.* (2001) and
Miller et al. (2002) evaluated four different receptor-oriented source apportionment
models (CMB, Principal Component Analysis, PMF, and UNMIX) by applying them to
simulated personal exposure data for select (VOCs). *Henry et al.* (1997) applied UNMIX
model on VOC source apportionment for the Houston Ship Channel COAST data.

In this study, concentrations of 54 different VOCs measured hourly between June
2 and October 31, 2003 were used to study the sources of VOCs in Houston. Ambient
VOC data were divided into weekly intervals and PMF was applied to hourly VOC data
in each interval to determine the source profiles and contributions at each site. A
nighttime data analysis was also performed at two sites to investigate the effect of
photochemical loss of reactive VOCs on source attribution of VOCs.

2.2. Data Collection

All ambient VOC concentrations were measured by automated gas
chromatography (autoGC) under the Texas Commission on Environmental Quality's
(TCEQ's) Enhanced Industry Sponsored Monitoring Program during the summer of 2003
at a number of sites in Harris County, Houston, TX. Wallisville Road, Lynchburg Ferry
and HRM-3 Haden Road sites, which are located in the Houston Ship Channel region,
were selected for source apportionment analysis; because the data set was larger and
better quality at these sites (Figure 3.1). The autoGC collected an approximate 40-minute

ambient air sample at each site each hour (referred to as one-hour or hourly data). Each

sample was analyzed for a range of VOCs, and concentrations were recorded hourly in

parts per billion by carbon (ppbC). Instrument calibration, operation and data quality

assurance followed techniques applicable to the Photochemical Assessment Monitoring

(PAMS) program (*U.S. Environmental Protection Agency*, 1999).

Figure 2.1. The locations of the study sites relative to the major sources.

■   1311-Crude petroleum and natural gas

♦   2821 -Plastics materials and resin

●   2869-Industrial organic chemicals

▲   2911-Petroleum refining

♦   4226 -Special warehousing and storage
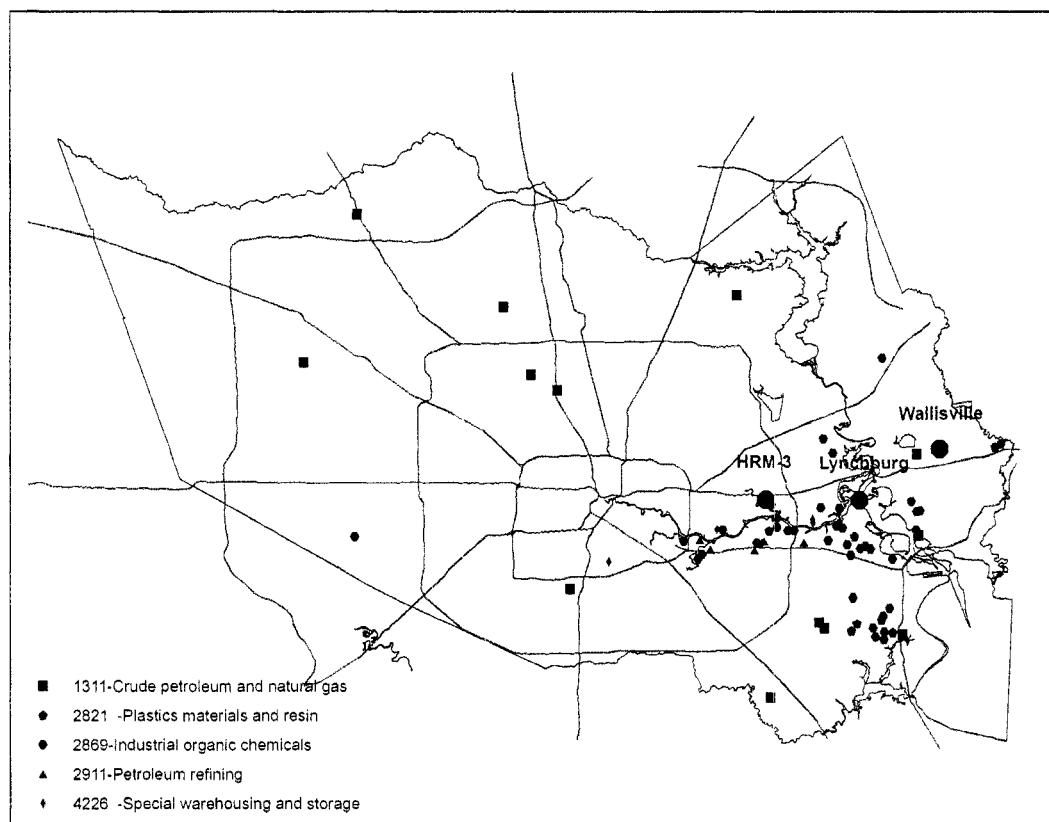
2.3. Methods

2.3.2. Positive Matrix Factorization (PMF) Model Description

PMF described in detail in the works of *Paatero and Tapper* (1994) and *Paatero* (1997) was used to analyze the volatile organic compound (VOC) data in Houston atmosphere. Given a data matrix X consisting of the concentration measurements of n chemical species in m samples, the objective of PMF is to determine the number of VOC source factors (p), the chemical composition profile of each source factor (f), the contribution of each source factor to each sample (g), and residuals e:

$$X_{ij} = \sum_{k=1}^{p} g_{ik} f_{kj} + e_{ij} \tag{1}$$

In PMF, the sum of the squares of residuals, e_{ij}, weighted inversely by the variation of the data points, s_{ij}^2, is minimized according to the following constrained weighted least-squares model;

$$\text{minimize } Q = \sum_{i=1}^{n} \sum_{j=1}^{m} \frac{e_{ij}^2}{s_{ij}^2} \tag{2}$$

$$\text{subject to } g_{ik} \geq 0, f_{kj} \geq 0 \tag{3}$$

The objective is to minimize Q. The constraints in Equation (4) denote the physically meaningful conditions that factors cannot have negative species concentration and ambient samples cannot have a negative factor contribution. Equation (3) is solved using a unique iterative algorithm in which matrices G and F vary simultaneously at each iteration step (*Paatero*, 1997).

2.2.3. PMF Model Implementation

In PMF model applications, missing values in the data are best handled so that the user specifies large uncertainties for them. By using the optional parameter "*missingneg r*" (r is a decimal value), one commands PMF to decrease the significance of all missing values in data matrix. This approach internally increases the uncertainty for missing data by the factor r and uses the value zero as the data value. With a suitable r=10,..., r=100 this allows these missing data to have a negligible effect on the isolated factors (*Paatero*, 2000). At the Wallisville Road, 1.9% of the data was missing; this ratio was 1.7% for HRM-3 and 7.0% for Lynchburg data. Concentrations of a number of compounds such as acetylene, n-pentane, isopentane, isoprene, 2-methylpentane and 3-methylpentane were missing for the first 9 weeks and the last week of the analysis period at Lynchburg. The data for those 10 weeks were analyzed separately, excluding these missing compounds from the analysis. All other missing values were handled by PMF using a *missingneg* value of 100 so that missing data were given low weights and had minimal effects on the factors. Since the analytical uncertainties were not available, the uncertainties for the normal data points were substituted with the 20% of the concentration values.

The minimum number of factors required to obtain a good fit between the model parameters and observed data was determined by the sum of the squares of the weighted residual, Q, determined in Equation (3). In a good fit, the value of Q should be approximately equal to the number of entries in the concentration matrix. However, some deviation can be expected because of missing data points. The optimal number of factors was found by trial and error and involved verifying that a solution also provided physically meaningful results. Another consideration for the determination of number of

factors is to examine the scaled-residual matrix (e_{ij} / s_{ij}), which is also calculated by the model. The elements of this matrix should be between -2.0 and 2.0 for a good fit to the actual values (*Junnto and Paatero*, 1994). In this work, scaled residuals varied between -2.13 and 2.75 with 93% of the values between –2 and +2 representing good agreement of the fitted values to the observed values. In addition, since rotational ambiguity exists in bilinear factor analysis models, a user-defined parameter, FPEAK is used to allow some modification of the derived rotations. Since there is no rule of selecting the correct FPEAK value, the valid range of FPEAK values, within which the Q value remained relatively constant, was determined by running the model with different FPEAK values. The FPEAK values that provide the most reasonable profiles ranged from 1.0 to 1.5 in all the weekly data sets for HRM-3, and from 0.5 to 1.4 for Lynchburg and Wallisville Road. Also, the seed of pseudo-random values for the PMF model were changed for different runs of the model and these trials produced almost identical factor profiles and contributions.

Assuming that all of the sources contributing to the VOC samples have been identified, the sum of the contributions should add to the measured total VOC concentration (*Jorquera and Rappengluck*, 2004). Thus, a multiple linear regression was performed to fit the total mass against the factor contributions, and the regression coefficients (the scaling constants, s_k) were used to convert the factor profiles and contributions into values with physically meaningful units (*Song et al.*, 2001).

$$x_{ij} = \sum_{k=1}^{p} g_{ik} f_{kj} = \sum_{k=1}^{p} g_{ik} \frac{s_k}{s_k} f_{kj} = \sum_{k=1}^{p} g'_{ik} f'_{kj} \qquad (4)$$

After the scaling, the factor profiles (f_{kj}') have units of *ppbC/ppbC*, and the factor

contributions (g_{ik}') have units of *ppbC*. In this regression, each of the s_k values must be

non-negative. If the regression produces a negative value, then too many factors have

been used.

In this analysis, approximately 98%, on average, of the scaled residuals calculated

by PMF were between –3 and 3, indicating a good fit of the modeled results (Figure 3.2).

Figure 2.2. Illustrative scaled-residual plots at each site.
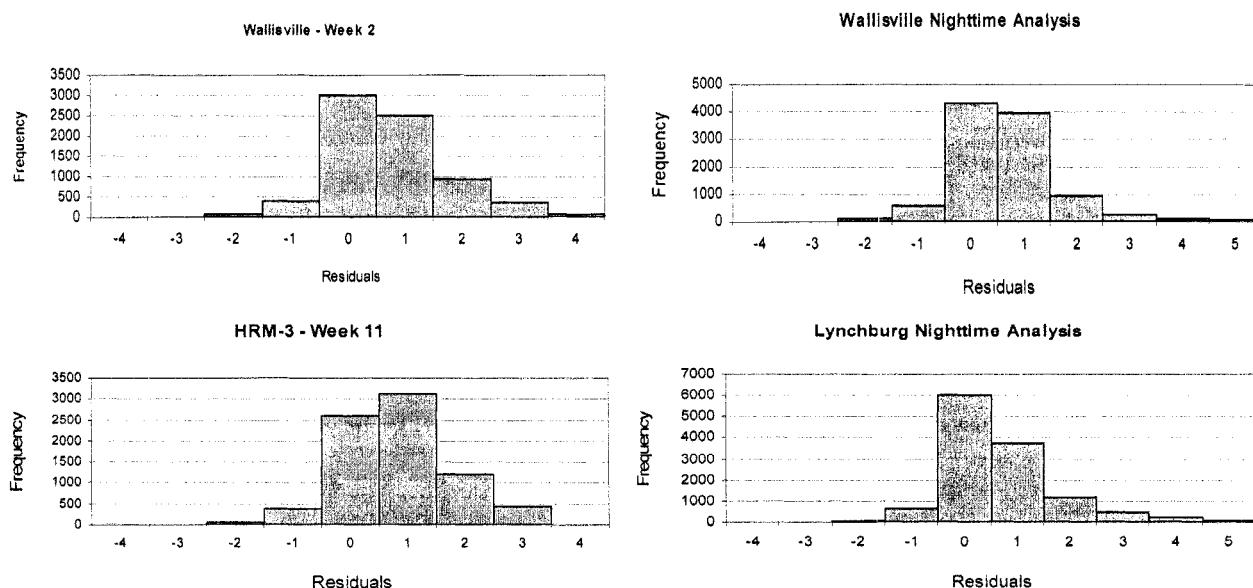
2.4. Results

Source apportionment of hourly speciated VOC data from three sites in Houston,

TX (Wallisville Road, HRM-3 Haden Road and Lynchburg Ferry) was performed to

isolate emission sources and quantify the contributions of these sources to total VOC

mass at these sites. Positive Matrix Factorization (PMF) was applied to hourly VOC data

divided into weekly intervals for the period of June 2 – October 31, 2003. Past applications of PMF have used multiple years of VOC data to resolve up to 15 sources (*Brown and Hafner*, 2003). The approach in this study is to use only one week of hourly data to focus on the most important sources during each weekly period. With this approach, it is possible to identify the different sources and transient emission events since some sources might be more significant than others in some of the weeks and they might not have any influence on VOC levels in some other weeks. Another advantage of this method is to be able to observe the temporal variations in a larger time scale and study the daily variations in each source contribution.

Examination of spatial and temporal characteristics of atmospheric constituents and relative abundances of certain chemical species is a useful approach prior to applying receptor modeling. Table 3.1 presents averages, standard deviations, and maximum concentrations for hourly average auto-GC measurements at Wallisville, HRM-3 and Lynchburg sites. The sum of individual VOCs in Wallisville data accounted for 87.5% of the total NMHC mass, 88.8% in HRM-3 data, and 84.7% in Lynchburg data.

Table 2.1. Statistical Summary of VOC concentrations (ppbC).

Wallisville				HRM-3				Lynchburg			
Species	Avg.	St. Dev.	Max	Species	Avg.	St. Dev.	Max	Species	Avg.	St. Dev.	Max
NMHC	143.0	139.7	1058.1	NMHC	240.2	313.7	5540.9	NMHC	319.6	377.9	3576.8
Propane	19.6	23.1	180.8	n-Butane	26.9	142.6	4280.0	Propane	30.3	40.9	543.7
Ethane	17.2	17.9	241.5	Isopentane	25.3	54.5	1337.6	Propylene	28.8	78.3	1281.9
Propylene	14.0	38.0	528.6	Propane	20.6	21.2	267.9	Ethane	21.8	22.1	221.7
n-Butane	11.0	16.6	329.8	Ethane	18.0	15.0	176.6	n-Butane	21.6	45.4	1155.8
Isobutane	10.8	17.7	289.5	Isobutane	13.3	20.6	523.6	Isopentane	20.6	39.1	814.5
Isopentane	9.3	14.5	418.1	n-Pentane	11.4	21.1	318.0	Isobutane	18.9	33.9	616.2
Ethylene	7.0	12.1	170.5	Ethylene	9.2	20.1	646.0	Benzene	16.9	100.2	2828.6
n-Pentane	4.9	5.9	55.9	Propylene	9.0	27.7	1271.0	n-Pentane	12.4	36.6	1164.7
n-Hexane	3.1	5.2	94.3	Toluene	8.3	10.6	347.5	Ethylene	12.2	26.2	536.1
Toluene	2.9	3.8	78.4	n-Hexane	6.4	7.9	93.9	Styrene	10.3	164.1	7897.5
Benzene	2.1	2.4	30.4	Benzene	4.7	6.2	152.2	Toluene	9.1	16.0	370.8
Cyclohexane	1.7	4.7	155.2	p-Xylene + m-Xylene	4.0	5.4	149.7	n-Hexane	8.6	19.3	575.1
2-Methylpentane	1.6	2.0	22.8	2-Methylpentane	3.7	7.6	126.0	Cyclohexane	5.2	15.9	361.9
t-2-Butene	1.6	0.5	8.2	1-Butene	3.5	13.4	388.8	p-Xylene + m-Xylen	3.8	6.4	114.3
3-Methylpentane	1.4	1.7	18.0	3-Methylpentane	3.3	6.2	108.6	3-Methylpentane	3.1	9.0	249.9
1-Butene	1.4	4.0	118.5	Cyclohexane	3.2	7.1	133.8	Methylcyclopentane	3.1	8.3	332.8
Methylcyclopentane	1.2	1.5	14.1	Methylcyclopentane	2.8	4.1	82.1	2-Methylpentane	3.0	7.6	189.5
Isoprene	1.2	1.7	40.7	Isoprene	2.8	3.4	30.9	1-Butene	2.7	9.6	247.9
p-Xylene + m-Xylene	1.1	1.4	23.0	2,2,4-Trimethylpentan	2.7	4.1	52.4	o-Xylene	2.7	16.1	716.6
Methylcyclohexane	1.0	1.4	25.7	Methylcyclohexane	2.0	2.3	24.7	1,3-Butadiene	2.6	6.2	174.1
2,2,4-Trimethylpentane	0.9	1.0	15.9	n-Heptane	2.0	2.6	25.8	Ethyl Benzene	2.3	14.6	453.0
Acetylene	0.8	0.8	10.2	1,3-Butadiene	1.9	5.5	123.8	2,2,4-Trimethylpenta	2.1	4.5	86.3
1,3-Butadiene	0.7	1.6	31.8	3-Methylhexane	1.7	2.4	44.6	n-Heptane	2.1	8.0	345.5
n-Heptane	0.7	0.8	10.0	Styrene	1.6	4.4	91.1	Methylcyclohexane	2.0	3.8	86.2
3-Methylhexane	0.6	0.7	5.9	n-Octane	1.5	2.7	48.6	Cyclopentane	1.9	27.4	1320.4
2-Methylhexane	0.5	0.6	5.4	Cyclopentane	1.5	16.0	884.0	3-Methylhexane	1.7	9.6	443.9
c-2-Butene	0.5	0.3	4.2	2-Methylhexane	1.4	2.1	49.1	2-Methylhexane	1.4	7.5	341.3
Cyclopentane	0.5	0.5	5.9	1,2,4-Trimethylbenzen	1.4	1.7	24.6	Isoprene	1.3	2.2	55.6
1,2,4-Trimethylbenzen	0.4	0.5	10.6	t-2-Pentene	1.3	4.5	108.3	1,2,4-Trimethylbenz	1.3	2.2	44.0
n-Octane	0.4	0.6	14.2	o-Xylene	1.3	1.7	55.3	n-Octane	1.2	3.9	145.8
o-Xylene	0.4	0.5	9.3	Ethyl Benzene	1.2	1.5	40.4	Isopropyl Benzene -	1.2	13.6	568.0
Ethyl Benzene	0.4	0.5	6.0	t-2-Butene	1.2	2.2	43.6	t-2-Butene	1.1	3.3	117.9
2,3-Dimethylbutane	0.4	0.5	5.3	Acetylene	1.1	1.4	20.8	Acetylene	1.0	2.7	50.5
1,2,3-Trimethylbenzen	0.4	0.5	6.6	2,3-Dimethylbutane	0.9	2.2	29.8	n-Decane	1.0	3.3	114.3
m-Ethyltoluene	0.3	0.4	7.1	c-2-Butene	0.9	1.9	39.6	c-2-Butene	0.9	3.0	79.5
n-Decane	0.3	0.4	15.5	m-Ethyltoluene	0.9	0.9	7.0	m-Ethyltoluene	0.8	1.7	64.2
2,3-Dimethylpentane	0.3	0.3	2.5	1,2,3-Trimethylbenzen	0.9	0.9	9.7	2,3-Dimethylbutane	0.8	2.0	45.8
Styrene	0.2	0.8	33.5	n-Decane	0.8	0.7	22.0	n-Undecane	0.7	2.0	55.0
2,3,4-Trimethylpentane	0.2	0.3	4.8	2,3,4-Trimethylpentan	0.8	1.2	13.0	n-Nonane	0.7	2.0	52.1
2,2-Dimethylbutane	0.2	0.3	5.3	2,3-Dimethylpentane	0.8	1.1	16.7	1,2,3-Trimethylbenz	0.7	1.0	22.1
n-Nonane	0.2	0.4	15.6	2,2-Dimethylbutane	0.7	2.8	71.2	t-2-Pentene	0.7	5.9	289.8
3-Methylheptane	0.2	0.2	5.5	1-Pentene	0.7	1.9	33.9	3-Methylheptane	0.7	4.6	220.2
2-Methylheptane	0.2	0.2	4.7	2,4-Dimethylpentane	0.7	1.1	16.0	2,3,4-Trimethylpenta	0.7	1.6	42.6
2,4-Dimethylpentane	0.1	0.3	5.3	3-Methylheptane	0.6	0.8	12.6	2-Methylheptane	0.6	3.2	148.7
n-Undecane	0.1	0.3	12.7	c-2-Pentene	0.6	2.2	57.5	2,3-Dimethylpentane	0.6	3.1	139.5
Isopropyl Benzene - C	0.1	0.3	3.1	n-Nonane	0.6	0.8	24.0	1-Pentene	0.5	1.1	17.6
t-2-Pentene	0.1	0.2	3.9	2-Methylheptane	0.5	0.7	10.2	2,2-Dimethylbutane	0.5	1.3	29.4
1-Pentene	0.1	0.2	2.1	n-Undecane	0.5	0.6	15.0	1,3,5-Trimethylbenz	0.4	1.0	26.2
p-Diethylbenzene	0.1	0.2	3.3	1,3,5-Trimethylbenzen	0.4	0.5	6.2	p-Diethylbenzene	0.4	0.6	12.1
1,3,5-Trimethylbenzen	0.1	0.2	5.1	Isopropyl Benzene - C	0.4	1.5	34.8	p-Ethyltoluene	0.4	1.0	37.2
p-Ethyltoluene	0.1	0.2	4.2	p-Ethyltoluene	0.4	0.4	3.9	2,4-Dimethylpentane	0.4	1.6	65.4
n-Propylbenzene	0.1	0.1	3.0	p-Diethylbenzene	0.3	0.3	3.1	o-ethyltoluene	0.3	0.8	17.1
o-ethyltoluene	0.1	0.1	3.7	o-ethyltoluene	0.3	0.3	6.6	c-2-Pentene	0.3	0.7	11.0
c-2-Pentene	0.1	0.1	1.7	n-Propylbenzene	0.2	0.3	2.8	n-Propylbenzene	0.3	0.7	25.6

Total NMHC mass measured at Wallisville was 143.0 ppbC. The average concentrations of the most abundant VOCs measured at this site over the whole analysis period showed that propane (19.6 ppbC) was the most abundant species, followed by ethane (17.2 ppbC), propylene (14.0 ppbC), n-butane (11.0 ppbC), isobutane (10.8 ppbC), isopentane (9.3 ppbC) and ethylene (7.0 ppbC). Ethane is mostly emitted from

natural gas (*Harley et al.*, 1992) while propane is present in natural gas emissions as well as in refinery gas emissions together with n–butane and isobutene (*Wiswanath*, 1994; *Na and Kim*, 2001). Because of varying rates of oxidation of the vapor-phase organic compounds, some highly reactive species, such as the light olefins, are depleted in a more rapid rate than less reactive compounds. With transport of emissions from distant sources, atmospheric oxidation removes the reactive species and the remaining fraction contains mostly the less reactive species, such as ethane and propane (*Gouw et al.*, 2005). Therefore, having longer lifetimes, ethane and propane tend to accumulate in the atmosphere and may cause an overestimation of natural gas emissions which is determined based on the concentrations of less reactive alkanes.

The main source of ethylene and propylene is petrochemical manufacturing facilities, although they also exist in vehicle exhaust emissions together with acetylene, isopentane, toluene and xylenes (*Jobson et al.*, 2004; *Na et al.*, 2001). Ethylene and acetylene provide tracers for engine exhaust emissions; they are formed during combustion, but are not present in unburned gasoline (*Harley and Cass*, 1995). Unburned gasoline emissions, liquid or evaporated gasoline, contain isobutane, n-butane, n-pentane and isopentane (*Watson et al.*, 2001).

Total NMHC mass at HRM-3 during analysis period was 240.2 ppbC. The average concentration of the most abundant compound, n-butane, 26.9 ppbC and the other major components of the total NMHC mass included isopentane (25.3 ppbC), propane (20.6 ppbC) and ethane (18.0 ppbC).

Lynchburg site had the highest total NMHC concentrations with 319.6 ppbC. Higher total NMHC mass measured at HRM-3 and Lynchburg sites is consistent with site

location as these two sites are in the middle of the largest industrial complexes in the Ship

Channel whereas Wallisville Road is located to the northeast of the Ship Channel.

Propane (30.3 ppbC) was the most abundant species at Lynchburg followed by propylene

(28.8 ppbC), ethane (21.8 ppbC), n-butane (21.6 ppbC), isopentane (20.6 ppbC), and

isobutane (18.9 ppbC).

Total NMHC concentrations at each site showed similar diurnal variations with

high concentrations in the morning and evening, and low concentrations in the afternoon

(Figure 2.3). This may be explained by the higher traffic emissions during the morning

and evening rush hours, photochemical destruction of reactive VOCs and the dilution of

the pollutants by the increase in the mixing height during the day. The high

concentrations of species such as butane, isobutane, ethylene and propylene suggest that

refineries, petrochemical production facilities and gasoline emissions are likely sources

of VOCs in Houston Ship Channel region. PMF was used to verify this, to identify other

significant sources of VOCs in the region, and to quantify how much each source affects

VOC levels at the three study sites.

Figure 2.3. Diurnal variations in the average concentrations of total VOC mass at each site.
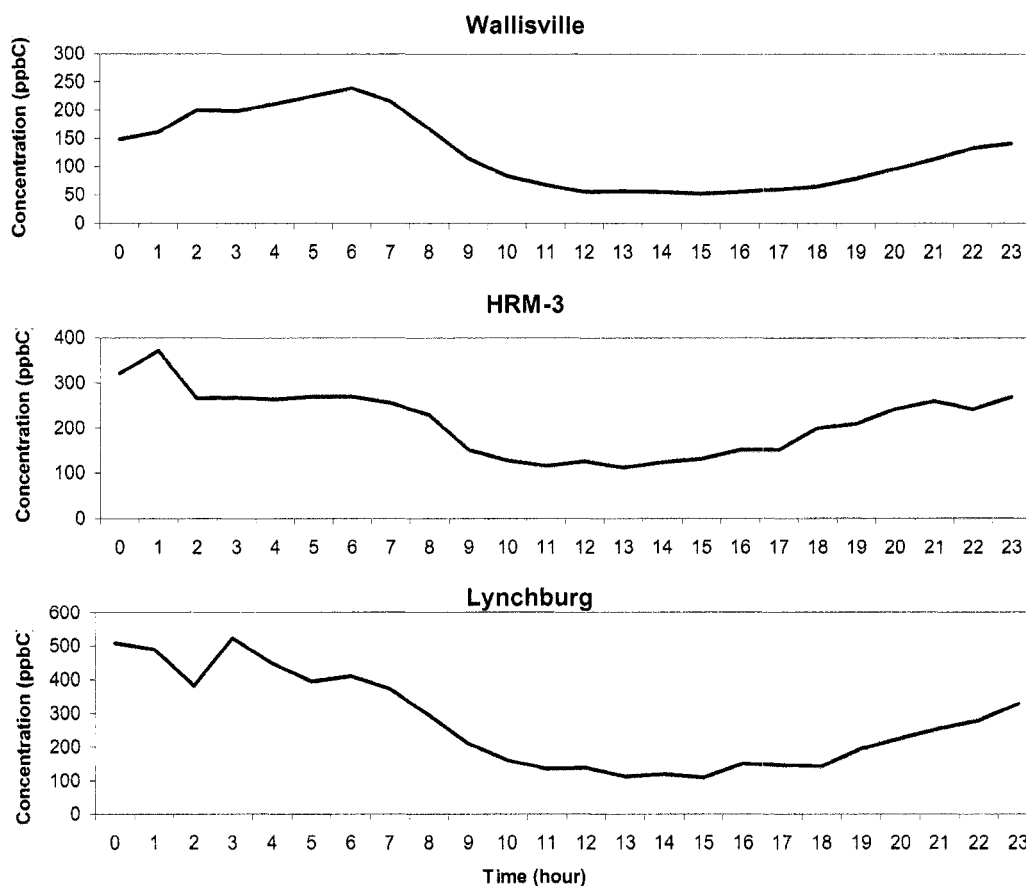
2.4.1. Wallisville Road

Hourly VOC data from Wallisville Road were divided into 21 weekly data sets. Four separate source factors were extracted from the samples collected at this site in each of the weekly data sets. The chemical composition of these profiles is consistent with the chemical composition of refining operations, petrochemical production, natural gas, liquid gasoline emissions, aromatics, vehicle exhaust and biogenic emissions based on the comparison of the factor profiles with previously reported profiles in the literature

and in EPA's SPECIATE database. Representative factor profiles are shown in Figure

2.4.

Figure 2.4. Representative factor profiles for Wallisville Road data.
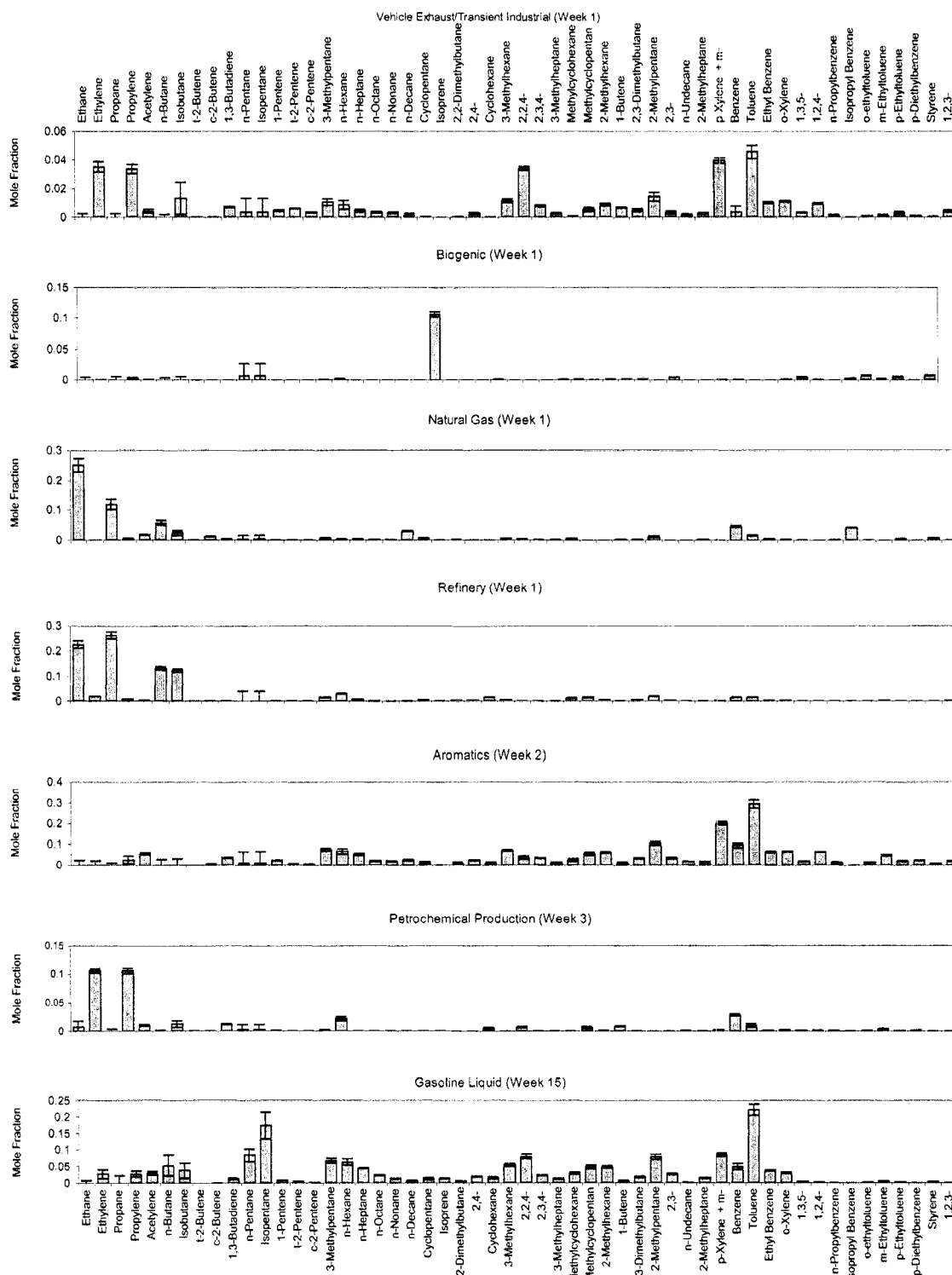
The refinery profile is characterized by propane, ethane, butanes, and pentanes in the factor profiles and this factor was resolved in all 21 weeks. Light olefins, specifically, ethylene and propylene, which are among the most reactive VOCs, are predominantly concentrated in a source factor consistent with the composition of petrochemical production emissions, which was isolated in 19 of the 21 analyzed weeks. A factor characterized by aromatics, specifically toluene and xylenes, was resolved in 9 weeks as well. Since aromatic hydrocarbons are emitted from industrial solvent use sources (*Harley et al.*, 1992) and motor vehicles (*Walsh*, 1994), this factor might either represent a solvent use or a gasoline source. Because of this ambiguity, this factor will be labeled "aromatics" for the rest of this work. Ethane and propane are the representative VOCs of natural gas emissions (*Fujita et al.* 1995) and a factor characterized by these alkanes was isolated in 16 of 21 weeks. Another factor, which mainly had toluene, xylenes and pentanes was found to be the consistent with the liquid gasoline profiles reported in the work of *Fujita et al.* (1995) which represented unburned gasoline due to misfiring and other engine malfunctions. For this reason, this factor will be labeled "liquid gasoline" for the rest of this report. A profile, which was resolved in the first week, is similar to vehicle exhaust emissions, due to the relatively high abundance of ethylene, propylene, toluene and xylenes. However, since this factor was resolved only in one week of data, it is likely that this factor represents a transient emission from an industrial source. Finally, a factor representing biogenic emissions was extracted in 6 weekly data sets. Biogenic VOC emissions from trees and shrubs are characterized by isoprene, which is commonly used as the marker of biogenic emissions despite its high reactivity (*Carter*, 1991; 1995). However, due to the high reactivity of isoprene, the biogenics factor contributions should

be treated with caution and viewed as a lower limit (*Fujita*, 2001; *Fujita et al.*, 1995). In this profile, isoprene constituted almost 100% of the mass since other biogenic species such as pinenes were not detected in the ambient samples. Isoprene can also be characterized by industrial emissions when emitted with other industrial VOCs such as 2-methylpentane, 3-methylpentane and 1,3-butadiene.

The weekly contributions of each factor calculated by PMF were averaged over the whole sampling period and the results were presented in Figure 2.5-a. At Wallisville, refinery factor had the largest contribution to VOC mass with 62 ppbC, and petrochemical production factor was the second major contributor to VOC mass with 39 ppbC. Other significant factors were natural gas (24 ppbC) and gasoline emissions (19 ppbC).

Biogenic emissions were directly related to plant growth period, sunlight intensity and ambient temperature (*Hagerman et al.*, 1997). For this reason, diurnal variation of biogenic emissions showed higher contributions during the day and lower contributions at night as shown in Figure 2.6. The contribution of biogenic emissions averaged approximately 6.8 ppbC during the sampling period. A source factor representing biogenic emissions was not resolved for the data at the other two sites, possibly because the Lynchburg and HRM-3 sites are closer to the highly industrial Ship Channel and farther from the forested areas. Aromatics emissions and vehicle exhaust/transient industrial factors had minor contributions to VOC concentrations at Wallisville.

Figure 2.5. Percent contributions to VOC mass at the three sites.

(a) Wallisville

(b) HRM-3

(c) Lynchburg
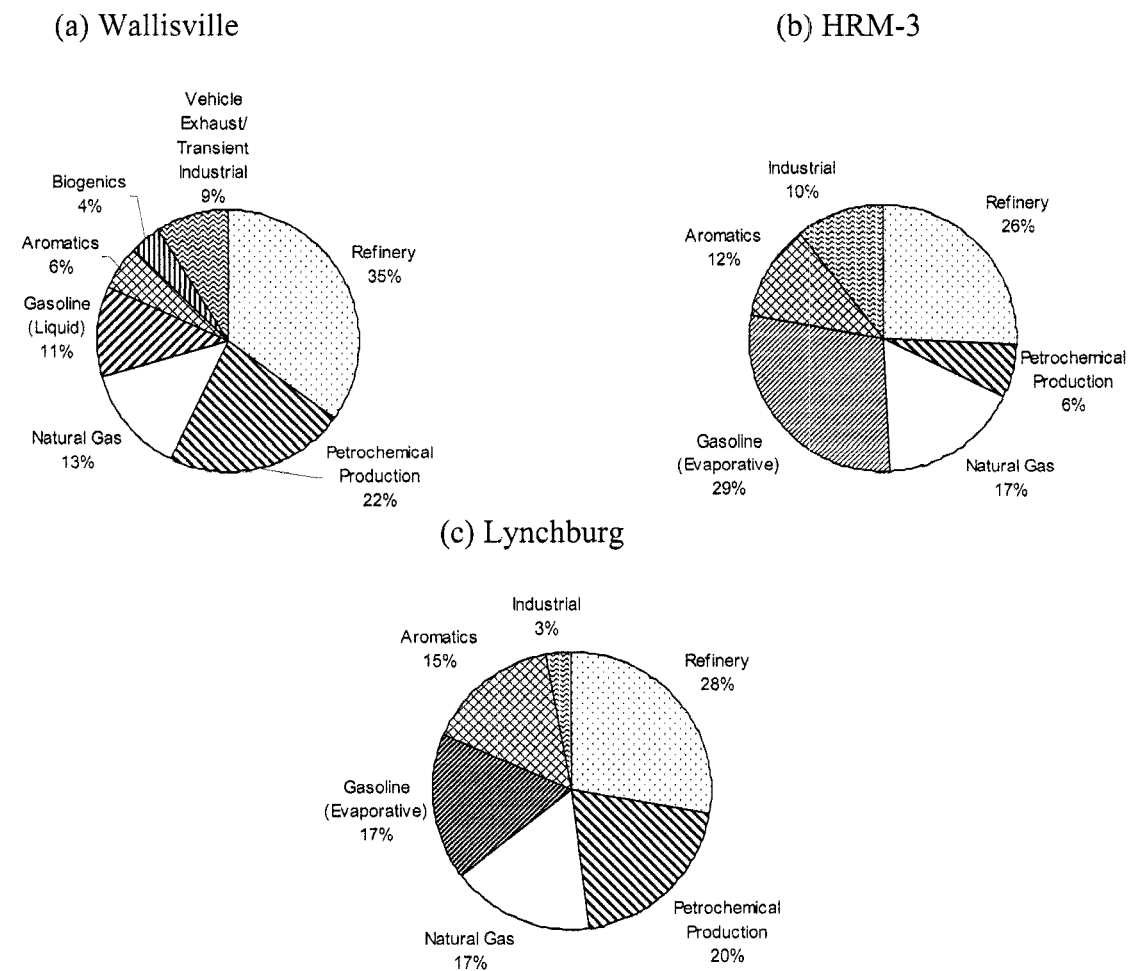
Figure 2.6. Time series plot of factor contributions for Wallisville Road data.
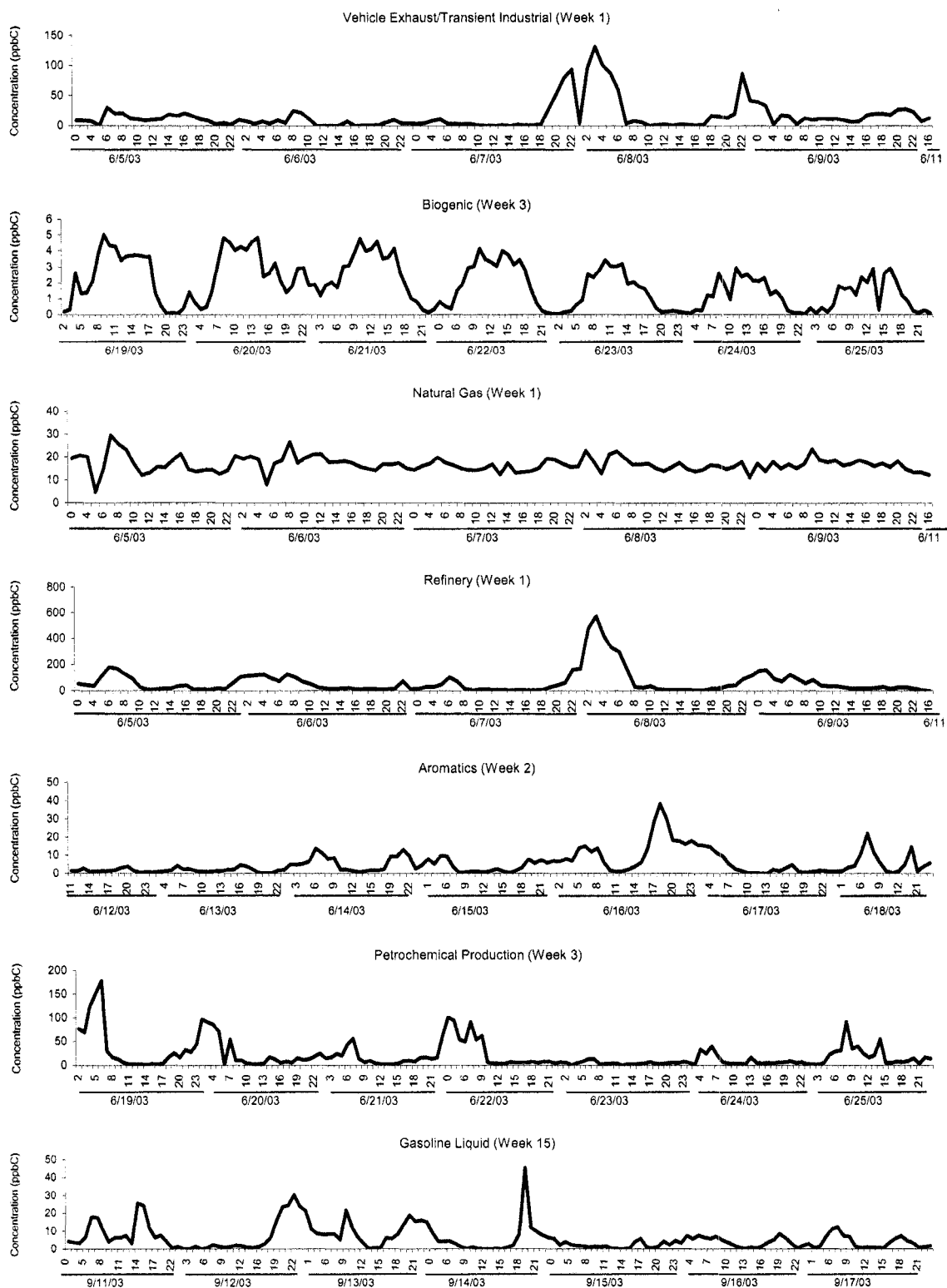
There are regular temporal variations in the source contribution estimates for the biogenic emissions factor but not for the other factors. This is shown in Figure 2.6 where the source contribution estimates calculated by PMF are plotted as a function of time.

2.4.2. HRM-3 Haden Road

Hourly VOC data from HRM-3 was divided into 22 weekly data sets. Four source factors were isolated in 12 weeks and three source factors in 10 weeks. The same profiles were obtained at this site as the ones at Wallisville, except that no biogenic and vehicle exhaust/transient industrial factors were resolved. An additional profile, in which n-butane, n-hexane, 2- and 3-methylpentanes and 2,2,4-trimethylpentane are present, is interpreted as industrial emissions. At HRM-3, a different profile was obtained for gasoline emissions containing only the butanes and pentanes, which are the gasoline components with the lowest boiling points. Therefore, this factor represents evaporative gasoline emissions (*Fujita et al.*, 1995). Representative factor profiles are shown in Figure 2.7.

Figure 2.7. Representative factor profiles for HRM-3 Haden Road data.
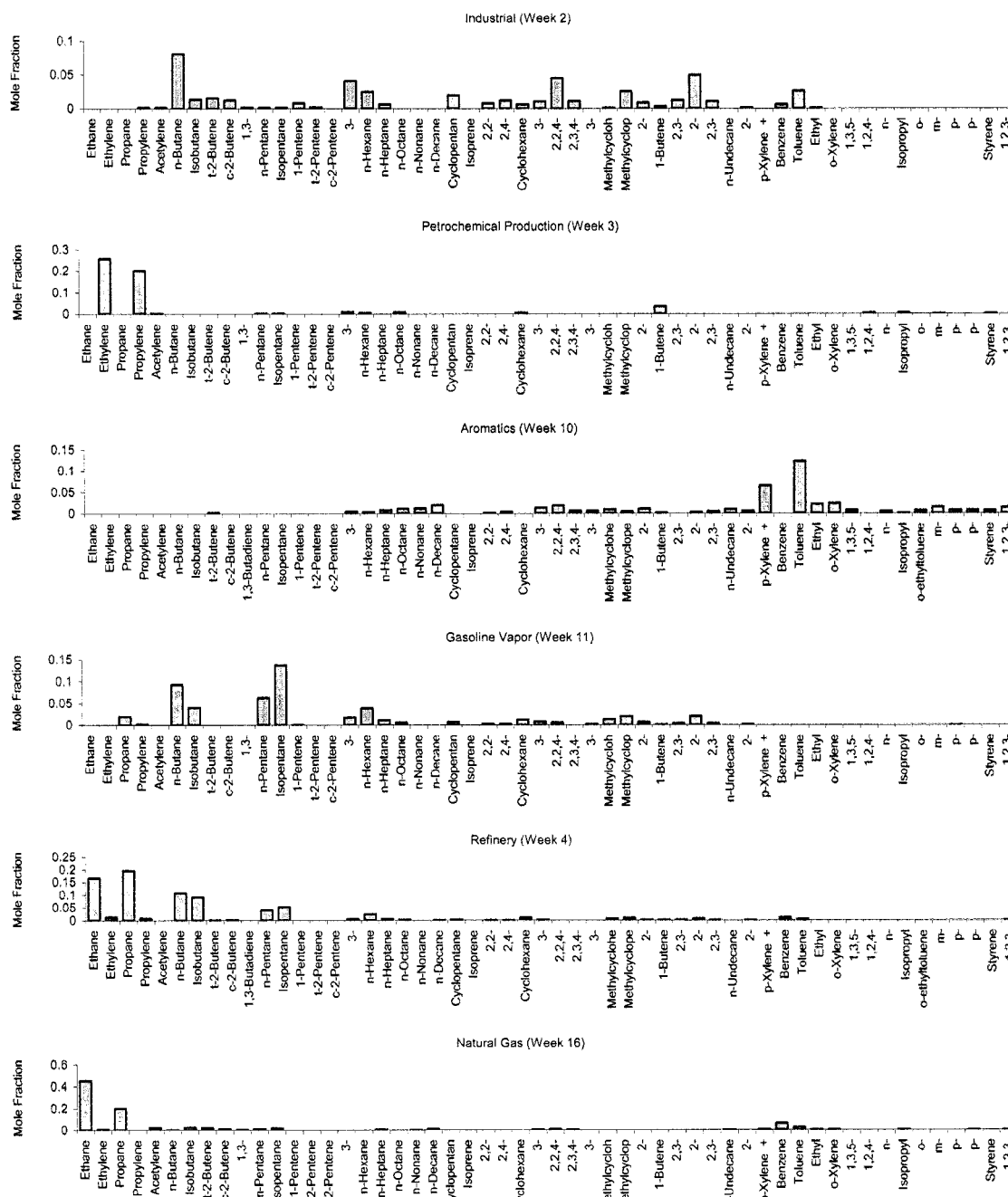
Refinery and aromatic emissions factors were resolved in all 22 weeks, whereas

gasoline vapor was isolated in 17 weeks and petrochemical production factor was isolated

in 10 of the 22 weeks. The other factors, natural gas and industrial emissions, were extracted from the data set in only 4 and 3 of the 22 weeks, respectively.

Figure 2.5-b shows the percent contributions of each factor at HRM-3 site. According to the results, gasoline and refinery factors were the two major contributors with 99 ppbC and 89 ppbC, respectively. The contribution from natural gas followed those two factors with 58 ppbC and the aromatics emission factor was the fourth largest contributor to VOC mass with 40 ppbC. Industrial emissions and petrochemical production factors contributed 38 ppbC and 22 ppbC to total VOC concentrations, comprising a small portion of the total mass.

2.4.3. Lynchburg Ferry

This study focused on 54 VOCs for the overall sampling period. However, a number of key compounds such as acetylene, n-pentane, isopentane, isoprene, 2-methylpentane and 3-methylpentane, were not reported for the first 9 weeks and the last week of the summer period. As a result, the data for those 10 weeks were analyzed separately, excluding these missing compounds from the analysis. This separate analysis contained fewer compounds but covered all of the periods from week 1 to week 9 and also week 21. The factors resolved for this period were interpreted by considering the missing compounds.

Hourly VOC data from Lynchburg Ferry was divided into 21 weekly data sets. Four factors were isolated in 8 weeks and three factors in 13 weeks. The same types of profiles were extracted from the Lynchburg data as the ones from HRM-3 data as shown in Figure 2.8.

Refinery and aromatic emissions factors were resolved in all 21 weeks, whereas gasoline vapor was isolated in 12 weeks and natural gas factor was isolated in 10 of the 22 weeks. Other source factors, petrochemical production and industrial emissions, were extracted from the data set in only 4 of the 22 weeks.

In Figure 2.5-c, the refining factor is the most important contributor with 114 ppbC at this site. The petrochemical production factor is the second major contributor to VOC mass with 83 ppbC, accounting for 20% of the total mass, although this factor was resolved only in 4 weeks. Gasoline and natural gas factors contributed 71ppbC and 68 ppbC to the total mass, respectively. The aromatics factor, which was dominated by toluene and xylene emissions, contributed 62 ppbC. The minor contributor, the industry factor accounted for only 3% of the total VOC mass, contributing 13 ppbC.

Figure 2.8. Representative factor profiles for HRM-3 Haden Road data.
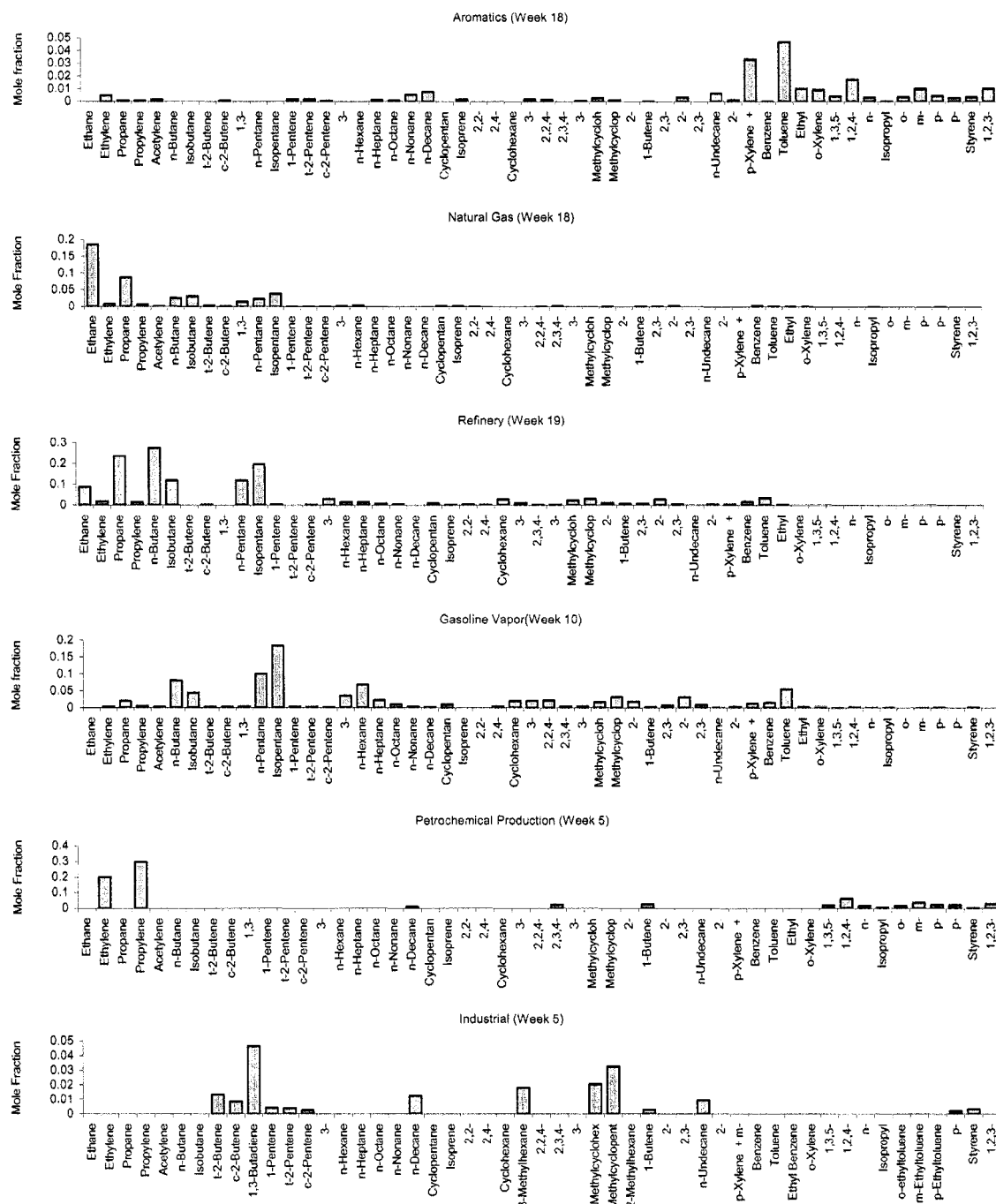
2.4.4. Comparison of the results at the three sites

VOC concentrations were much lower at Wallisville compared to HRM-3 and

Lynchburg, consistent with the relative proximities of the sites to the industrial facilities.

Similar factors were resolved at each site, and therefore it can be deduced that the same

types of sources influence the VOC emissions throughout the Ship Channel region. As

can be seen in Figure 2.5, refining operations dominated the VOC composition at all

three sites, which is expected for this region that is surrounded by some of the world's

largest refinery complexes. However, the contribution of evaporative gasoline emissions

was slightly higher than refinery emissions at HRM-3. Since HRM-3 site is located to the

south of a major interstate highway, the relatively higher contribution of evaporative

gasoline emissions can be explained by the evaporation of the VOCs due to the vehicle

refueling, running losses, diurnal or hot soak. Since exhaust emissions of VOCs have

been reduced due to the substantial improvements in emission control of new cars in

recent years, evaporative emissions of gasoline have become relatively more important in

terms of VOC emissions from automobiles (*Tran et al.*, 2003). Evaporative gasoline

emissions are also originated from the loading of tank truck, transportation and unloading

from tank trucks at service stations and distribution depots (*Fujita et al.*, 1995). The

evaporative gasoline factor was a major contributor to VOC mass together with the

refinery factor at HRM-3 and the third largest contributor at Lynchburg. However, the

factor, associated with gasoline emissions at Wallisville site, had toluene and xylenes

together with pentane in its profile, which suggested that this factor probably represented

liquid gasoline emissions due to spillage or seepage of gasoline (*Fujita et al.*, 1995). The

gasoline factors were not resolved in each week although they are associated with traffic

emissions, however the aromatics factor, which can also be associated with gasoline emissions, was resolved in the other weeks, suggesting that mobile sources are likely important in the region in addition to the industrial sources.

The natural gas factor was resolved in 76% of the weeks at Wallisville whereas it was resolved in 48% of the total number of weeks at Lynchburg and 18% at HRM-3. This factor was not a major contributor in any of the sites, but the contribution was lower at Wallisville than at the other sites. Since this factor may also represent the accumulation mass due to the longer lifetime of ethane and propane, it can be concluded that air masses were fresher at Wallisville. It was also supported by less diurnal changes in VOC concentrations shown in Figure 2.2 at Wallisville than at HRM-3 and Lynchburg, where air masses were more aged.

Petrochemical production factor was resolved in 90%, 45% and 19% of all of the weeks at Wallisville, HRM-3, and Lynchburg sites, respectively. This factor was the second major factor contributing to VOC mass at Wallisville and Lynchburg although it was resolved in only 4 weeks at Lynchburg, which suggests that petrochemical production facilities play a major role in total VOC emissions around the Ship Channel. This is caused by the large number of petrochemical plants located to the south of Lynchburg site. The lower contribution of this factor at HRM-3 compared to the other two sites is consistent with the concentration measurements of ethylene and propylene as the average concentrations of these two VOCs were lower at HRM-3 than at Lynchburg and Wallisville.

The industrial emissions factor was only resolved in 3 and 4 weeks at HRM-3 and Lynchburg sites, respectively, and that factor was found to be a minor contributor to

NMHC mass at both sites. Since this was such a minor contributor, no further
investigation of this factor was pursued.

The results of the analysis of variance (ANOVA) have shown that the relationship
between total VOC mass and factor scores could be considered statistically significant at
a 99% confidence level for all the three sites. The adjusted coefficient of multiple
determination, R_a^2, indicated that 85%, 88%, and 73% of the variability of VOC mass can
be explained by the PMF model for the VOC measured at Wallisville, HRM-3 and
Lynchburg, respectively. The regression coefficients were statistically significant at the
99% confidence level. A residual analysis has been performed and the residuals showed
no major trend, indicating that the regression model between measured and calculated
values was not biased by limiting the analysis to the top 3 or 4 source factors. Figure 2.9
shows that the resolved sources effectively reproduced the measured values and
accounted for most of the variation in the VOC mass concentrations.

Figure 2.9. Measured versus calculated VOC mass concentration at the three sites.
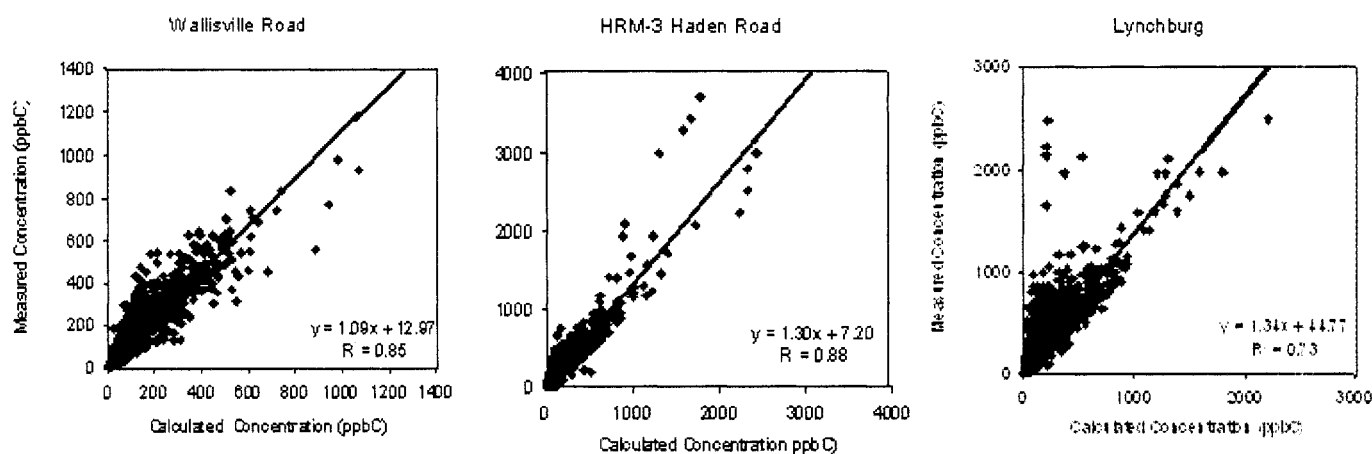
The contribution of VOCs to the production of the photochemical ozone is related to their reaction with hydroxyl radicals and ozone in the complex photo-oxidation mechanism (*Na et al.*, 2003). Previous work has shown that propylene, ethylene, isoprene and 1,3-butadiene have the highest contribution to the photochemical ozone production (*Ryerson et al.*, 2003). Highly reactive species, propylene and ethylene are mainly emitted from petrochemical facilities, which are abundant in the Houston Ship Channel (*Ryerson et al.*, 2003). This suggests that emissions from the petrochemical manufacturing plants are significant contributors to ozone formation in Houston. While the carbon-based concentrations of ethane, propane and n/i-butane are higher than the other VOCs, their ozone formation potentials are low, meaning that while these species are abundant, they are not as important as the reactive olefins to ozone production in Houston (*Carter*, 1991, 1994). However, because of their very high concentrations in the Houston atmosphere, the reactions of alkanes may be more important in ozone formation in Houston than they are in other urban areas (*Allen et al.*, 2004; *Katzenstein et al.*, 2003).

2.4.5. Nighttime Data Analysis

PMF was also performed on the nighttime VOC data from July 2003 at Wallisville Road and Lynchburg Ferry. The data between the hours of 9pm and 6am local time were used to minimize the effect of photochemical reactions on model results. The analysis of the nighttime data is also important because the mixing heights are low, so the point source emissions are not much diluted and mostly industrial as mobile and biogenic emissions are minimal at nighttime. Using nighttime data only in this analysis resulted in the resolution of same type of factors dominated the VOC emissions, but the

contributions were higher in the nighttime analysis since the loss of species concentrations due to the photochemical reactions and the dilution effect was minimum. The evaporative gasoline emissions were not resolved, since emissions from vehicles are low and the evaporation is less during nighttime. On the other hand, industrial factors such as refining, petrochemical, and aromatics emissions were still resolved due to the continuing activity of the industrial facilities in the region during the night.

Nighttime data were not divided into weekly periods for analysis, instead were analyzed as a full data set. Here, it is important to emphasize that n-pentane and isopentane concentrations were missing in all of the July samples from the Lynchburg data. Since these VOCs are significant components of gasoline emissions, either in vaporized form or in liquid form, and also of refining emissions and vehicle exhaust emissions, it is important to approach the interpretation of factor profiles keeping this fact in mind.

To be able to compare the results of both nighttime and all-day analysis, the source contributions for the month of July were averaged for the all-day data. At Wallisville, petrochemical production factor was the most significant factor with 48 ppbC (35%); refinery factor was also a dominant contributor to VOC mass with 44 ppbC (32%). Other factors contributing to VOC mass during July were natural gas with 26 ppbC (19%), aromatics with 11 ppbC (8%) and biogenic emissions with 7 ppbC (5%).

For the nighttime data at Wallisville, total VOC mass was measured as 167 ppbC and total apportioned mass was calculated as 163 ppbC showing that PMF well apportioned total VOC mass. Factor profiles are shown in Figure 2.10. Refining source factor accounted for 39% of total calculated VOC mass, contributing to 63 ppbC and

petrochemical production factor was an equally significant contributor to VOC mass with 62 ppbC accounting for 38% of the total mass. The aromatics factor, which is dominated by toluene and xylene emissions, contributed 24 ppbC (15%). A factor consistent with vehicle exhaust or transient industrial emissions, mainly characterized by n-hexane, ethylene, benzene, and cyclohexane, accounted for only 9% of the total VOC mass, contributing 14 ppbC to the total mass. This factor might represent vehicle exhaust emissions since it has ethylene, acetylene, benzene and n-hexane in the profile, but no toluene and xylenes were resolved in this factor. High n-hexane fraction together with cyclohexane, 1,3-butadiene, 1-butene and methylcyclopentane suggest that the same factor might also be representing an industrial source. Thus, this factor might be a mix of vehicle exhaust and industrial emissions.

Figure 2.10. Factor profiles for nighttime data at Wallisville Road.
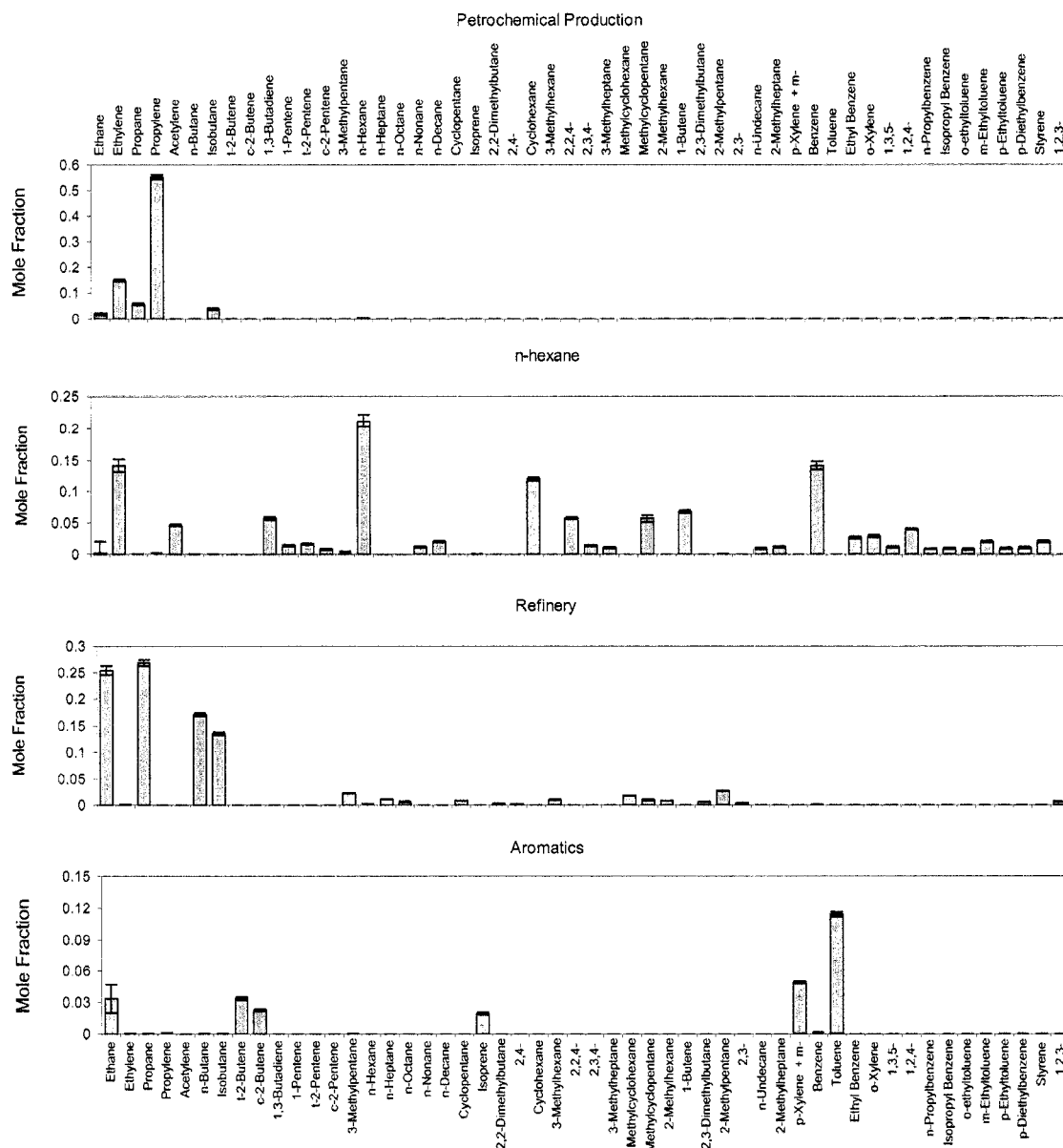
The contributions of each factor were higher for nighttime data compared to the all-day data, as the effect of the photochemical activity was minimized during nighttime period. Since biogenic emissions are directly related to plant growth period, sunlight intensity and ambient temperature (*Hagerman et al.* 1997), diurnal variation of biogenic emissions showed higher contributions during the day and lower contributions at night

(Figure 2.6). For the same reason, the representative compound of biogenic emissions, isoprene, has higher concentrations in the all-day data than it does in nighttime data. This might be the reason that a biogenic emissions factor was not resolved for the nighttime data. Natural gas factor, resolved in 2 of the 5 weeks in the month of July when all-day data were analyzed, was not resolved for nighttime data. However, another factor representing a mix of vehicle exhaust and industrial emissions was resolved for the nighttime data. The difference between the measured concentrations of n-hexane, benzene, ethylene, cyclohexane and acetylene in nighttime and all-day samples explains the resolution of this factor, as the nighttime concentrations were much higher than the all-day concentrations.

At Lynchburg, the source contributions calculated for the month of July for each factor was averaged for the all-day analysis. Refinery factor had the highest contribution to VOC mass with 100 ppbC accounting for 29% of total mass, and the aromatics factor had a contribution of 84 ppbC comprising 24% of the total VOC mass. Other factors resolved were petrochemical production with contribution of 68 ppbC (20%), evaporative gasoline emissions with 52 ppbC (15%), natural gas with 31 ppbC (9%) and finally an industrial emissions factor having 1,3-butadiene, methylcyclohexane, propylene, and t-2-butene in its profile had a minor contribution of 13 ppbC (4%).

For the nighttime data, total VOC mass was measured as 368 ppbC and total apportioned mass was calculated as 348 ppbC at Lynchburg for the four-factor solution. The profiles of the resolved factors are shown in Figure 3.11. The factor, which is dominated by benzene, toluene and propylene emissions, contributes 99 ppbC (29%). This factor might be a representative of evaporative losses from petroleum storage

facilities located all around the Ship Channel. The reason that benzene dominates this factor instead of other aromatic compounds is related to the fact that benzene concentration measurements are more than 100% higher in the nighttime samples than in the all-day samples whereas the concentrations of other aromatics are similar between day and night samples. The most abundant VOCs in the nighttime samples are propylene and benzene whereas in all-day samples benzene follows propylene, propane, n-butane and isobutane. For nighttime analysis, refining source factor accounted for 28% of total calculated VOC mass, contributing to 96 ppbC. Natural gas factor accounted for 22% of the total mass with 76 ppbC and petrochemical production factor was also a significant contributor to VOC mass with 75 ppbC accounting for 22% of the total mass. Results of the PMF calculations for nighttime compared to all day samples are summarized in Table 2.2.

Figure 2.11. Factor profiles for nighttime data at Lynchburg.
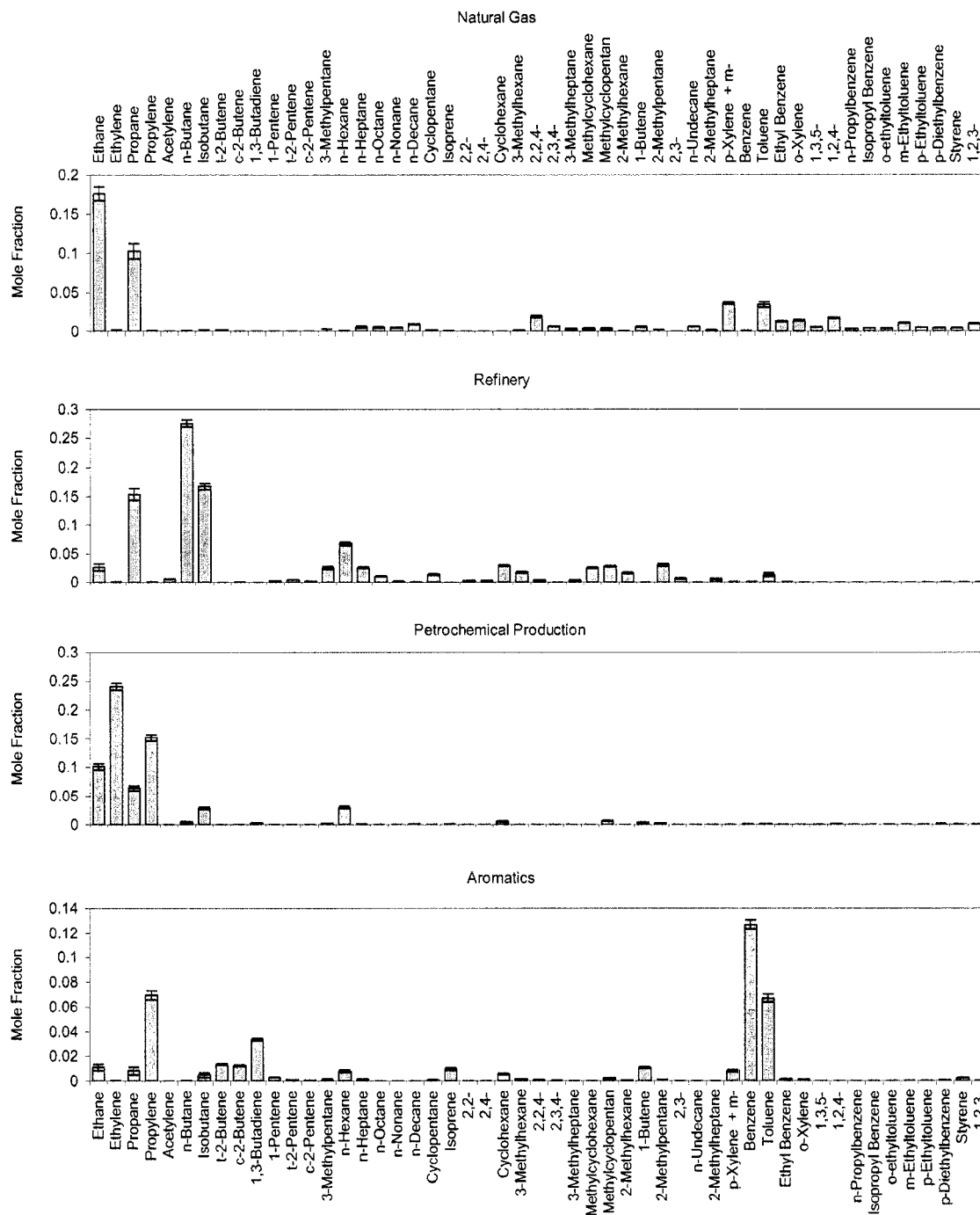
Table 2.2. Comparison of the factor contributions to VOC mass for July data using all-day data and nighttime data only at Wallisville and Lynchburg.

Factor	Wallisville (All-Day Data)		Wallisville (Nighttime Data)		Lynchburg (All-Day Data)		Lynchburg (Nighttime Data)	
	Contribution (ppbC)	%	Contribution (ppbC)	%	Contribution (ppbC)	%	Contribution (ppbC)	%
Biogenic	7.35	5						
Industrial					13.46	4		
Gasoline (Evaporative)					52.00	15		
Natural Gas	26.10	19			31.29	9	76.46	22
Petrochemical Production	48.06	35	62.43	38	68.25	20	75.48	22
Refinery	43.93	32	62.98	39	100.18	29	96.51	28
Aromatics	11.18	8	23.74	15	83.98	24	99.59	29
Transient Industrial			14.14	9				

The contribution of each source factor was higher in the nighttime data than the all-day data except the refinery factor. Since the effect of the photochemical activity was minimized during nighttime period, it is expected to observe higher contributions from petrochemical production factor and aromatics factor as compounds such as ethylene, propylene, and toluene are highly reactive VOCs and their activity is limited during the nighttime. However, refinery factor represents emissions of less reactive VOCs, such as n-butane, isobutane, propane and ethane, therefore concentrations of these compounds can be expected to remain roughly the same during the daytime. While the contribution of refining factor was approximately the same on daytime and nighttime analysis at Lynchburg, it was found to be higher on nighttime samples at Wallisville. Since

Lynchburg site is located very close to the petroleum refining complexes in the Ship

Channel and since the VOCs emitted from refineries are not highly reactive, they are not

expected to be consumed photochemically in the short transport times to the site.

However, Wallisville is located to the northeast of the Ship Channel and not as close to

the industrial complexes. Therefore, it is more likely that the VOCs emitted from the

refineries are oxidized photochemically on the way to the receptor site at Wallisville.

2.5. Conclusion

Analysis of the data collected at three sites in Houston during the summer of 2003

resulted in isolating and evaluating 3 or 4 major source factors of 54 VOCs for each

weekly period in the Houston Ship Channel region. The most important isolated factors

affecting these three sites were found to be consistent with emissions from refineries,

petrochemical production facilities, gasoline and natural gas/accumulation emissions,

which indicated the importance of the reactive compounds that have high ozone

formation potential as well as the less reactive VOCs that have longer lifetimes in the

atmosphere. Using nighttime data only resulted in the resolution of same type of factors

dominated the VOC emissions, but the contributions were higher in the nighttime

analysis since the loss of species concentrations due to the photochemical reactions was

minimum. The evaporative gasoline emissions were not resolved, since emissions from

vehicles are low and evaporation is less during nighttime. On the other hand, industrial

factors such as refining, petrochemical, and aromatics emissions were still resolved due

to the continuing activity of the industrial facilities in the region during the night.

CHAPTER 3

Evaluation of VOC Emission Inventory with Source

Apportionment

3.1. Introduction

In this chapter the results of Chapter 2 will be compared to emission inventory information and analyzed in more detail. In Section 2, the source contributions calculated for each hour will be related to the ozone formation using a quantitative analysis method. In Section 3, we will compare self-reported emissions of VOCs in Houston, TX to the results of the multivariate receptor modeling performed at three receptor sites near the Houston. The hourly concentrations of 54 VOCs for the period June through November 2003 were analyzed by Positive Matrix Factorization (PMF) receptor model in Chapter 2. Utilizing the hourly source contributions, Section 3 will look at the potential source directions using a method called "conditional probability function" and then compare them to the locations of the specific point sources in the emission inventory. The consistencies or inconsistencies between the compositions and the locations of reported emissions and major sources as derived from the ambient data using PMF will be interpreted in an attempt to determine the adequacy of existing inventories. Finally, Section 4 will analyze the influence of the event emissions on the source contributions.

3.2. Comparison of Source Attribution with Ozone Formation

3.2.1. Cross-correlation analysis

The contribution of VOCs to the production of the photochemical ozone is related to their reaction with hydroxyl radicals and ozone in a complex photo-oxidation mechanism (*Na et al.*, 2003). Previous work has shown that propylene, ethylene, isoprene and 1,3-butadiene have the highest contribution to the photochemical ozone production in Houston (*Ryerson et al.*, 2003). Propylene and ethylene are highly reactive species that are mainly emitted from petrochemical facilities, which are abundant in the Houston Ship Channel (*Ryerson et al.*, 2003). This suggests that emissions from the petrochemical manufacturing plants are significant contributors to ozone formation in Houston. While the ambient concentrations of ethane, propane and n/i-butane are higher than the other VOCs, their ozone formation potentials are low, and as a result while these species are abundant, they are not as important as the reactive olefins to ozone production in Houston (*Carter*, 1991; *Carter*, 1994). However, because of their very high concentrations in the Houston atmosphere, the reactions of alkanes may be more important in ozone formation in Houston than they are in other urban areas (*Allen et al.*, 2004; *Katzenstein et al.*, 2003). This section will analyze the dependence between the calculated hourly source contributions and measured ozone concentrations to present evidence supporting the importance of alkanes and alkenes to ozone formation in the Houston atmosphere.

The cross correlation function or CCF, is a standard method of estimating the degree to which two time series are correlated and is obtained by evaluating the cross correlation coefficients between the elements of these two time series, x(t) and y(t). That is, for each lag k (positive or negative) in the time series, the CCF estimates the

correlation between x(t) + k and y(t) where t=0,1,2...n-1 and n is the length of each time series.

The cross correlation r at lag k is defined as

$$r_{xy}(k) = \frac{\sum_t [(x(t+k) - \mu_x)(y(t) - \mu_y)]}{\sqrt{\sum_t (x(t+k) - \mu_x)^2} \sqrt{\sum_t (y(t) - \mu_y)^2}}$$

(1)

where μ_x and μ_y are the means of the corresponding series. If the above is computed for all lags k, the result is a cross correlation series, twice the length as the original data. The lags represent the time periods separating data in one time series from the data in the other time series when calculating the cross correlation coefficients. By default, the lags range from $-(\sqrt{n}+10)$ to $+(\sqrt{n}+10)$. The denominator in Equation 1 serves to normalize the correlation coefficients such that $-1 <= r_{xy}(k) <= 1$, the bounds indicating maximum correlation and a value of zero indicating no correlation.

If the population cross correlation of lag k is zero, then for fairly large n, $r_{xy}(k)$ will be approximately normally distributed, with mean zero and standard deviation $1/(n-|k|)^{1/2}$. Since roughly 95% of a normal population is within 2 standard deviations of the mean, a test that rejects the hypothesis that the population cross correlation of lag k equals zero when $| r_{xy}(k) |$ is greater than $2/(n-|k|)^{1/2}$ has a significance level of approximately 5% (Minitab StatGuide, 2006).

All the cross-correlations between the ozone time series and the source contribution time series were calculated using a statistical software package, Minitab 14, and the results are presented in the next section..

3.2.2. Results of the Ozone Time Series Analysis

Measured air quality during the entire sampling period, June-October 2003

identified 13 exceedances of the ozone standard at each site and investigated where ozone

levels exceeded one hour standard of 120 ppbV (Table 3.1).

Table 3.1. Days of exceedance of 1-hr ozone standard of 125 ppb at each site (all ozone concentration values are in ppb).

O_3 exceedance days	Wallisville	HRM-3	Lynchburg
June 9, 11am			129
July 17, 11am			136
July 17, 12pm			149
July 17, 1 pm		161	
July 17, 2pm		150	
July 17, 3pm		138	
July 18, 3pm	143		
July 18, 4pm	147		
July 18, 5pm	129		
July 19, 1pm	127		
August 8, 2pm	130		169
August 8, 3pm	133		136
August 8, 4pm	139		127
August 23, 1pm			130
August 23, 2pm			131
August 23, 3pm	132	125	152
August 23, 4pm	143	135	142
August 23, 5pm		139	
September 13, 12pm	131		
September 13, 1pm	139	126	143
September 13, 2pm		144	146
September 13, 3pm		143	
October 21, 2pm	151		140
October 21, 3pm	141		
October 23, 12pm		125	
October 23, 1pm		133	
October 23, 2pm		133	
October 23, 3pm		125	

Cross correlations for ozone concentrations between the sites for the entire sampling period have very significant peaks (correlation coefficient of about 0.8) for lag = 0 (Figure 3.1). This means that at each site the maximum ozone concentrations are observed at the same time.
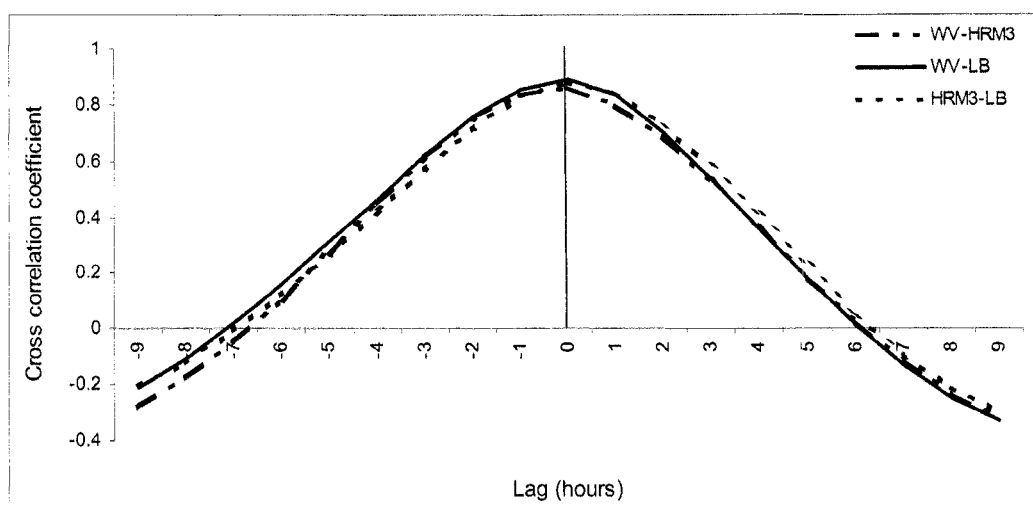
Figure 3.1. Cross correlation between study sites Wallisville (WV), HRM-3, and Lynchburg (LB) for ozone.

The cross correlations were also calculated using data at one-hour temporal resolution for source contribution estimates and ozone concentrations, and the results were summarized in Table 3.2. The cross-correlation coefficients (CCC) between the ozone and the source contribution time series, and the time lags, which correspond to the highest correlation coefficients, were reported in Table 3.2. In most cases, the ozone standard exceedances corresponded to the peak values in the time series of the source contributions with lags ranging from 8 to13. This is consistent with the atmospheric chemistry of ozone formation where photochemical reactions of VOCs and NOx lead to ozone accumulation. For Wallisville and Lynchburg data, the ozone time series show good correlations with the time series of petrochemical production and refining emissions, whereas for HRM-3 data, the correlations of ozone time series with aromatic emissions were more significant.

The statistical significance of the calculated correlation coefficients was assessed by the value reported in the second column of Table 3.2. As explained in Section 3.2.1, if the CCC is greater than the test statistic, $2/(n-|k|)^{1/2}$, then the CCC is significant at 95% confidence level. Since all of the cross correlation coefficients were larger than the corresponding test statistics, it can be stated with 95% confidence that the calculated correlation coefficients were statistically significant.

Some of these results are also presented in Figures 3.2 through 3.4 where parts (a) show the plots of the cross correlation coefficients (CCC) against the time lags. The source contribution time series are lagged by the number of hours that correspond to the highest correlation coefficients in the top figures and plotted together with the ozone time series in the part (b) of Figures 3.2 to 3.4. These figures are the representative plots from each receptor site and for each different source type. More plots for the other periods of ozone standard exceedances are presented in the Appendix.

There is a time lag ranging from 8 to 13 hours between the maximum values of ozone concentrations and the contributions of certain VOC sources, because ozone is produced as a result of chemical reactions between VOCs and nitrogen oxides. That means ozone reaches maximum concentration several hours after large amounts of VOCs are emitted. Positive values of the lag correspond to the time series of source contributions leading the ozone time series consistent with the precursor nature of VOCs to ozone formation. The actual magnitude of cross correlation coefficients is much lower for some periods, and this is related to the larger variability observed in the time series of that particular source because source contributions are affected by the variability in local emissions as well as meteorological factors.

Table 3.2. The results of the cross-correlation analysis for the ozone time series and the source contributions during the ozone standard exceedance periods.

Wallisville						
O_3 exceedance days	CCC	$2/(n-|k|)^{1/2}$	Lag (hours)	Ozone (ppb)	Source	Source Contribution (ppbC)
8-Aug						Not enough ambient data
23-Aug	0.63	0.22	13	143	Pet. Prod.	237
23-Aug	0.67	0.22	11	143	Refinery	571
13-Sep	0.83	0.22	13	139	Pet. Prod.	68
13-Sep	0.49	0.12	9	139	Refinery	251
21-Oct	0.70	0.21	8	151	Refinery	577

Lynchburg						
O_3 exceedance days	CCC	$2/(n-|k|)^{1/2}$	Lag (hours)	Ozone (ppb)	Source	Source Contribution (ppbC)
9-Jun	0.52	0.22	12	129	Refinery	551
9-Jun	0.40	0.22	12	129	Pet. Prod.	509
17-Jul	0.56	0.21	2	136	Gasoline	126
8-Aug	0.45	0.27	14	169	Refinery	574
23-Aug	0.54	0.22	12	152	Refinery	1906
13-Sep	0.55	0.16	11	146	Refinery	575
21-Oct						No ambient data

HRM-3						
O_3 exceedance days	CCC	$2/(n-|k|)^{1/2}$	Lag (hours)	Ozone (ppb)	Source	Source Contribution (ppbC)
17-Jul	0.56	0.23	0	161	Refinery	196
23-Aug	0.59	0.22	14	139	Aromatics	236
13-Sep	0.76	0.22	11	143	Aromatics	938
23-Oct	0.40	0.17	10	133	Aromatics	84

(CCC=Cross correlation coefficient)
If CCC>$2/(n-|k|)^{1/2}$ then the correlation is significant at 95% confidence level.
n is the length of each time series, k is the time lag.
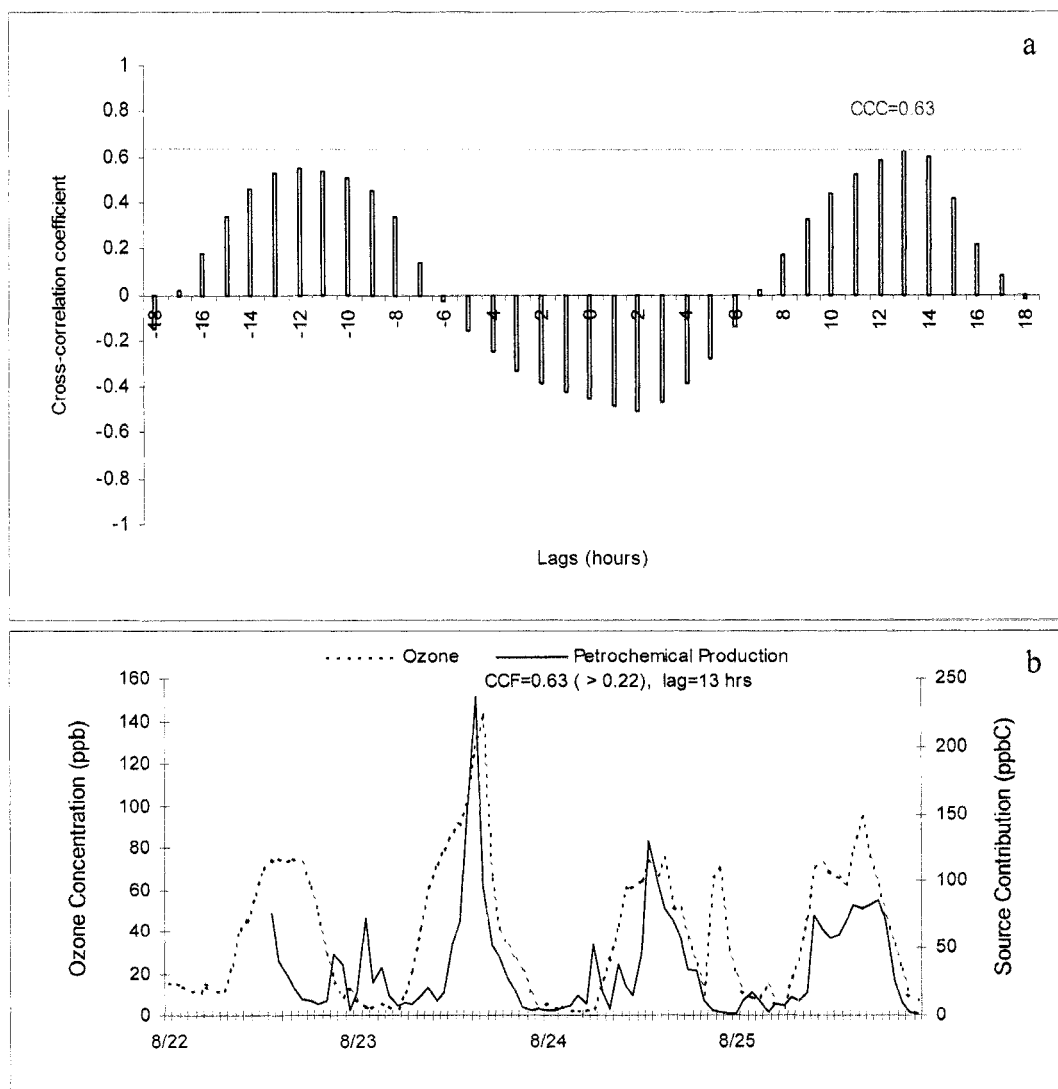
Figure 3.2. Cross correlation function between ozone and petrochemical production time series for the same period at Wallisville (a), and 1-hour ozone time series and lagged contributions of petrochemical production source at Wallisville (b).
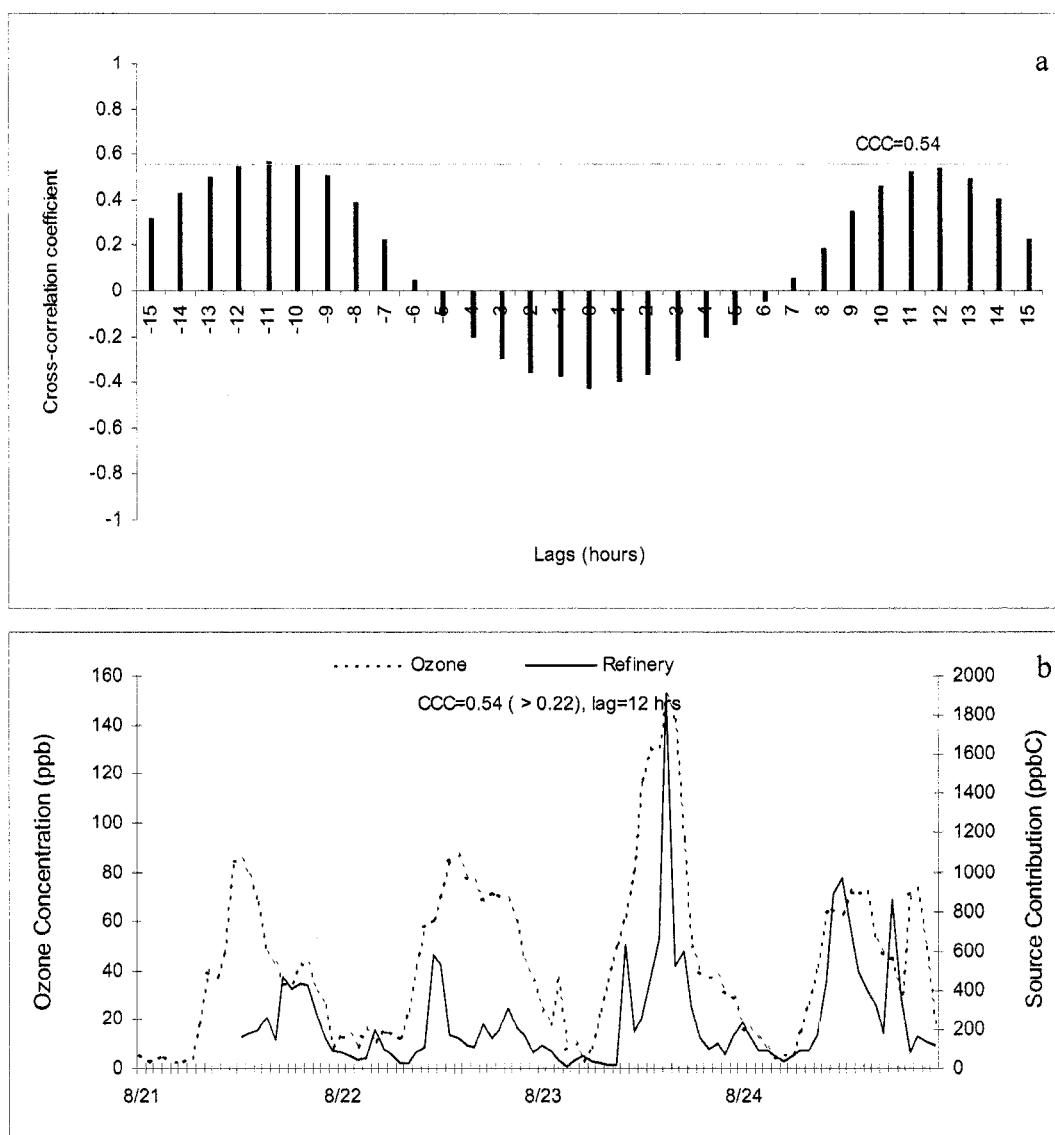
Figure 3.3. Cross correlation function between ozone and refinery emissions time series for the same period at Lynchburg (a), and 1-hour ozone time series and lagged contributions of refinery emissions source at Lynchburg (b).
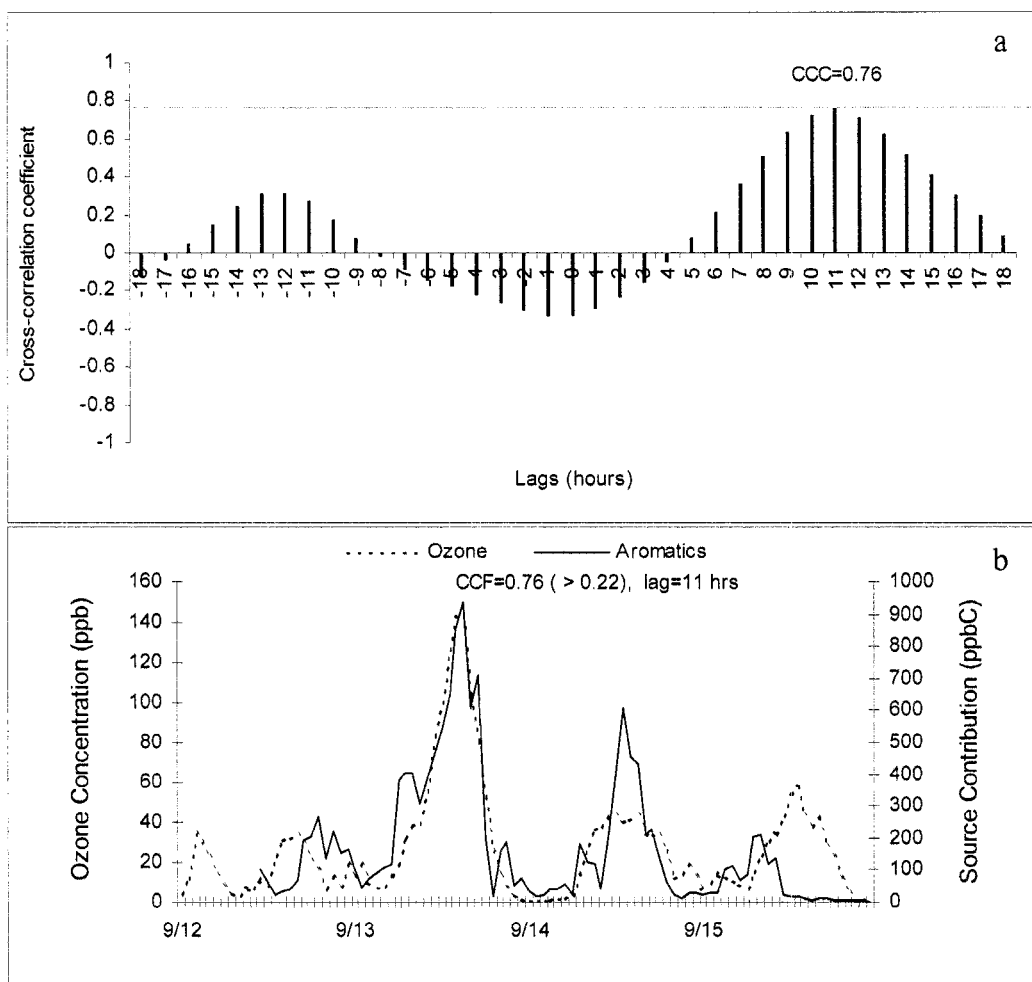
Figure 3.4. Cross correlation function between ozone and aromatics emissions time series for the same period at HRM-3 (a), and 1-hour ozone time series and lagged contributions of aromatics emissions source at HRM-3 (b).

The results of this analysis confirmed that very high contributions of the dominant

sources of VOCs such as refineries and petrochemical plants during times that are

favorable to ozone formation led to ozone concentrations that exceed air quality standards

at the three sites. The results also revealed that markers of refining emissions such as

propane, butanes, ethane and pentanes can also lead to ozone violations as well as highly

reactive compounds present in petrochemical emissions such as ethylene and propylene.

All these observations are consistent with the findings of *Allen et al.* (2004) who

analyzed the OH and MIR reactivities of selected VOCs, including highly reactive VOCs

(ethylene, propylene, 1,3-butadiene, 1-butene), alkanes (ethane, propane, n-butane, n-

pentane, isobutene), aromatics (toluene, xylenes, and benzene) and isoprene, at each site

for the days when ozone exceeded 1-hr standard and compared the hourly VOC

reactivities with 5-minute ozone concentrations.

3.3. Identification of Source Regions and Comparison of Source Attribution to Point Source Emission Inventory

3.3.1. Conditional Probability Function (CPF) Analysis

A conditional probability function (CPF) analysis (*Kim et al.*, 2003; *Kim and Hopke*, 2004) was performed on the results of the source apportionment to help interpret the findings. CPF (*Ashbaugh et al.*, 1985) is used to analyze the effects of point sources from different wind directions using the source contribution estimates from PMF together with the wind direction values measured at that site (*Begum et al.*, 2005; *Kim and Hopke*, 2004; *Kim et al.*, 2003). Wind direction here refers to the azimuth angle (measured clockwise from north) that the wind is blowing from. CPF is the fraction of total samples within wind sector, $\Delta\theta$, having a source contribution estimate higher than a predetermined threshold criterion value, usually some fractional value of distributed data. The CPF is then normalized by the total number of occurrences from the same wind sector for that specific factor. Hourly source contribution estimates of each factor were matched to hourly wind data measured at each site and CPF was calculated as

$$CPF_{\Delta\theta} = (m_{\Delta\theta} / n_{\Delta\theta})*W(n_{\Delta\theta}) \qquad (2)$$

$$W(n_{\Delta\theta}) = 0.1*n_{\Delta\theta} \text{ when } 0 < n_{\Delta\theta} \leq 9$$

$$W(n_{\Delta\theta}) = 1 \qquad \text{when } n_{\Delta\theta} \geq 10$$

where $m_{\Delta\theta}$ is the number of occurrences from wind sector $\Delta\theta$ that exceeded the criterion value, $n_{\Delta\theta}$ is the total number of data from the same wind sector and $W(n_{\Delta\theta})$ is the weight function. Since small values of $n_{\Delta\theta}$ produce high CPF values with high uncertainties, CPF

values were down-weighted using a weight function, W ($n_{\Delta\theta}$) when $n_{\Delta\theta}$ is less than 10. In this study 24 wind sectors with $\Delta\theta=15°$ were used. The hours when the wind speed is less than 1 mile per hour were excluded. 50th and 75th percentile of all contributions from each source were tested as the criterion value and 75th percentile (highest 25%) of the source contributions was chosen. CPF values were then plotted as polar graphs that show the fraction of samples coming from a given direction having "high" values, and point to regions associated with these high values.

3.3.2. Processing the VOC Emissions Inventory

Point source emissions were taken from the speciated emissions inventory prepared by the Texas Commission on Environmental Quality (TCEQ). The inventory is subsetted from a version of the inventory (version 15b) used by TCEQ modeling staff for modeling the August/September 2000 episode in Houston, TX. The inventory includes the description, location and emission rates of 18 VOC classes in total pounds per day (lb/day) from all the individual sources in an industrial facility and covers the emission sources in Harris County plus seven surrounding counties and contains 11,810 records. This study focused on the VOC point sources in Harris County, specifically on the sources around the heavily industrialized Houston Ship Channel area. The point source emissions studied included the petrochemical production, refining, aromatics, natural gas and evaporative gasoline emissions. Other sources determined by the source apportionment in Chapter 3, such as biogenics, gasoline liquid emissions and transient industrial emissions were not studied. This is because biogenics are considered to be area sources and were not included in this inventory, and the other sources were minor

contributors to NMHC (non-methane hydrocarbon) mass at the sampling sites. The fractional contributions and emission inventories were adjusted by removing the contributions of biogenic emissions, gasoline liquid emissions and transient industrial emissions and then renormalizing the sum of the remaining fractional source contributions to unity. Only records with VOCs greater than zero are included in the inventory and emissions are listed by emission point.

Before the emissions inventory is compared with the source contributions, the emission rates need to be converted to molar units (ppbC) since the source contributions calculated by PMF are in ppbC. For this purpose, Point ID numbers of each production unit of each plant in the inventory were matched to the source classification codes obtained from "EPA's Technology Transfer Network Ozone Implementation - Plant Index Page" (www.epa.gov/ttn/naaqs/ozone/areas/plant/ms3361pv.htm). Volumetric gas flow rates of stack gases were taken from the same source for each unit in the industrial facilities. Flow rates, which were in cubic feet per second (cfs), were converted to m^3/day, and the equation (3) was used to convert the emission rate to molar concentration units.

$$ppbC = No.\,of\,Carbons \times \frac{1}{MW_{voc}[g\,/\,mol]} \times 1000 \times (E\left[\frac{lbs}{day}\right] \times \frac{1}{F(m^3\,/\,day)} \times 454000\frac{mg}{lbs}) \times R\left[\frac{L.kPa}{mol.K}\right] \times T_{air}[K] \times \frac{1}{P_{air}[kPa]} \quad (3)$$

where MW refers to the molecular weight of the VOCs, F is the stack volumetric gas flow rate, E is the emission rate from the inventory, R is the universal gas constant (8.3144 L.kPa/mol.K), T_{air} is the ambient temperature in K, and P_{air} is the air pressure (101.325 kPa = 1 atm). Emissions from each production unit were weighted by the inverse distance between the emission point and the receptor.

In the inventory, emitted species are either included as a specific chemical species such as propylene, ethylene, butadiene, isoprene, styrene, and benzene, or as a group of species such as C2C3 (ethane, propane), butenes (t-2-butene, 1-butene, c-2-butene), butanes (isobutane, n-butane), pentanes (isopentane, n-pentane), pentenes, c5cyclos (cyclopentane, cyclopentene), hexanes, hexenes, c6cyclos (methylcyclopentane, cyclohexane), c7c10aromatics, c7c11other, and xylenes (m,p-xylene, o-xylene).

In order to compare the source types in the source apportionment results and in the emissions inventory, the representative species of certain types of sources were matched to the individual species or groups of species listed in the inventory. For instance, the natural gas source is mainly represented by ethane and propane as discussed in Chapter 2. The emission sources emitting only these two compounds in the group C2C3 were selected to be used in the comparison of the emissions in the inventory and the contributions of natural gas emission sources determined by PMF.

For each receptor site, emissions from point sources were split by wind direction into one of 24 wind sectors ($\Delta\theta = 15°$). Only the emission sources in 24km by 24km area around each receptor site (up to 12km from the receptor) were included in the calculations. The fraction of total number of units within the wind sector, $\Delta\theta$, having an emission rate higher than a predetermined threshold criterion value of all emission rates to the total number of units in the same wind sector was calculated and plotted as polar graphs which will be discussed in detail in the next section. As the threshold criterion value, 75th percentile of all the emission rates in the inventory for specific types of sources was chosen.

3.3.3. Comparison of the CPF plots and the source locations in the emissions inventory

The main goal of this section is to identify the wind directions associated with high source contributions calculated by the receptor modeling and compare these results to the locations and the compositions of the real sources of VOCs as reported in the emissions inventory to determine the accuracy of the reported emissions. The results of the Conditional Probability Function (CPF) analysis of the source contributions and wind directions were compared to data in the emission inventory in Figures 3.5, 3.6, and 3.7 for Wallisville, Lynchburg and HRM-3 sites, respectively. In these figures, two overlaid polar plots show the fraction of the highest 25% of all the source contributions and the emission rates within a wind sector, $\Delta\theta$, for a specific source type and point to the regions associated with high emissions.

In Figure 3.5 it is clear that high contributions from all types of sources are strongly associated with winds from west and southwest directions at the Wallisville site, where there are many large complexes at distances up to 28 km. The distance-weighted emissions plots also show that the highest 25% of the emission rates from the industrial complexes in the 24 km x 24 km domain around the Wallisville site lie in the southwest direction of the site. Only for the petrochemical production source, the CPF plot did not agree with the emissions plot very well in catching the high emissions from the sources to the east of the Wallisville site, probably because the probability of the winds blowing from that direction was low.
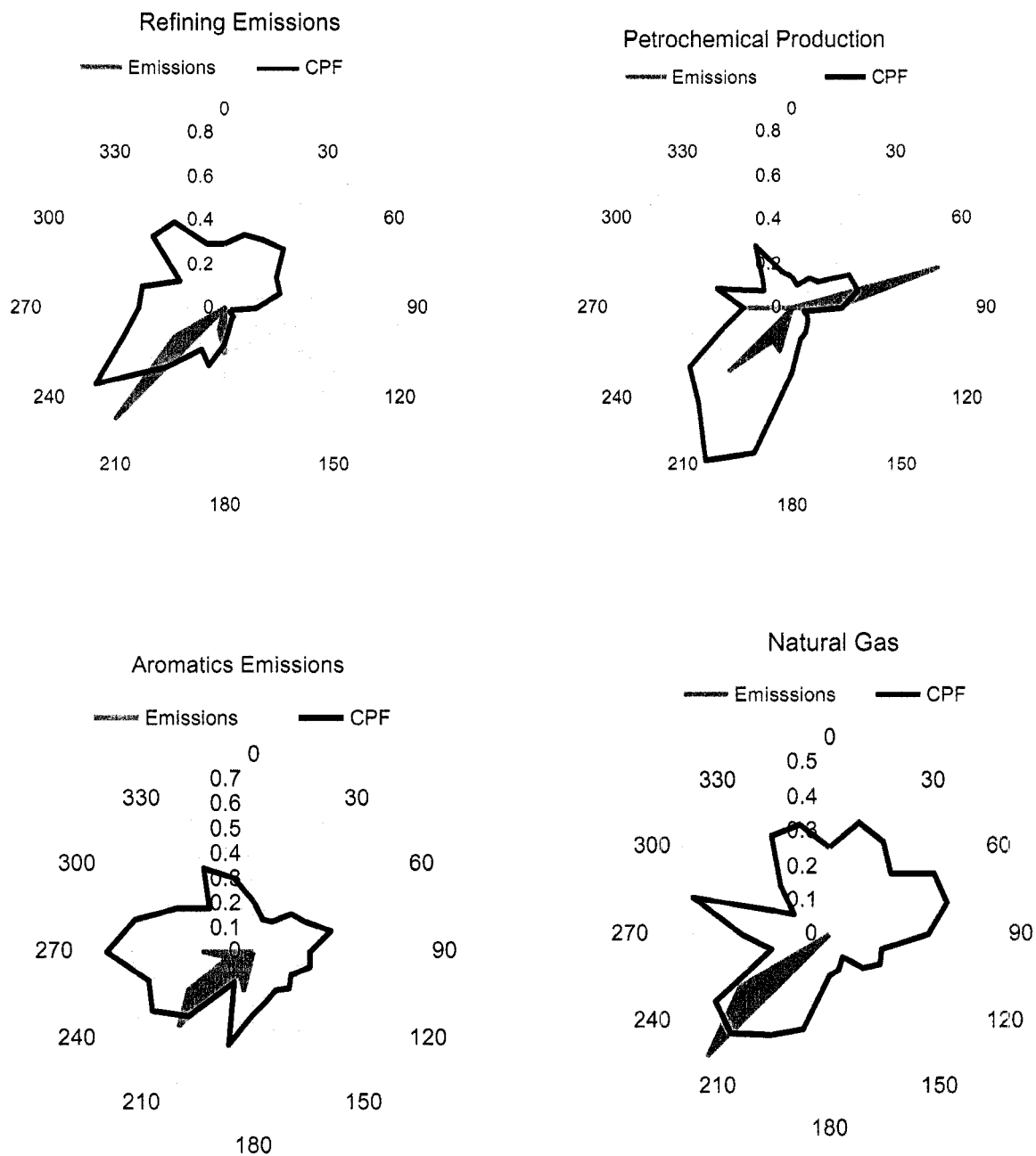
Figure 3.5. Comparison of polar plots of emission rates (left) and source contribution estimates (right) for Wallisville.

Figure 3.6 shows the results for the Lynchburg site. According to the overlaid

plots for petrochemical production emissions, high source contributions are strongly

associated with the winds from the 165°-210° sector and thus the plants located to the

south of the monitoring site are probably responsible for the high concentrations of VOCs

at this site. The emissions plots for the other sources mostly point to the southwest

direction, but CPF plots could also identify the emissions from the sources to the west of

the Lynchburg site, right around the HRM-3 site, which were underreported in the

inventory (emissions possibly from the facilities such as Chevron USA, Elf Atochem

North America, Crown Central Petroleum, GB Biosciences, Dynegy, Paktank,Valero

Refining, and Reichhold Chemicals).

At HRM-3, the wind directions that correspond to the high emissions were

consistent with the locations of the high emitting sources in the inventory, especially for

refining and petrochemical production sources (Figure 3.7). For aromatics and gasoline

emissions, the sources to the southeast of HRM-3 site could not be identified by the CPF

analysis, because the winds were blowing mostly from the west and southwest during that

period.

In general, the CPF plots showed greater range in direction than the

corresponding emissions plots, however the highest CPF values agreed well with the

directions of the high emission sources reported in the inventory.

Petrochemical Production

Refining Emissions

Aromatics Emissions

Natural Gas

Gasoline Evaporation
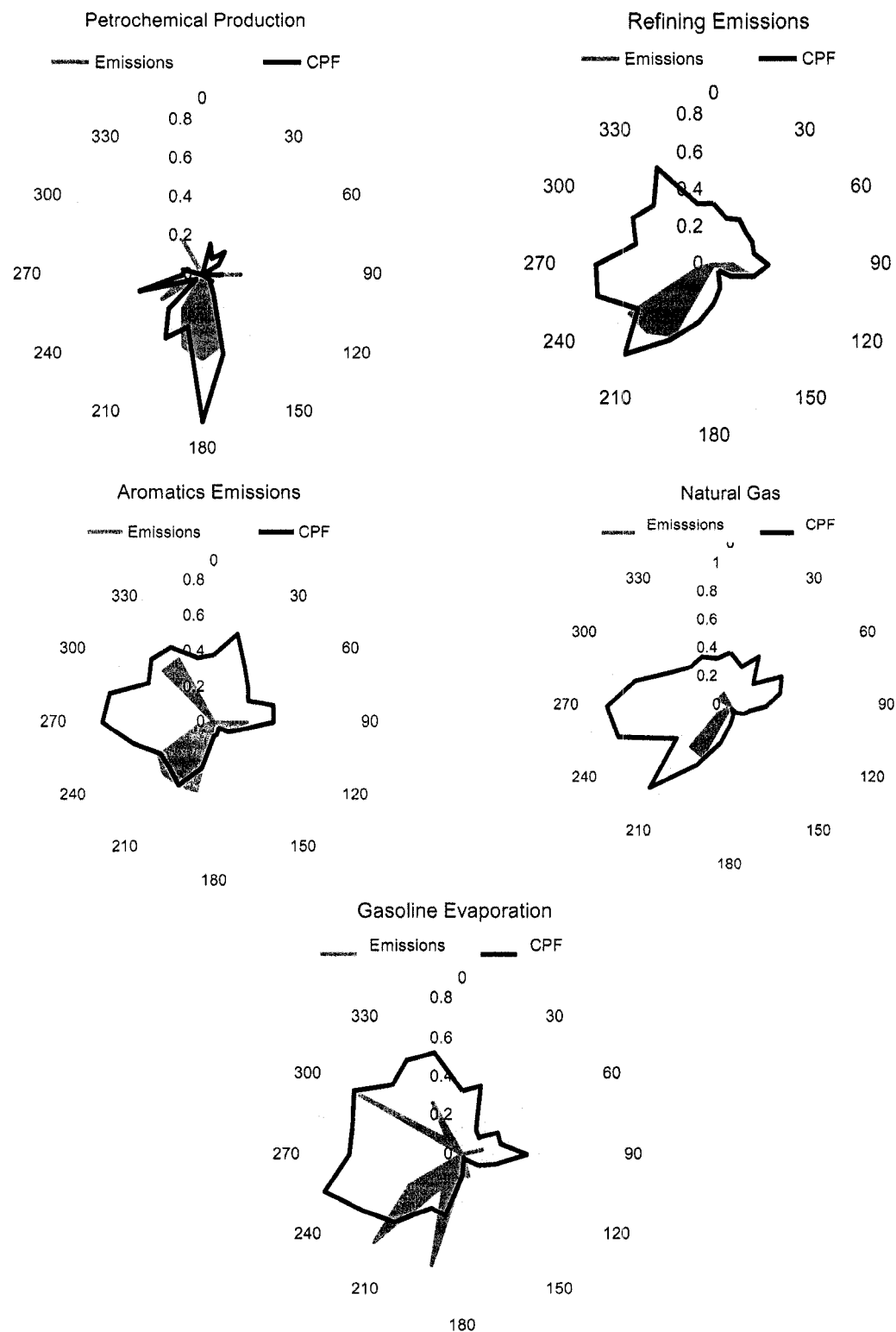
Figure 3.6. Comparison of polar plots of emission rates (left) and source contribution estimates (right) for Lynchburg.

Petrochemical Production

Refining Emissions

Aromatics

Natural Gas

Gasoline Evaporation
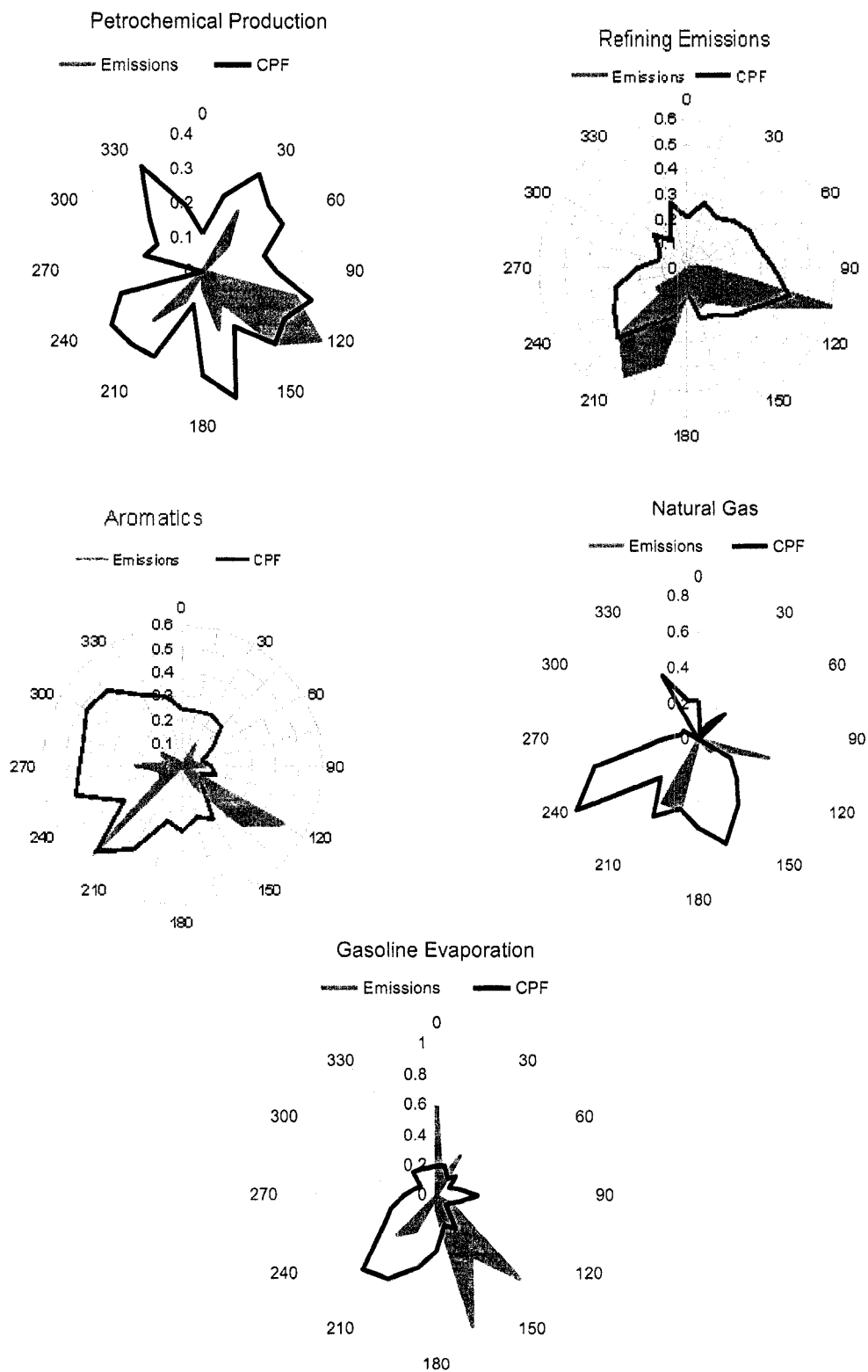
Figure 3.7. Comparison of polar plots of emission rates (left) and source contribution estimates (right) for HRM-3.

As a result of the analysis in Chapter 2, the most important contributions to VOC concentrations at each site have been found to be from petrochemical production and the refining operations, the rest of the discussion will mostly focus on these two source categories. Figures 3.8a and 3.8b show the relationships between the source contributions represented as CPF plots and the sources in the emissions inventory on a map of the Houston Ship Channel area enclosing the three monitoring sites. These figures also show the locations of VOC sources that emit predominantly refining gases (butanes, ethane, propane and pentanes) (Figure 3.8a) and petrochemical products ethylene and propylene (Figure 3.8b) at a rate exceeding 25 pounds per day.

Tables 3.3 through 3.8 list the largest sources of VOCs in the inventory associated with petrochemical production and refining operations together with their distances and the directions to the three monitoring sites. The distance and the direction of the point sources were calculated using the coordinates of the monitoring sites and the sources in the inventory. Tables 3.3 through 3.8 give the emissions of light olefins and refining gases in lbs/day, their distance-weighted emissions, and the percentage of these emissions in the total emissions of all VOCs from these industrial complexes.

Figures 3.8a and 3.8b should be examined together with Tables 3.3 through 3.8 in order to specify a few major sources responsible for the high VOC concentrations at the three monitoring sites. All three CPF plots for the refining emissions source in Figure 3.8a point to the same direction, 210°-250° direction, in addition to the 90°-120° direction at HRM-3. This corresponds to the directions of the same largest five sources in Tables 3.3, 3.4 and 3.5, while at the Lynchburg site these sources are present in a different order compared to the other two sites. These five sources account for 88% on average of the

total emissions from the refining complexes in the geographical area studied. Since HRM-3 is the closest one to these facilities, the distance-weighted emission rates that influence the concentrations at this site were the highest (315.80 lbs/day/km), Lynchburg was the second with 216.18 lbs/day/km and the farthest site, Wallisville, had the least effect of the emissions from these five industrial complexes (96.97 lbs/day/km). According to the emissions inventory, a high percentage of the emissions of all the industrial complexes representing the refinery source factor are refining gases (butanes, propane, ethane and pentanes) (Tables 3.3, 3.4 and 3.5). Therefore, both the location and the composition of the refinery source resolved by the receptor modeling were consistent with the emissions inventory.

The CPF plots for the petrochemical production factor point to slightly different directions at each site, and thus, to different point sources. At Wallisville, unlike the refining emissions, there are more petrochemical point sources in the vicinity of the site and in the 210°-240° direction, emitting high amounts of ethylene and propylene (Figure 3.8b). In the same figure, it can be observed that the ethylene and propylene concentrations at Lynchburg are strongly associated with the winds from the south. In fact, there are many large sources of these two light olefins to the south of the site. The olefin concentrations at HRM-3 seem to be influenced by the emissions from several directions since there are many sources surrounding the site in short distances. The listed sources in Tables 3.6, 3.7 and 3.8 account for 94% on average of the emissions of ethylene and propylene from all of the sources reported in the inventory. At Wallisville, 50% of the emissions were from sources in the direction of 210°-240°, and 40% of the emissions were from two facilities in 80°-90° direction, Chevron and Amoco Chemicals.

At HRM-3, the directions of the highest CPF values were consistent with the directions of the largest emitting sources of olefins in the region. 64% of the emissions were from the sources in the 140°-180° range, 17% were from 115°-125°, and 12% were from 210° - 230° directions. At Lynchburg, according to the emissions inventory, the facilities to the south of the site, in the direction of 165°-190°, emit 40% of the total emissions whereas around 47% of the emissions were from 240°-250° direction, dominated by one largest source in the inventory, Enron Methanol, located in that direction.
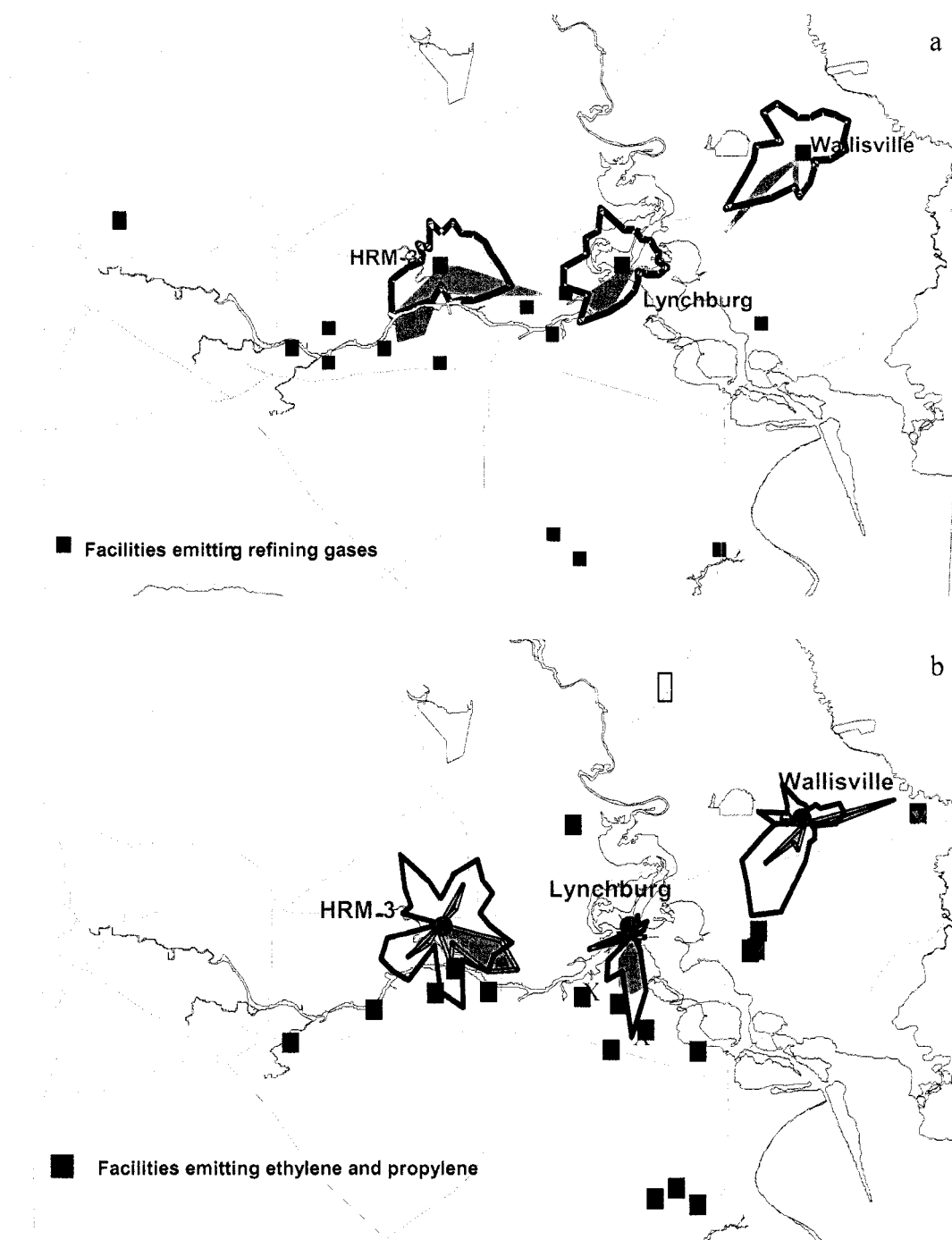
Figure 3.8. Location of the monitoring sites, Wallisville, Lynchburg and HRM-3 with respect to the Houston Ship Channel and nearby sources of refining emissions (a) and petrochemical production emissions (b).

Table 3.3. Major refining emission sources around Wallisville.

Facility Name	Distance-Weighted Emissions (lbs/day/km)	Total Emissions (lbs/day)	% Refining Gas* Emissions	Distance (km)	Azimuth (deg)
Shell Oil Co	29.158	507.473	88	18	232
Crown Central	27.751	660.820	82	24	242
Lyondell-Citgo Refining	18.643	488.572	81	26	243
Valero Refining Texas	11.591	321.551	88	28	246
Houston Fuel Oil Term.	9.826	134.373	72	13	235
Exxon Mobil Pipeline	3.760	132.550	87	35	199
Oil Tanking Houston	2.411	38.266	84	16	239

*Ethane, propane, butanes, pentanes

Table 3.4. Major refining emission sources around Lynchburg.

Facility Name	Distance-Weighted Emissions (lbs/day/km)	Total Emissions (lbs/day)	% Refining Gas* Emissions	Distance (km)	Azimuth (deg)
Shell Oil Co	74.553	507.473	88	7	229
Crown Central	49.112	660.820	82	13	249
Houston Fuel Oil	43.443	134.373	72	3	238
Lyondell-Citgo	30.778	488.572	81	16	250
Valero Refining Texas	18.291	321.551	88	17	254
Oil Tanking Houston	7.091	38.266	84	5	252
Exxonmobil Corp	5.353	39.486	81	7	106
Exxon Mobil Pipeline	5.332	137.012	87	27	186
Phillips Pipe Line Co	2.362	25.644	83	11	242

*Ethane, propane, butanes, pentanes

Table 3.5. Major refining emission sources around HRM-3.

Facility Name	Distance-Weighted Emissions (lbs/day/km)	Total Emissions (lbs/day)	% Refining Gas* Emissions	Distance (km)	Azimuth (deg)
Crown Central	119.538	660.820	82	5	211
Shell Oil Co	75.252	507.473	88	7	127
Lyondell Citgo Refining	65.433	488.572	81	8	222
Valero Refining Texas	37.656	321.551	88	8	235
Houston Fuel Oil Term.	17.919	134.373	72	7	103
Oil Tanking Houston Inc	7.222	38.266	84	5	112
Phillips Pipe Line Co	4.872	25.644	83	5	176

*Ethane, propane, butanes, pentanes

Table 3.6. Major petrochemical production emission sources around Wallisville.

Facility Name	Distance-Weighted Emissions (lbs/day/km)	Total Emissions (lbs/day)	% Ethylene+ Propylene Emissions	Distance (km)	Azimuth (deg)
Amoco Chemicals	97.841	598.914	98	6	87
Enron Methanol Co	78.673	1443.940	64	18	237
Chevron Chemical Co	40.602	251.134	87	6	85
Equistar Chemicals	35.663	521.754	99	15	213
Fina Oil & Chemical	24.101	340.732	91	14	220
Mobil Chemical Co	17.725	503.845	81	28	242
Millennium	10.219	142.673	81	14	211
Phillips Chemical	7.211	149.477	99	21	240
Exxon Chemical Co	6.755	7.755	97	8	196
Exxonmobil Pipeline	5.486	37.420	100	7	197

Table 3.7. Major petrochemical production emission sources around Lynchburg.

Facility Name	Distance-Weighted Emissions (lbs/day/km)	Total Emissions (lbs/day)	% Ethylene+ Propylene Emissions	Distance (km)	Azimuth (deg)
Enron Methanol Co	184.772	1443.940	64	8	242
Equistar Chemicals	86.400	521.754	99	6	174
Fina Oil & Chemical	78.273	340.732	91	5	190
Amoco Chemicals	37.421	598.914	98	16	66
Mobil Chemical Co	27.920	503.845	81	18	248
Millennium	24.618	142.673	81	6	168
Chevron Chemical Co	15.511	251.134	87	16	65
Phillips Chemical	14.475	149.477	99	10	249
Exxon Chemical Co	8.175	9.175	97	6	101
Montell Usa Inc	7.607	112.728	100	15	170
Equistar Chemicals	6.341	50.225	94	8	331
Amoco Chemical	3.373	30.970	47	9	254

Table 3.8. Major petrochemical production emission sources around HRM-3.

Facility Name	Distance-Weighted Emissions (lbs/day/km)	Total Emissions (lbs/day)	% Ethylene+ Propylene Emmision	Distance (km)	Azimuth (deg)
Enron Methanol Co	297.545	1443.940	64	5	142
Mobil Chemical Co	51.978	503.845	81	10	225
Equistar Chemicals	48.182	571.979	99	12	120
Phillips Chemical	38.628	149.477	99	4	175
Fina Oil & Chemical	33.691	340.732	91	10	115
Amoco Chemicals	23.596	598.914	98	26	75
Crown Central	13.075	14.075	69	6	209
Millennium	11.294	142.673	81	13	117
Amoco Chemical	10.760	30.970	47	3	157
Chevron Chemical Co	9.844	251.134	87	26	75
Equistar Chemicals	5.453	50.225	94	9	41

96

3.3.4. Comparison of the source attribution with the emissions in the inventory

Distance-weighted VOC emissions, converted to ppbC units according to

Equation 3, from each point source in the domain of each receptor site were averaged for

each factor and plotted in pie charts (Figures 3.9a, 3.10a, 3.11a). In Figures 3.9b, 3.10b,

and 3.11b, the average source contribution estimates from PMF calculations for each

factor for the whole modeling period were also plotted for the comparison with the

emission inventory. Finally, the ratios of average source contribution estimates from

PMF calculations to the emissions reported in the inventory were calculated for each

factor and presented in Figures 3.9c, 3.10c and 3.11c.

At Wallisville, the inventory is dominated by the petrochemical production and

refining emissions while it highly underestimates the natural gas emissions. The ratio of

the contribution of refinery factor to the emissions from the refining gases in the

inventory is 2.23, for petrochemical production factor 0.98, for aromatics 1.06 and for

natural gas factor 112.38.

At Lynchburg, natural gas emissions make up only 0.2% of all emissions in the

inventory whereas PMF estimated the fraction of natural gas emissions as 17%. Other

than natural gas, the percent distribution of the contribution of VOC emission sources is

in agreement with that of the inventoried sources. The ratio of source contributions for

refining factor to emission inventory value is 1.58, for petrochemical production factor

1.43, for aromatics 2.89, for evaporative gasoline 1.80 and for natural gas factor 167.08.

At HRM-3, the composition of VOC emissions is in agreement with both in the

inventory and in the PMF results (Figures 3.11a, 3.11b). The fraction for refining and

gasoline emissions were approximately the same, however, the contribution of petrochemical production was underestimated in PMF results. The effect of natural gas emissions from the sources around this site was much higher than the other sites. The ratio of source contributions for refining factor to emission inventory value is 1.62, for petrochemical production factor 0.60, for aromatics 1.04, for evaporative gasoline 1.78 and for natural gas factor 27.81.

All these results suggest that VOC emissions from point sources at all sites are dominated by refining and petrochemical production sources. Refineries contribute between 29-38% of the VOC point source emissions in the inventory, and petrochemical production facilities contribute between 20-52%. The emission inventory for refining emission sources located in the 24km by 24km domain around Wallisville site was underestimated by a factor of 2.2, around HRM-3 and Lynchburg by a factor of 1.6. Emission inventory for petrochemical production emission sources was underestimated by 1.4 for Lynchburg while the PMF results were underestimated by a factor of 1.6 at HRM-3. The contributions of petrochemical production emissions both in the inventory and in the PMF results for Wallisville were about the same. Evaporative gasoline emissions represented by the emissions of pentanes and butanes contributed 25-29% of the VOC point source emissions and were also underestimated by a factor of 1.8 at HRM-3 and Lynchburg. Natural gas emissions contributed between 0.2-1% of the total VOC emissions in the inventory and therefore were highly underestimated at all sites, especially at Wallisville and Lynchburg. This significant underestimation can probably be explained by the accumulation mass due to the longer lifetime of ethane and propane or because of area sources from small leaks in the natural gas distribution system in the

region. Because of varying rates of oxidation of the vapor-phase organic compounds, some highly reactive species, such as the light olefins, are depleted in a more rapid rate than less reactive compounds. With transport of emissions from distant sources, atmospheric oxidation removes the reactive species and the remaining fraction contains mostly the less reactive species, such as ethane and propane (*Gouw et al.*, 2005). Therefore, having longer lifetimes, ethane and propane tend to accumulate in the atmosphere and may cause an overestimation of natural gas emissions which is determined based on the concentrations of less reactive alkanes.

(a)

(b)

Emissions Inventory

PMF
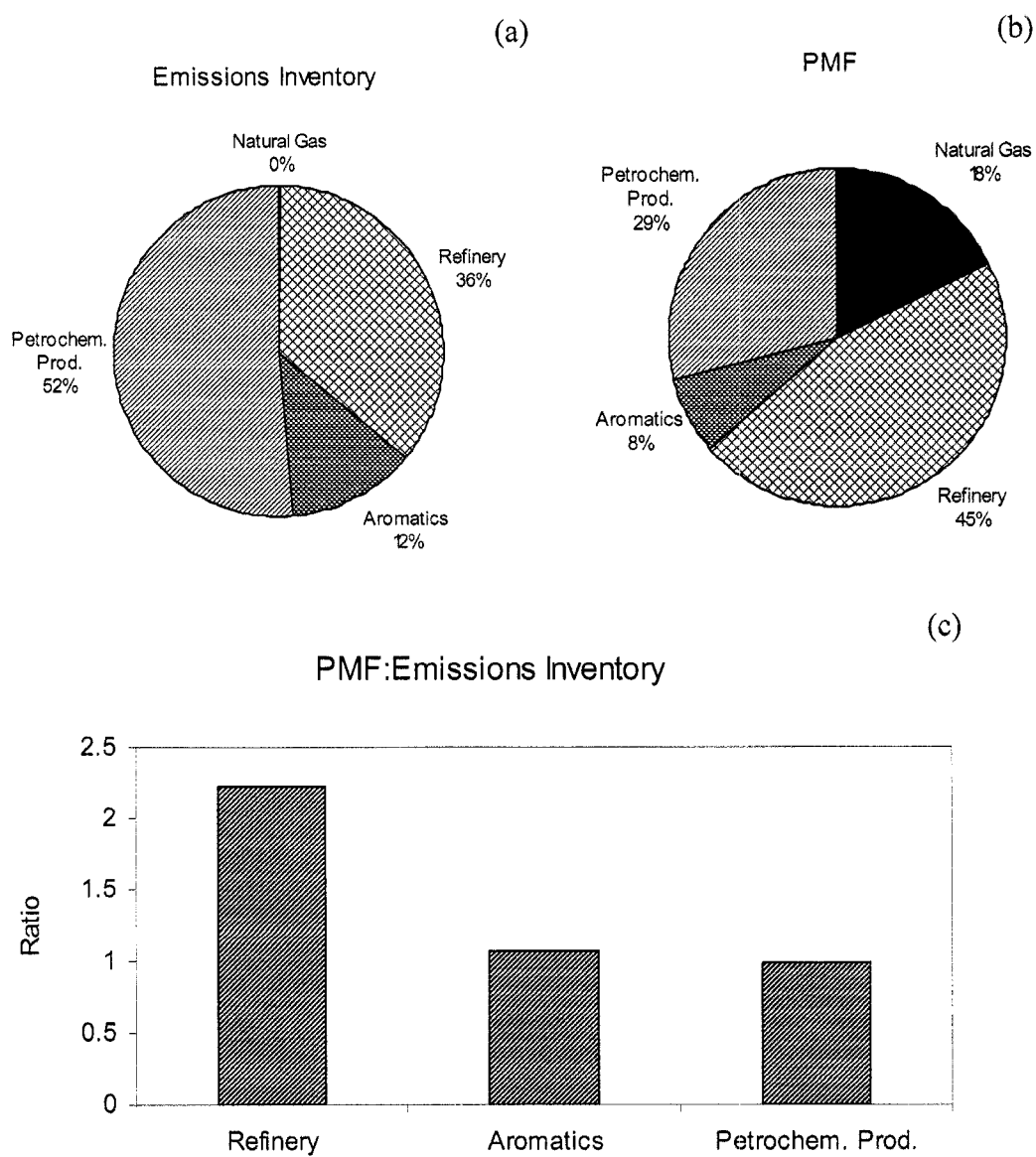
Figure 3.9. Comparison of PMF results with the emission inventory for Wallisville data.
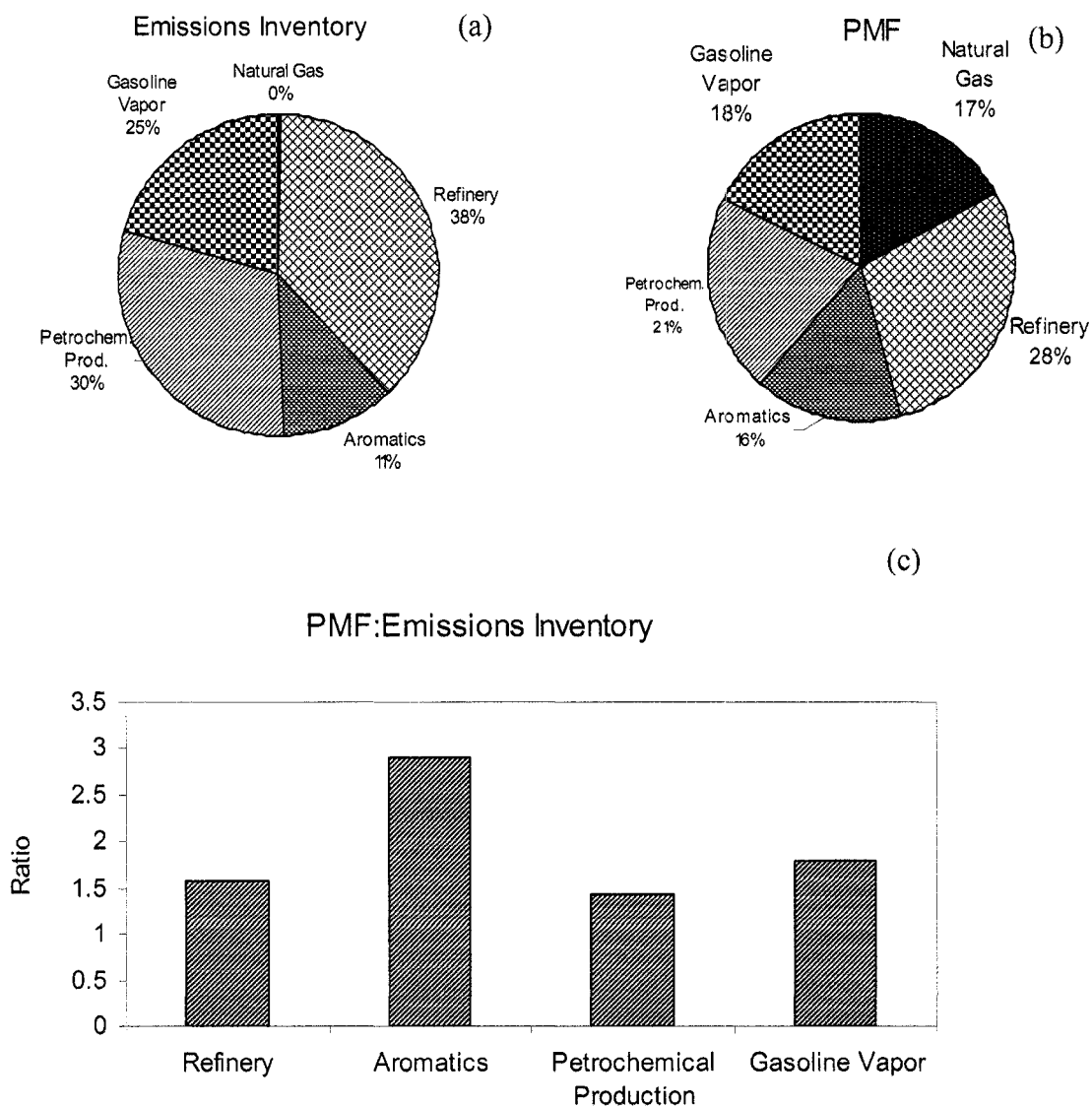
Figure 3.10. Comparison of PMF results with the emission inventory for Lynchburg data.
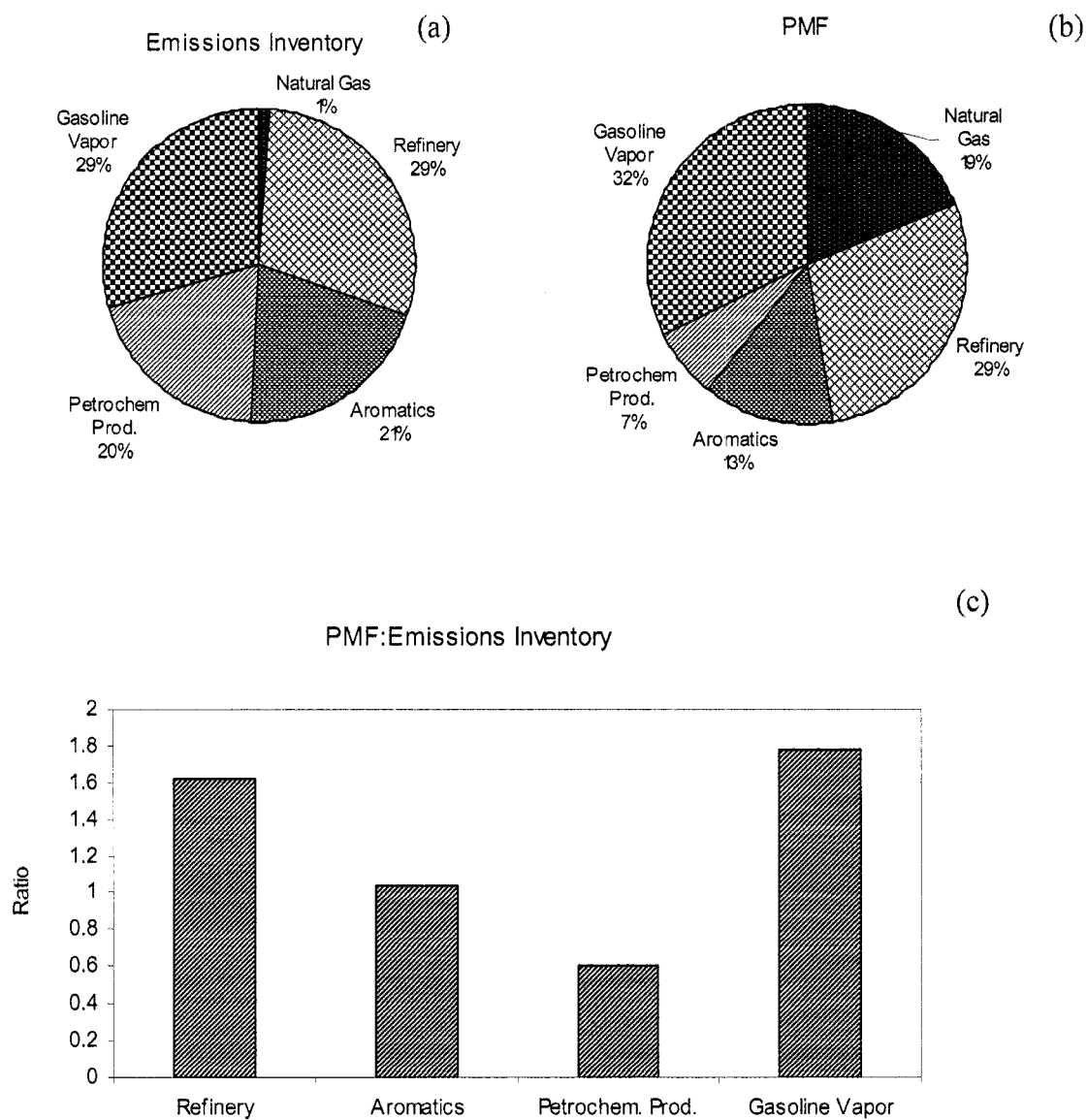
Figure 3.11. Comparison of PMF results with the emission inventory for HRM-3 data.

Henry et al. (1997) performed a similar analysis using SAFER multivariate receptor model on VOC data at one monitoring site in Houston Ship Channel, and their model could resolve three industrial source factors. They used the relationship between the wind directions and the source contributions to identify the location of these sources. Their observational based methods could only identify the location and compositions of a small nearby chemical plant. They concluded that the composition and the location of the sources as deduced from the ambient data are not consistent with the reported industrial emissions.

Estes et al. (2002) compared VOC:NOx ratios at and around seven monitors in the Ship Channel area and calculated discrepancies from 0.95 to 12 for ethene and 1.9 to 16 for propene between ambient and inventory ratios. *Jolly et al.* (2004) used a similar approach including only the point source emissions and determined the ranges of discrepancies that fall inside the ranges of the study of *Estes et al.* (2002). The present study used a different approach comparing the contributions of VOC point sources to the VOC levels at the monitors with the inventoried emissions of the same source categories. Since the comparison has been done based on the source types rather than different VOC classes in the present study, the ratios of PMF source contributions to emission inventory can be compared to the results of the earlier studies. The ratio for the petrochemical production source, containing primarily ethene and propene emissions was from 1.9 to 3.4 at the three sites in this study, which is in the range of the earlier two studies but more consistent between the monitoring sites.

Brown et al. (2004) focused on top-down evaluation methods using surface and aloft (via aircraft) ambient data available for Houston/Galveston area. The integrated

results from surface and aloft data analysis showed that total VOC as identified using VOC:NOx ratios was underrepresented in the emission inventory by a factor of 2 to 10. Olefins, and specifically propene, are underestimated in the inventory by a factor of 2 to 5. Total aromatics were also underrepresented by a factor of 2 to 5. Total paraffins, especially ethane and propane were also underestimated in the emission inventory by a factor of 3 to 8. However at the Deer Park site pentanes tended to be over represented in the inventory. Their results are consistent with the results of the present study although a different approach is applied in evaluating the accuracy of the emission inventories.

There are some uncertainties in these calculations that need to be mentioned. First of all, emissions outside the domain of 24km x 24km around the monitors were not included in the calculations for the comparison of the emissions inventory and the source contributions.

Secondly, the loss of emissions due to reactions was not accounted for, since daily emissions were used and hourly ambient concentration data for the whole day were used in PMF calculations. Again for the same reasons, the effect of variable mixing heights were not eliminated or minimized, because mixing heights are relatively low in the early morning hours.

Another area of uncertainty is that it was assumed that winds from a specific direction bring air solely from that direction, without considering the changing wind direction. However, in reality, wind trajectories are rarely straight. This might be the reason for the discrepancy between the source contributions and emissions in some wind sectors adjacent to each other (e.g. HRM-3 in Figures 3.8a).

One further point of consideration is that the point source emission inventory data comes from the companies, and the reported VOCs are sometimes only partly speciated or not speciated at all. As a result, and additional consideration is that only speciated VOCs are included in the emission inventory.

Finally, for some of the point sources in the inventory, no information was available regarding the source type, source classification codes or volumetric flow rates. Thus, those sources were not included in the calculations and so in certain wind directions there might be some other sources of which the emissions were not accounted for.

3.3.5. Nighttime Data

Section 2.4.5 reported the application of positive matrix factorization model on the nighttime VOC data in July 2003 at Wallisville and Lynchburg. The data between the hours of 9pm and 6am local time were used to minimize the effect of photochemical reactions when calculating the source contributions. When the loss of emissions due to photochemical reactions and the effect of variable mixing heights were accounted for, PMF had resolved different factors at both locations than the factors resolved from the all-day samples. In order to evaluate the effect of emission inventories more accurately, the source contributions calculated using nighttime data were used together with wind directions to compute conditional probability function for the factors that are comparable to the sources in the inventory. Figures 3.12 and 3.13 shows the comparison of the CPF plots for nighttime data with the emissions plots from Figures 3.5 and 3.6. From these figures, it is clear that daytime CPF plots show greater range in direction than

corresponding plots at night and nighttime CPF plots agree better with the emissions plots. This can be interpreted as that the effect of photochemical loss due to the reactions in the atmosphere and also the lower mixing height in the early morning hours increases the reliability of the modeling results.
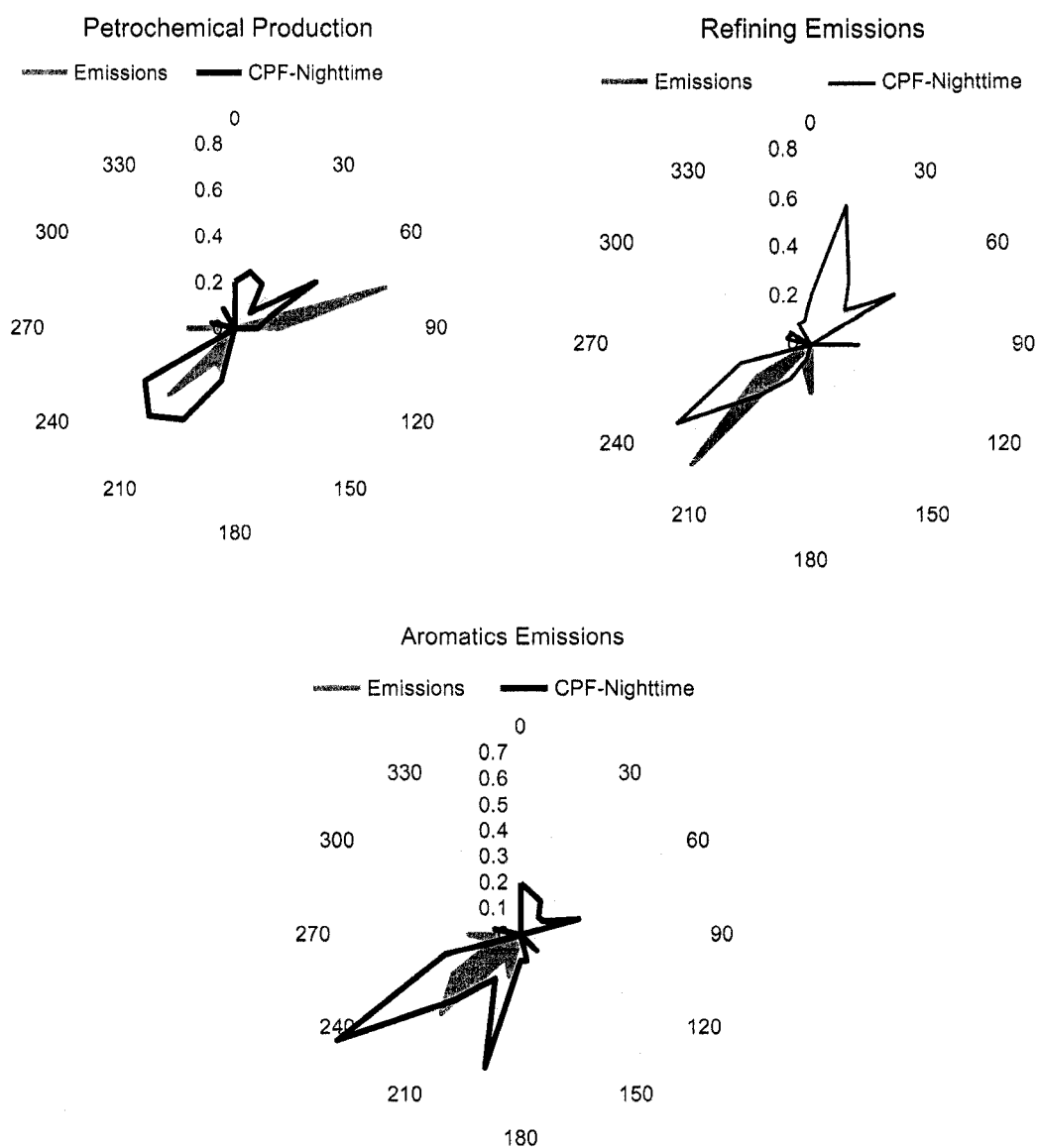
Figure 3.12. Comparison of polar plots of emission rates (left) and source contribution estimates (right) for nighttime data at Wallisville.

Petrochemical Production

Emissions   CPF-Nighttime

```
          0
      0.6
330          30
      0.4
300               60
      0.2
270                    90

240               120

   210        150
```

Refining Emissions

Emissions   CPF-Nighttime

```
          0
         1
330    0.8    30
      0.6
300          60
      0.4
70    0.2          90

240               120

   210        150
        180
```

Natural Gas

Emisssions   CPF-Nighttime

```
          0
         1
330    0.8    30
      0.6
300          60
      0.4
      0
270               90

240               120

   210        150
        180
```
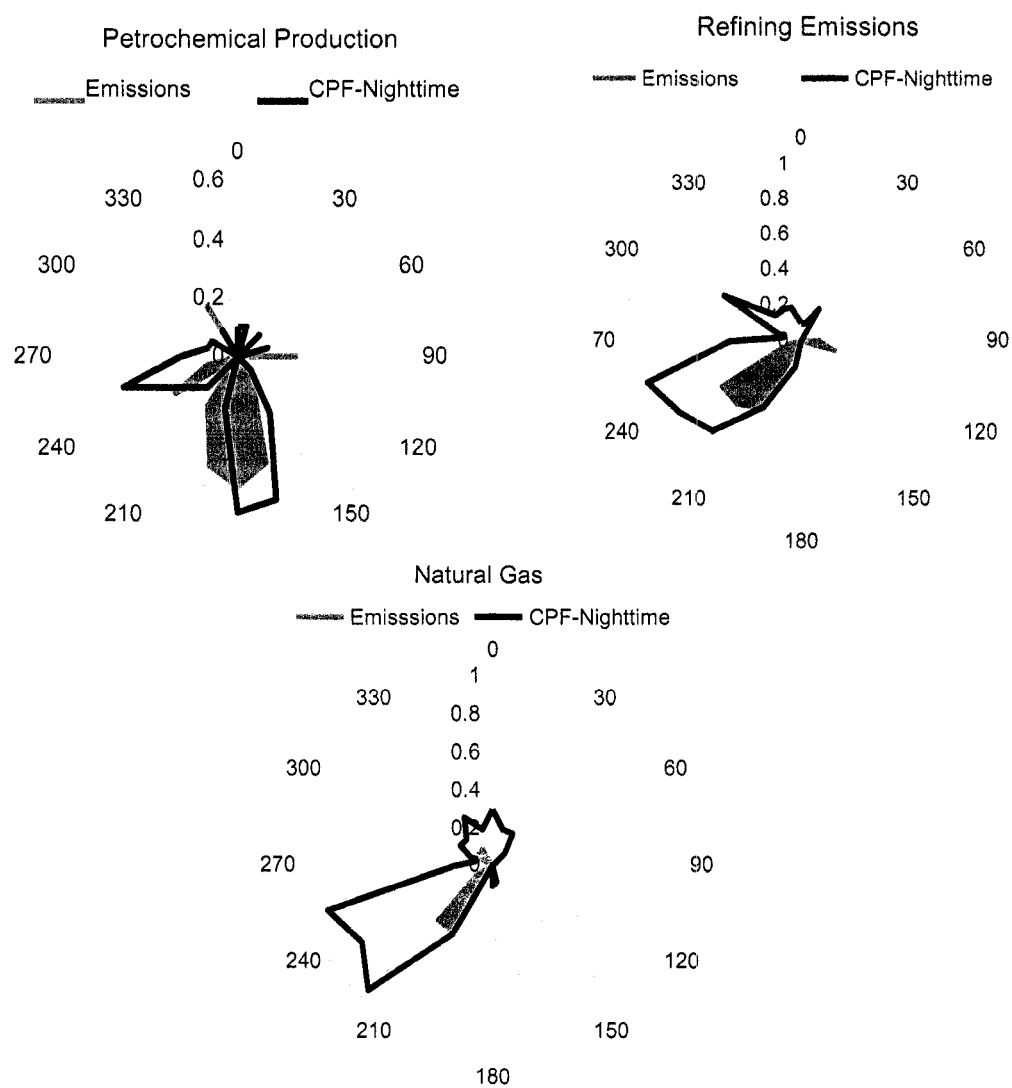
Figure 3.13. Comparison of polar plots of emission rates (left) and source contribution estimates (right) for nighttime data at Lynchburg.

3.4. Event Emissions

In this section, the upset emissions from the industrial facilities in the Harris County, Houston, TX were studied. Since light olefins, especially ethylene and propylene play the most important role in rapid and efficient ozone formation, and since roughly 40% of the total mass reported in the event data base was HRVOCs (*Murphy and Allen*, 2005), the focus of this section was directed to the emissions from the petrochemical plants mostly emitting light olefinic compounds (*Buzcu and Fraser*, 2006).

The event emissions data is available online for the events starting from January 31, 2003 (*TCEQ*, 2004). Since the original source apportionment analysis (*Buzcu and Fraser*, 2006) was performed on the VOC data for the period of June 1 - October 31, 2003, the event emissions for that period only were studied in this section.

Event emissions are of concern because they release emissions much greater than regular amounts in a very short time periods. Of all the events studied in this analysis, 75% lasted less than 24 hours; 62% emitted 100-1,000 lbs; 16% emitted 1,000-10,000 lbs; and 3% emitted more than 10,000 lbs of ethylene or propylene.

A total of 33 entities in Harris County reported events with ethylene and propylene emissions between June 1 and October 31, 2003. Of these entities, 67% are classified in the category of "Industrial Organic Chemicals", and the rest are plastic material manufacturers, refineries, and pipelines.

Time series for the event emissions of ethylene and propylene were developed following the procedure suggested by *Murphy and Allen* (2005) by determining the emission rates during each of the 1-h time blocks (Figure 3.14). The average emission

rate from all the facilities in Harris County has been calculated as 942 lbs per hour from

the 2000 TCEQ emissions inventory and plotted as a horizontal line in Figure 3.14. The

event emissions exceeded the average value 47 times during the period of 5 months

(June-October, 2003). The highest rate was 16,334 lbs/hour, which is 17 times the

average value. In 14 instances, the emission rates were 2-4 times the average emission

rate, and for the rest, the rates of the event emissions were very close to the average rate

of 942 lbs/hr.
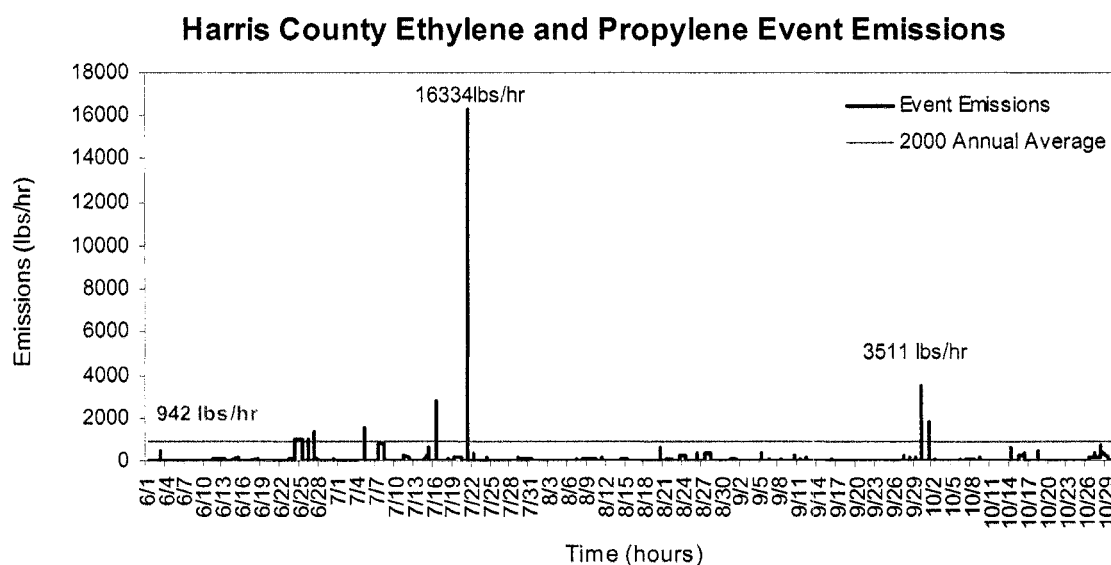
Figure 3.14. Time series of the event emissions of ethylene and propylene for the period June-November, 2003 for Harris County, TX compared to the 2000 annual average rate.

The total of the ethylene and propylene event emissions over the five month

period were 179,863 lbs. Ethylene emissions (total of 116, 576 lbs) were more frequent

and of greater magnitude than propylene emissions (total of 63,287 lbs). Although the

total ethylene and propylene mass emitted from the facilities reporting event emissions is

only 5% of the total ethylene and propylene emitted from all facilities in Harris County,

single event emissions can affect the VOC concentrations in the region significantly for short amounts of time.

Murphy and Allen (2005) demonstrated that event emissions of HRVOCs have the potential to affect the ozone formation significantly, given the suitable atmospheric conditions using ambient data and photochemical modeling for an episode. Our goal is to investigate if the event emissions can explain the episodes of high source contributions from the petrochemical facilities to the ethylene and propylene concentrations. For this purpose, the impact of all of the reported event emissions during the summer of 2003 on the source contributions of petrochemical emissions at three receptor sites was investigated (see Chapter 2). In this analysis, wind trajectory data and other atmospheric parameters were also utilized by performing dispersion calculations of the plume originating from the source of emissions for the entire period of the event emissions. The three-dimensional HYbrid Single-Particle Lagrangian Integrated Trajectory (HYSPLIT 4.7) model (February 2005 version; *Draxler and Rolph*, 2003) was used to reconstruct the air parcel movement and to calculate the concentrations of the ethylene and propylene for each hour for the duration of the event. Dispersion calculations were performed on a concentration grid with 0.01-deg resolution and with a span of 0.5 deg from the center of the grid, which is the emission source. The computations were performed using archived meteorological data set (EDAS 80 km).

The computation start time must be entered to HYSPLIT in UTC (Universal Time). To convert Central Standard to UTC, 6 hours should be added to the local time. For example for a model run starting at 14:00 (2 pm) Central Standard Time (CST) is

entered as 20 UTC the same day. For a run starting at 19:00 (7 pm) CST is entered as 1

UTC the next day (consider the day when converting start times).

Since the amount of the VOCs released from the facilities were reported in

pounds (lb), the concentrations calculated by the dispersion model were in pounds per

cubic meter (lb/m^3). These concentrations were converted to ppbC units in order to be

able to make the connection with the source contributions using Equation 5:

$$ppbC = No.\,of\,Carbons \times \frac{1}{MW_{VOC}[g\,/\,mol]} \times 1000 \times (C\left[\frac{lbs}{m^3}\right] \times 454000\frac{mg}{lbs}) \times R\left[\frac{L.kPa}{mol.K}\right] \times T_{air}[K] \times \frac{1}{P_{air}[kPa]} \quad (5)$$

where C is the concentration of olefins in lbs/m^3, R is the universal gas constant (8.3144

L.kPa/mol.K), T_{air} is the ambient temperature in K, P_{air} is the air pressure (101.325 kPa =

1 atm), and MW is the molecular weight of the compound (MW$_{ethylene}$=28,

MW$_{propylene}$=42)

The modeling of 163 events emitting ethylene or propylene from June 1 to

October 31, 2003 from the 33 facilities in Harris County revealed that 42% of these event

emissions did not reach any of the study sites because of the direction of the wind. The

event plume passed over HRM-3 in 44% of all the events; the percentage was 38% for

Lynchburg and 35% for Wallisville. For 63% of the event emissions that reached the

study sites, the modeled concentrations of ethylene or propylene at the sites were low

enough that they were unlikely to have any additional influence on the source

contributions calculated at those sites. These low concentrations are due to the distance

between the receptor sites and the emission sources and the dilution of pollutants on their

way to the receptor sites. For the events that last several hours, or days, the changing wind direction, speed, and other atmospheric parameters disperse the pollutants in multiple directions in lower concentrations, whereas the emissions from the shorter-lasting events reach the receptors more quickly resulting in higher pollutant concentrations at the receptors if the wind blows in that direction.

For 3-5% of the events, the modeled emissions and the source contributions could not be compared due to the lack of the ambient concentration data. The influence of the modeled event emissions on the calculated source contributions could be detected for 26% of the events reaching the Wallisville site. This ratio was much lower for HRM-3 and Lynchburg sites with 7% and 5%, respectively, because the petrochemical production factor was resolved in 19% of the 21 weeks at Lynchburg and 45% of 22 weeks at HRM-3 whereas it was resolved in 90% of 21 weeks at Wallisville (*See Section 2.4.4*). Thus, there were more data available to compare the modeled event emissions and the source contributions for Wallisville site. However, at most times the quantity of the source contribution data was not sufficient for this type of a comparison at the other two sites.

Some examples of these results are presented in Figures 3.15-3.17. Figure 3.15 represents the impact of an emission event on the source contributions of the petrochemical production at Lynchburg and Wallisville sites. Starting on July 29, 2003 11:23 PM, 2,013 lbs of ethylene was released from a chemical plant (Sunoco R&M Bayport Polypropylene) for 41 hours. The increase in the source contributions corresponded to the times when the modeled concentrations of ethylene reached a maximum at around 11 PM on July 30 at Lynchburg (Figure 15a) and 2 AM on July 31 at Wallisville (Figure 3.15b). The position of the plume at these times was shown in Figures

3.15c and 3.15d. This event did not influence the ethylene concentrations at HRM-3 site, because the plume did not go to that direction during the release.

At Lynchburg, from August 8 through the end of the sampling period, no petrochemical production factor was resolved. In fact, except two events, emissions were not significant enough to have an influence on the ethylene and propylene concentrations. Those two events included 12,000 lbs of propylene emissions that were released from BP Basell on August 27, 2003 for 24 hours and 217 lbs of propylene emitted from ExxonMobil on September 12 for 1 minute. The 1-hour averaged concentrations of all of the modeled emissions were plotted in Figure 3.16a, where these two events dominated the time series and there is no source contributions calculated for the whole period. Figures 3.16b and 3.16c illustrate the movement of the propylene plume from these two facilities directed towards Lynchburg site. Interestingly, the time series of the ambient measured concentrations of ethylene and propylene did not show any increase due to these event emissions on the same days when the event emissions reached the site as shown in Figures 3.16d, and 3.16e.

Finally, Figure 3.17 shows an event that caused an increase in the source contributions at HRM-3 on September 30, 2003. The ethylene emissions of 194 lbs released from Equistar Channelview Complex on September 30 at 9:25 PM for 6 minutes were transported to HRM-3 site upon release. Although the emitted amount is relatively small, the instantenous release of the emissions, the proximity of the site to the source, and the wind direction helped the emissions reach the site very fast and in high amounts.
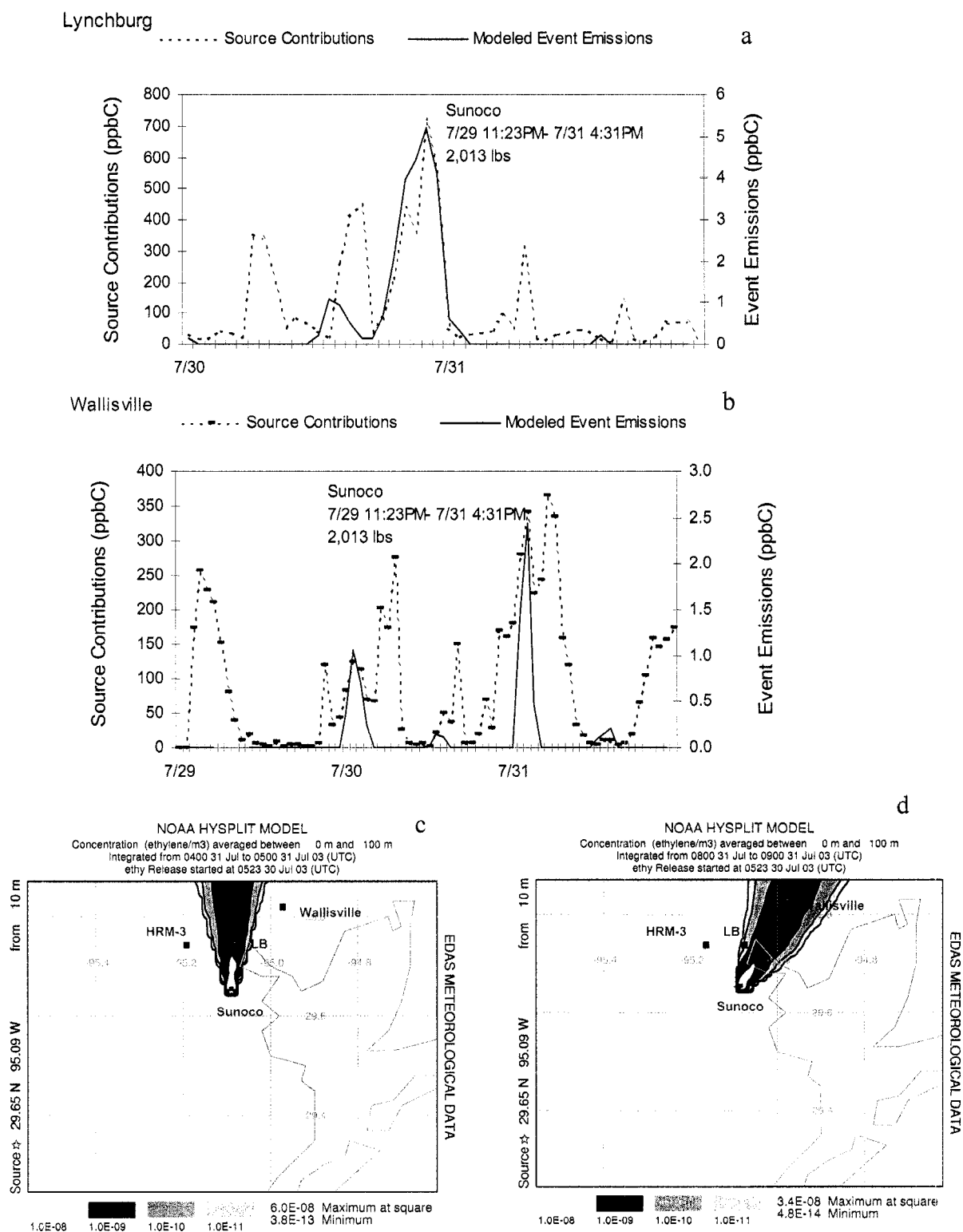
Figure 3.15. The impact of the modeled event emissions from Sunoco Plant on the source contributions at (a) Lynchburg and (b)Wallisville, and the results of the dispersion model for (c) 4-5 UTC and (d) 8-9 UTC.
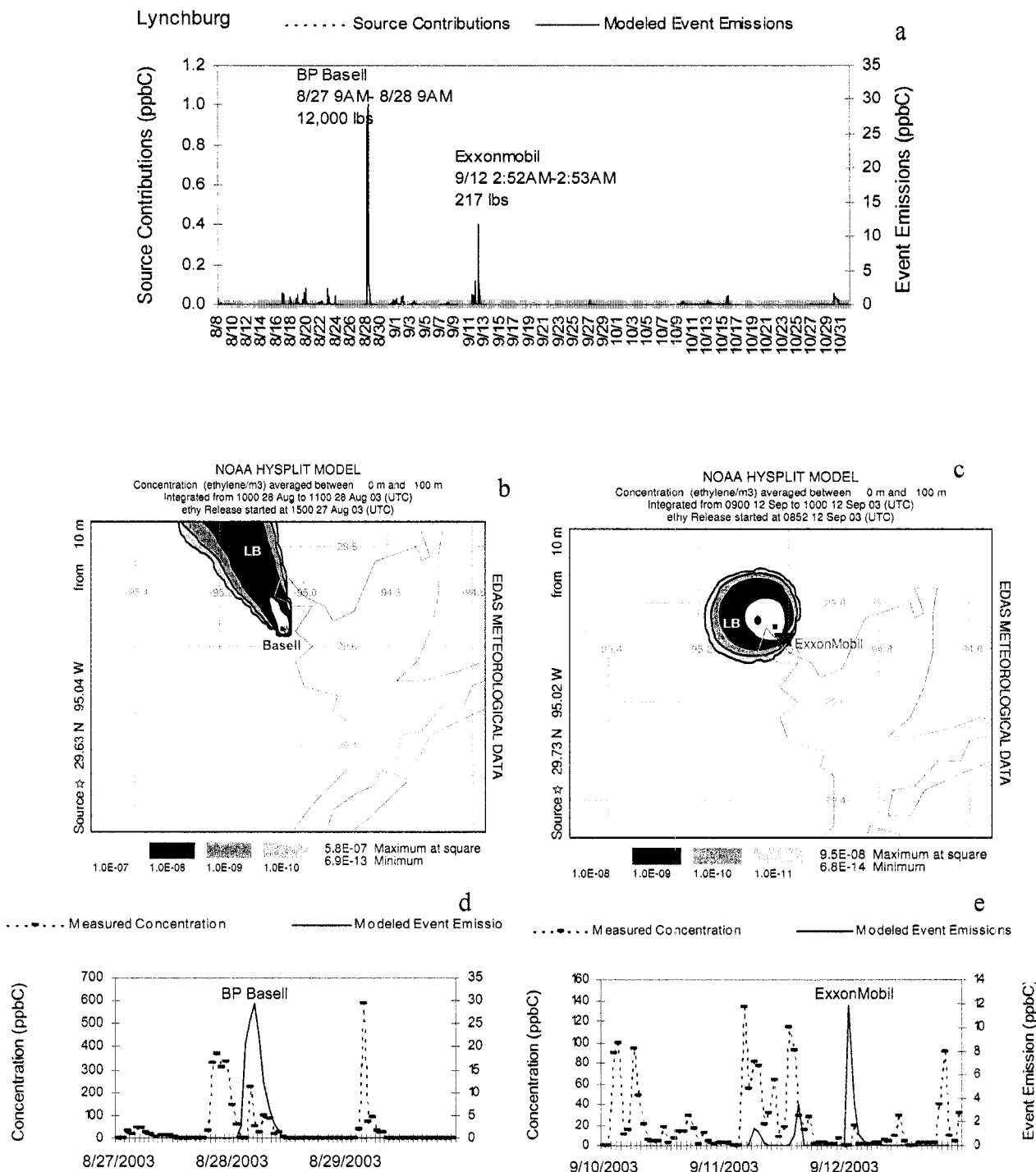
Figure 3.16. The time series of the modeled event emissions from BP Basell and ExxonMobil and source contributions at (a) Lynchburg and the results of the dispersion model for the emissions from (b) BP Basell and (c) ExxonMobil. Measured ethylene and propylene concentration compared with the event emissions for (d) BP Basell and (e) ExxonMobil events.
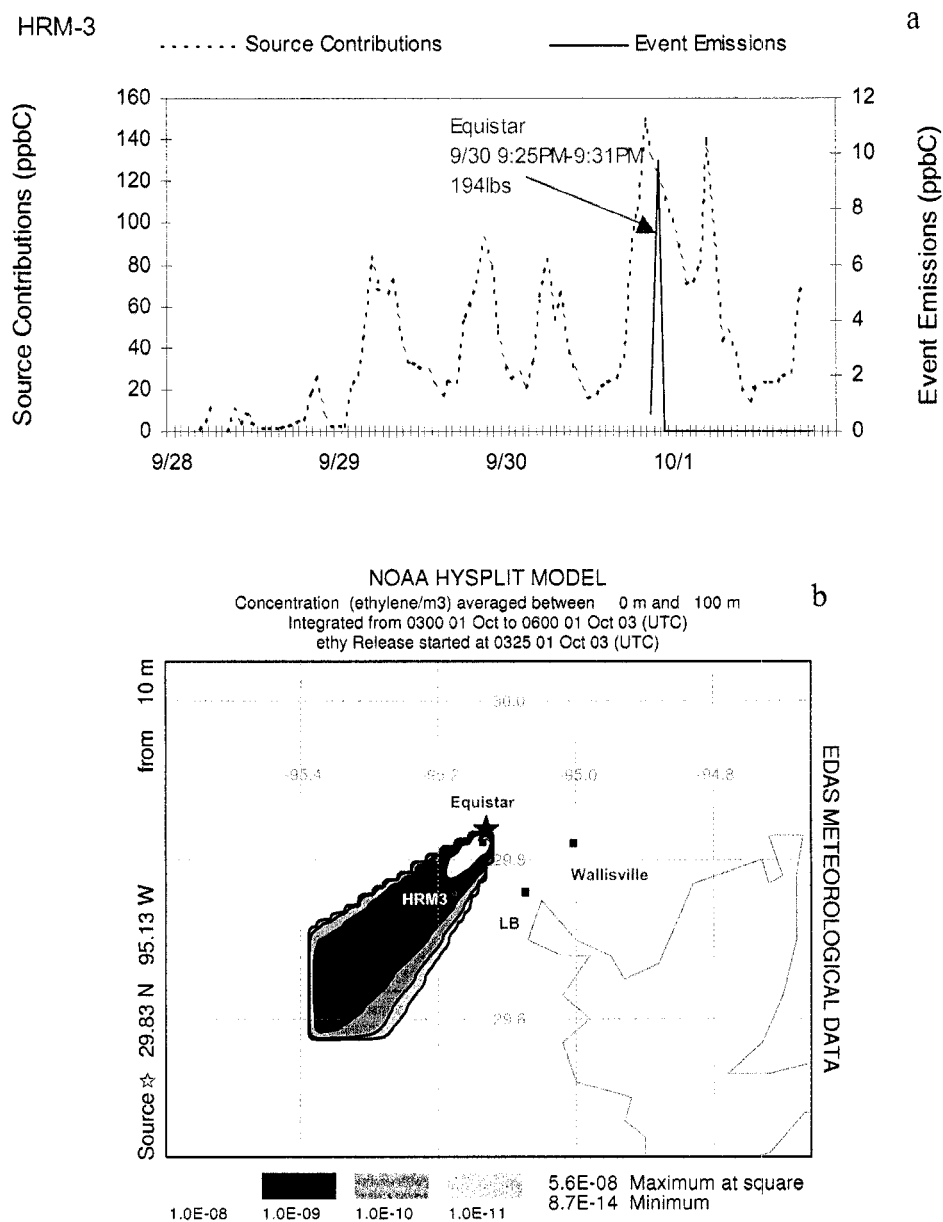
Figure 3.17. The impact of the modeled event emissions from Equistar on the source contributions at HRM-3 (a), and the results of the dispersion model (b).

3.5. Conclusions

This chapter first studied the correlations between the calculated hourly source contributions and measured ozone concentrations separated by a number of hours to present evidence supporting the importance of alkanes and alkenes to ozone formation in the Houston atmosphere. The results of this analysis confirmed that very high contributions of the dominant sources of VOCs such as refineries and petrochemical plants during times that are favorable to ozone formation led to peak ozone concentrations at the three sites.

The source contributions calculated in Chapter 2 were then compared to the emissions of volatile organic compounds in Houston, TX. In general, the composition and the location of the sources developed from the source apportionment results were consistent with the reported industrial emissions, although some small discrepancies were found as mentioned in the discussion. We observed that the results for the nighttime data showed a better agreement with the emissions data indicating that minimizing the effect of photochemical loss due to the reactions in the atmosphere and also the lower mixing height in the early morning hours increased the reliability of the modeling results.

Relative contributions of the important sources of VOCs calculated by PMF were then compared with speciation information included in the corresponding emission inventory. Measurements and source apportionment calculations established that the ethylene and propylene emissions and thus the contribution of petrochemical facilities, to VOC levels at Lynchburg site were higher than the inventoried emissions. For this reason, inventoried emissions used as inputs to photochemical models are unlikely to reproduce ozone concentrations accurately. Compared to the PMF results, the inventory

underestimated the petrochemical production emissions and aromatics emissions at Lynchburg. However, both types of emissions were consistent with source apportionment results at Wallisville and HRM-3 except petrochemical production contributions were underestimated in the PMF results. Emissions of refining gases in the inventory were underestimated for each site. The fractional contribution from natural gas emissions was two orders of magnitude higher than the inventoried emissions on average for Wallisville and Lynchburg, and only 28 times higher for HRM-3. This shows that natural gas emissions from the industrial facilities in the region were significantly underestimated in the inventory or sources, such as area sources, are also important contributors. There were a small number of point sources of ethane and propane emissions reported in the inventory, and the relatively large sources were closer to HRM-3 site, which supports this finding.

Finally, the event emissions of ethylene and propylene from the industrial complexes in Harris County, Houston, TX between June and November 2003 have been examined and their effects on the calculated source contributions have been studied. Of these event emissions, 42% did not reach any of the study sites because of the direction of the wind. The event plume passed over the study sites in 40 % of all the events. For 63% of the event emissions that reached the study sites, the modeled concentrations of ethylene or propylene at the sites were so low that they did not have any additional influence on the source contributions calculated at those sites. For 3-5% of the events, the modeled emissions and the source contributions could not be compared due to the lack of the ambient concentration data. The influence of the modeled event emissions on the

calculated source contributions could be detected for 26% of the events reaching the

Wallisville site. This ratio was much lower for HRM-3 and Lynchburg sites.

CHAPTER 4

Secondary Sulfate Formation on Mineral Dust Surfaces

4.1. Secondary Particle Formation and Evidence of Heterogeneous Chemistry during a Wood Smoke Episode in Texas

4.1.1. Introduction

Biomass burning, including prescribed burning and forest wildfires, leads to substantial atmospheric emissions of particulate matter and other pollutants. These emissions may significantly impact air quality over length scales of hundreds to thousands of kilometers during periods of intense fire activity (*Crutzen and Andreae*, 1990). A variety of methods have been used to quantify the contributions of biomass burning emissions to ambient air quality, including measuring the chemical composition of atmospheric particles, using back-trajectory analysis (*Andreae*, 1983), and determining the composition of trace gases (*Blake et al.* 1997).

In this work, the air quality impacts of fires in Texas will be examined. *Dennis et al.* (2002) and *Junquera et al.* (2005) have examined the overall magnitude of both prescribed burns and wildfires in Texas and have demonstrated that emissions from fires regularly have a significant impact on regional air quality. *Fraser and Lakshmanan* (2002) quantified the molecular marker in particle phase, levoglucosan, of biomass combustion during a regional haze episode in Texas to track the transport of biomass combustion aerosols, and demonstrated that air quality impacts can be substantial during extreme fire events.

To further examine the role of fires on air quality in Texas, the impact of wildfires on fine particulate matter concentration and composition during an August-September, 2000 episode will be evaluated. *Yue and Fraser* (2004b) have studied the sources of organic particulate matter during this fire episode by quantifying polar organic compounds in samples collected at three sites in Houston. Significantly higher concentrations of levoglucosan and other high molecular weight acids were observed on days when fires occurred, indicating that wood combustion was a major source of particulate matter generally, and polar compounds specifically, in this episode. To study the significance of fires as a source of particulate matter during this period, this chapter will report source apportionment calculations for three sites in Houston. Source contributions will be reported for days when particulate matter concentrations were greatly influenced by forest fires, and separately on other days not influenced by wood smoke (*Junquera et al.*, 2005). The Chemical Mass Balance (CMB) approach will be used to estimate the contributions of primary and secondary sources to $PM_{2.5}$ levels. These results will indicate that, in addition to being a significant source of carbonaceous aerosol, fires can lead to significant enhancements of particulate sulfate concentrations, and that this excess sulfate can be accounted for if heterogeneous sulfate formation reactions are occurring on the wood smoke surfaces.

4.1.2. Sampling and Analysis

4.1.2.1. Wood smoke episode

In late August and early September 2000, Texas experienced hot, dry weather for several days creating conditions conducive to wildfires across the state. Multiple

wildfires occurred and smoke from the wildfires reduced visibility and impaired air quality in the Houston area. This period will be referred to as the wood smoke episode. This episode coincided with a major air quality field study, the Texas Air Quality Study (TexAQS 2000). Consequently, for this period, extensive modeling data sets and observational data are available.

An inventory of the emissions associated with wildfires during the wood smoke episode have been assembled by *Junquera et al.* (2005) using procedures first described by *Dennis et al.* (2002). The period of most intense fire activity was from August 30 to September 8, with the highest fire emissions occurring on September 4 and 6, as shown in Figure 4.1. In contrast, relatively little fire activity occurred from the beginning of August to August 29 in the Houston area.

These wildfires led to significant increases in ambient fine particulate matter concentrations. 24-hour averaged $PM_{2.5}$ mass concentrations for the day with peak fire activity (September 6, 2000) averaged 39 $\mu g/m^3$ at multiple sampling sites throughout Houston, as compared to an average of 10 $\mu g/m^3$ on the days (August 25-28, 2000) immediately preceding the fires (*TCEQ*, 2005; *Junquera et al*, 2005). For sulfate, the 24-hour averaged mass concentrations were 13.5 and 3.8 $\mu g/m^3$, on September 6 and the days preceding the fire events, respectively.
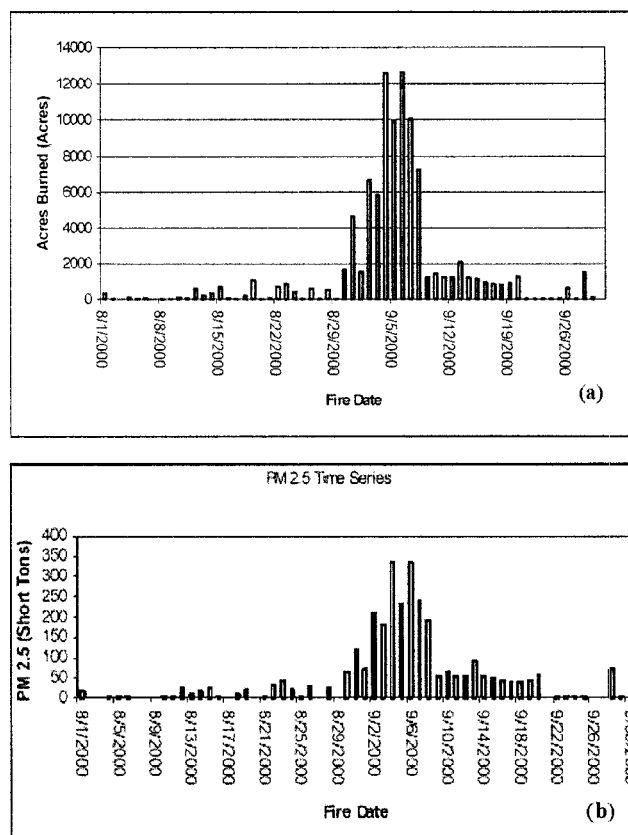
Figure 4.1. (a) Acres burned (b) Estimates of Emissions of PM$_{2.5}$ from fires in southeast Texas during August and September, 2000. (Junquera et al., 2005)

4.1.2.2. Ambient sampling

In order to resolve the sources of fine particulate matter on days with low and intense fire activity, samples of atmospheric fine particles were collected at three sites in Houston as described in the work of *Yue and Fraser* (2004a, b). The three sampling locations are shown in Figure 4.2 and included one near the coast (La Porte), one in an industrial location (HRM-3) and one in a suburban neighborhood (Aldine). In La Porte, the sampling site was located on the grounds of a municipal airport located at the edge of the small residential community of La Porte. Industrial sources bordered this residential

community on the north and east. The sampling site HRM-3 was located directly

adjacent to the highly industrialized Houston Ship Channel. Finally, the sampling site at

the suburban Aldine site was located on the grounds of an elementary school,

approximately 20 kilometers from the industrial source region.
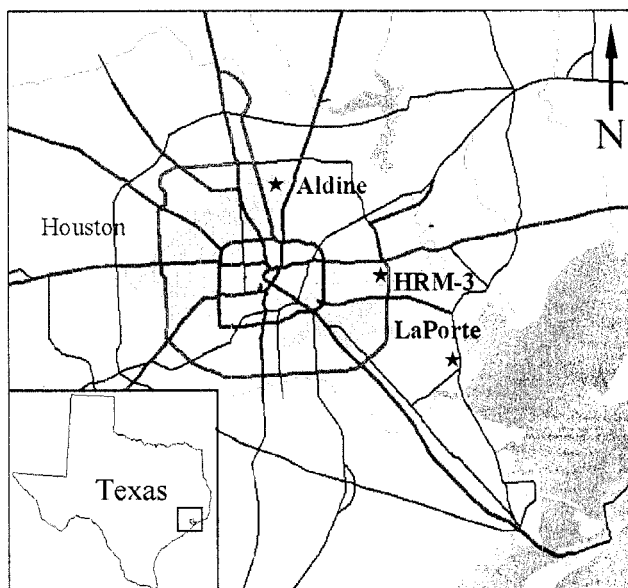
Figure 4.2. Location of the three sites in Houston.

Samples were collected every other day between August 15 and September 30

2000, and the samples collected on August 15, 21, 27, September 2, 6, 8, 14, 20, and 30

were analyzed for organic speciation.

The organic speciation of fine PM is described in detail in the work of *Yue and*

Fraser (2004a, b), and will only be summarized here. Samples of fine particles were

collected by a high volume air sampler (TSP Volume Controlled High Volume Air

Sampler; Thermo Andersen, Smyrna, GA) attached to a fine particles inlet (High Volume

Virtual Impactor; MSP, Minneapolis, MN) at a flow rate of 1.1 m^3 min^{-1} for 24 hours.

The filters were then stored in pre-baked glass jars and frozen until analysis. Organic

particulate matter was extracted with a suite of solvents under ultrasonic agitation and the

extract was reduced in volume with rotary evaporation and nitrogen blowdown. After the

extraction, the samples were analyzed using a Hewlett-Packard 6890 GC and a HP 5973

MS detector using authentic standards to calibrate instrument response (*Yue and Fraser*,

2004a, b).

4.1.3. Methods

4.1.3.1 Receptor modeling

The impact of forest fires on fine particulate matter concentrations and

composition was examined using the Chemical Mass Balance model (CMB) (*Watson et*

al., 1998) to calculate the contributions of the important sources to total PM$_{2.5}$ mass at the

receptors.

The CMB model estimates source contributions using the chemical composition

of primary emissions and the concentrations of these same constituents in the ambient

atmosphere. Thus, CMB requires both accurate speciation of pollutants in ambient air and

representative source profiles.

In the CMB model, the concentration (c_{ik}) of chemical species i at receptor k, is

given by

$$c_{ik} = \sum_{j=1}^{m} a_{ij} s_{jk} + e_{ik} \qquad (1)$$

where c_{ik} is the concentration of species i at the receptor k, a_{ij} is the concentration of species i in the emissions from source j, s_{jk} is the mass contribution of source j to receptor k, and e_{ik} is the difference between the measured and calculated species concentration (*Watson et al.* 1990). The CMB model estimates the contributions from chemically distinct source types by using an effective variance weighted least-squares solution to Equation (1) to solve for the unknown source contributions, (s_{jk}). In the present work, Equation (1) was solved using the chemical mass balance model CMB 8.2, which is described in detail in *Watson et al.* (1998).

Several considerations must be taken into account in constructing source profiles for use in CMB modeling. First, the analytical procedure used in the analysis of ambient samples should be equivalent to that used in the analysis of source samples to prevent procedural biases. Also, the chemical composition of source profiles used in CMB model must be significantly different from each other so that they do not lead to collinearity between sources. Profiles of the chemical and molecular composition of emissions from fine particle sources used in this work were taken from the results of different studies, all of which used analytical procedures equivalent to those used in the analysis of the ambient samples (*Yue and Fraser*, 2004a, b).

The composition of fine particulate matter emitted from catalyst-equipped gasoline-powered vehicles obtained from *Schauer et al.* (2002) was used as the representative source profile for gasoline vehicles. The chemical and molecular composition of emissions from two heavy-duty tractor-trailers operated on the Urban Dynomometer Driving Schedule for Heavy-Duty Vehicle cycle was used as the diesel-powered vehicle source profile (*Fraser et al.*, 2002).

Dennis et al. [2002] found that wildfires represent a significant fraction of the emission inventory of Southeast Texas. *Wiedinmyer et al.* (2001) determined that pine and hardwood oaks cover a majority of land use areas in Texas. Hence, pine and oak wood smoke profiles were adopted from the work of *Schauer et al.* (2001) as representatives of wood combustion source category. Since pine and oak wood smoke sources are very similar to each other, using two profiles at the same time caused collinearity problems. Therefore, model performance was tested using oak and pine profiles separately. Since the use of the pine smoke profile improved the model performance, and since the fires that occurred during the episode under study were primarily in pine forests (*Junquera et al.*, 2005), the pine smoke profile was used in this work.

Meat cooking emission profiles were taken from the results of the source tests reported by *Schauer et al.* (1999). In that work, significant quantities of n-alkanoic and n-alkenoic acids were measured in particles generated in meat cooking operations. Therefore, these fatty acids were used in this study as markers of meat cooking emissions.

There is strong evidence that plant leaf abrasion contributes an unspecified amount of fine particulate leaf wax particles to the atmosphere (*Mazurek et al.*, 1991). Leaves act as a sink for anthropogenic and natural airborne material, which under suitable conditions are resuspended into the atmosphere. Odd carbon number n-alkanes as a group ranging from C_{27} to C_{33} can serve as a marker that could be used to trace fine particulate vegetative detritus released to the urban atmosphere (*Rogge et al.*, 1993a). Organic compound speciation of $PM_{2.5}$ analyzed by *Rogge et al.* (1993a), and the chemical

speciation from *Hildemann et al.* (1991) were combined as the source profile for vegetative wax particles.

The composition of samples of paved road dust collected and analyzed by *Hildemann et al.* (1991) and the molecular composition of the same samples reported by *Rogge et al.* (1993b) were used as the source profile of road dusts.

4.1.4. Results and Discussion

4.1.4.1. Measurements of $PM_{2.5}$ and Source Attribution Using Organic Molecular Markers

The filter data were separated in two sets for analysis. In the first case, the concentrations of organic compounds in $PM_{2.5}$ samples collected on August 15, 21, 27, September 2, 14, 20, and 30 were averaged together and used in CMB calculations [*Yue and Fraser*, 2004a, b] as days not affected by the wood smoke period. These data will be labeled non-wood smoke period. As a second case, in order to investigate the influence of the regional haze episode attributed to forest fires in Eastern Texas on particulate matter concentrations in Houston [*Junquera et al.*, 2005], the contribution of the same sources was calculated for a set of the samples that were collected on two days (September 6 and 8) when the fire activity was most intense. Note that September 2 was included in the averaging for the days with low contributions for fires because the ambient sites used in this work were not impacted by fires on this date. The fires on September 2 were east of the sites and winds were out of the west, advecting the fire plumes away from the sampling sites.

The PM$_{2.5}$ mass concentrations and the concentrations of major chemical components of PM$_{2.5}$ are given in Table 4.1 for both the non-wood smoke period and the wood smoke episode.

Table 4.1. PM$_{2.5}$ mass and chemical composition during the observation period. Data are divided into woodsmoke period (filters collected on September 6 and 8) and non-woodsmoke period (all other filters analyzed). All concentrations are in micrograms per cubic meter.

	Aldine		HRM-3		La Porte	
Component	Non woodsmoke period	Wood smoke episode	Non woodsmoke period	Wood smoke episode	Non woodsmoke period	Wood smoke episode
PM$_{2.5}$ Mass	15.0	28.5	17.0	25.3	11.0	26.8
Organic Carbon*	4.7	10.1	4.2	8.0	2.7	8.1
Elemental Carbon	0.5	0.6	0.6	0.6	0.3	0.5
Nitrate	0.3	0.3	0.4	0.3	0.2	0.2
Sulfate **	5.3	8.8	5.4	9.5	5.3	8.7
Ammonium	1.2	2.9	1.2	3.1	1.2	2.9
Crustal Material	0.5	0.3	1.5	0.3	0.3	0.3

* Unscaled value of organic carbon mass.
** The mass of secondary sulfate is scaled to represent ammonium sulfate.

Source apportionment for the days not influenced by wood smoke episode

A total of 23 organic compounds plus 3 chemical constituents, as shown in Figure 4.3, were selected to be used in chemical mass balance calculations. An important consideration in the selection of marker compounds is that the species be chemically stable (species that cannot be significantly depleted nor formed by chemical reactions during the transport from sources to receptors), and that the species adequately span all source categories to be isolated [*Schauer et al.*, 1996]. Even though oleic acid is an

olefinic compound susceptible to ozone attack, this compound is a key tracer for aerosols from meat cooking and thus should be included in the analysis (Schauer et al., 1996).

The precision of mass concentration of each species should also be included in the model calculations. For the individual organic compounds analyzed using GC-MS, 20% of the concentrations of the compounds were assigned as the precision values based on the precision of the measurements determined experimentally [*Yue and Fraser*, 2004a, b]. Bulk chemical composition of particulate matter was determined using X-ray fluorescence (XRF) and thermal-optical transmission (TOT) by Research Triangle Institute (RTI) in compliance with established EPA protocols [*US EPA*, 1999]. The method detection limits of the three inorganic constituents involved in the chemical mass balance calculations were used for their precision values.

Marker compounds used in the chemical mass balance model include silica (sic), aluminum (alc), elemental carbon (ecc), n- heptacosane (c27c), n-octacosane (c28c), n-nonacosane (c29c), n-triacontane (c30c), n-hentriacontane (c31c), n-dotriacontane (c32c), n-tritriacontane (c33c), 17α(H)-21β(H)-29-norhopane (nhopc), 17α(H)-21β(H)-hopane (hopc), 22R+S 17α(H)-21β(H)-30-homohopane (hhopc), 22R+S 17α(H)-21β(H)-30-bishomohopane (bhopc), levoglucosan (levoc) pyrene (pyc), chrysene/triphenylene (chrc), benzo[k]anthracene (bkfc), benzo[b]anthracene (bbfc), benz[a]pyrene (bapc), indeno[1,2,3-cd]pyrene (i123c), benzo[ghi]perylene (bghic), palmitic acid (c16:0c), stearic acid (c16:1c), palmitoleic acid (c18:0c), and oleic acid (c18:1c).

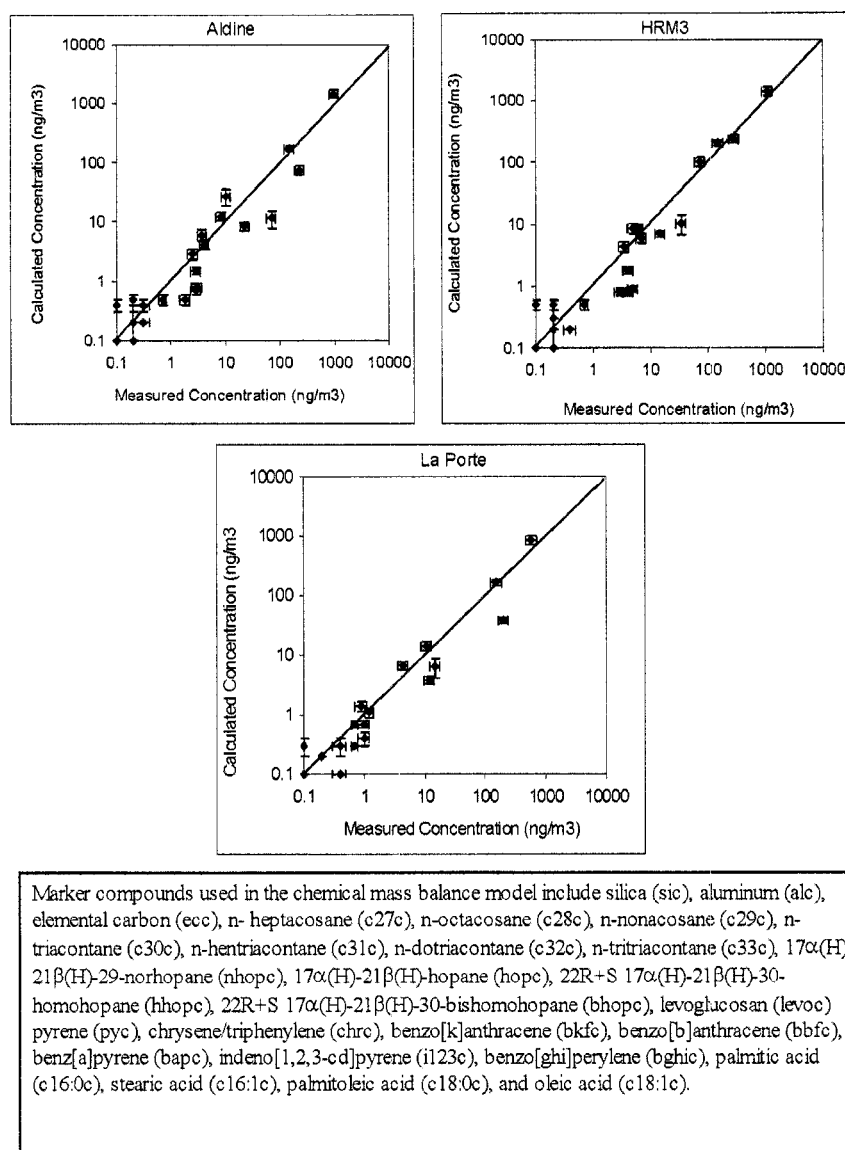**Figure 4.3**. Comparison of source allocation model calculations of molecular marker species concentrations to measured ambient concentrations for the days not affected by wood smoke.

A comparison of the calculated and measured ambient concentrations of each marker species at each site is given in Figure 4.3. In general, reconstructed molecular marker concentrations agreed with measured concentrations over a span of 3 orders of

magnitude. Since the source contribution estimates calculated by CMB are based on least-squares linear regression, they are not unique and therefore several performance measures and statistics such as t-statistics, R^2 and chi-squared values, are needed to help evaluate the accuracy of CMB source contribution estimates. All t-statistics values were greater than 2, which is a valid range as stated by Watson et al. [1990]. R^2 values were in the range of 0.67-0.73 and the corresponding chi-square values were less than 6.5, all of which indicate a good fit between reconstructed compound concentrations and measured values.

Fine particulate matter mass contributions on non-wood smoke days from six primary sources including gasoline-powered vehicle exhaust, diesel-powered vehicle exhaust, meat cooking, vegetative detritus, wood combustion and road dust, were calculated as well as other organics and secondary sulfate concentrations (Table 4.2). Also, OC attributed to each individual primary source is listed separately in Table 4.2. The road dust contribution was not statistically different than zero at Aldine and La Porte; therefore this source was excluded from the model. Although road dust had a small contribution to fine PM mass at HRM-3, it was statistically different from zero, and thus was included in the model calculation for this site. The presence of the road dust source in the calculations of source contribution estimates at HRM-3 may be a result of unpaved road surfaces in industrial facilities located near the Houston Ship Channel.

Table 4.2. Source contributions at three sites to ambient $PM_{2.5}$ mass and organic carbon (OC) concentrations (in micrograms per cubic meter) for the days not affected by wood smoke. Organic carbon masses have not been scaled to represent mass of organic compounds.

Source Categories	Aldine		HRM-3		La Porte	
	$PM_{2.5}$ Mass	$PM_{2.5}$ OC	$PM_{2.5}$ Mass	$PM_{2.5}$ OC	$PM_{2.5}$ Mass	$PM_{2.5}$ OC
Gasoline Vehicles	2.51± 0.94	1.10 ± 0.41	2.02± 0.67	0.89 ± 0.29	1.00± 0.40	0.44 ± 0.18
Diesel Vehicles	3.16± 0.44	1.01 ± 0.14	3.77± 0.45	1.21 ± 0.14	2.19± 0.28	0.70 ± 0.09
Vegetative Detritus	0.59± 0.09	0.19 ± 0.03	0.32± 0.05	0.10 ± 0.02	0.31± 0.04	0.10 ± 0.01
Meat Cooking	1.14± 0.26	0.39 ± 0.09	0.52± 0.14	0.18 ± 0.05	0.71± 0.16	0.24 ± 0.05
Wood Combustion	0.74± 0.18	0.41 ± 0.10	0.84± 0.15	0.47 ± 0.08	0.44± 0.10	0.25 ± 0.06
Road Dust	n.i.	n.i.	0.17± 0.04	0.05 ± 0.01	n.i.	n.i.
Sum of Apportioned $PM_{2.5}$ Mass	8.14± 1.09		7.64± 0.83		4.65± 0.52	
Sum of Apportioned OC		3.11 ± 0.46		2.90 ± 0.34		1.73 ± 0.21
Measured OC		6.54		5.88		3.77
Other Organics		3.43		2.98		2.04
Secondary Sulfate	5.28		5.40		5.30	
Sum of $PM_{2.5}$ mass apportioned to primary sources, other organics and secondary sulfate	16.85		16.02		11.99	
Measured $PM_{2.5}$ mass	15.00		16.99		11.00	

The apportioned mass due to the primary sources of $PM_{2.5}$ given in Table 4.2 (non-woodsmoke days) represents 54% of measured $PM_{2.5}$ mass at Aldine, 45% of $PM_{2.5}$ at HRM-3, and 42% of $PM_{2.5}$ at La Porte. The primary sources contributing to $PM_{2.5}$ mass at each site include diesel -powered vehicles with 21%, 22%, and 20%, gasoline

vehicles with 17%, 12%, and 9%, wood combustion with 5%, 5% and 4%, and meat cooking with 8%, 3%, and 6% of apportioned $PM_{2.5}$ mass at Aldine, HRM-3 and La Porte, respectively. The contribution of diesel-powered vehicles was found to be considerably higher than gasoline vehicles at each site. The higher contribution of the meat cooking source at Aldine is reasonable when considering that this site is located near a residential area where meat cooking operations are expected to be more frequent than they are at the other non-residential sites. The measurements in the work of *Yue and Fraser* [2004b] also showed that the levels of octadecenoic acid ($C_{18:1}$), which was found in the emissions from meat cooking processes, were the highest at Aldine. Vegetative detritus was a minor contributor to $PM_{2.5}$ mass at all locations.

The concentrations of organic carbon and sulfate attributable to primary sources were calculated by multiplying the primary source contribution estimates by the coefficients determined from the chemical composition profile of each source. The OC contribution from individual sources is listed separately in Table 4.2. At all three sites, less than 1% of sulfate was attributed to the primary sources, so the primary sulfate contribution is not listed separately. The OC and sulfate measured in the $PM_{2.5}$ samples in excess of the primary contributions was attributed to secondary particle formation. Since secondary ammonium sulfate aerosol is a major source of fine PM in the Southeast Texas region, the excess sulfate is labeled as "secondary sulfate". With bulk compositional analysis showing sufficient $PM_{2.5}$ ammonium to neutralize sulfate, with a molar ammonium to sulfate ratio averaging 1.7 ± 0.34 [*Russell et al.*, 2004], the secondary formation of sulfate will likely be in the form of ammonium sulfate, and the mass of secondary sulfate was scaled to represent ammonium sulfate.

For organic carbon during the non-wood smoke period, primary sources have been found to account for the majority of the measured fine particle OC concentrations at each site. Secondary organic aerosol (SOA) is not included in the OC apportionment calculations. The sum of OC from the source contributions determined by CMB represents 66%, 69% and 64% of the measured OC concentration in Aldine, HRM-3 and La Porte, respectively. Five sources have been identified that contribute to the organic carbon in $PM_{2.5}$ at Aldine and La Porte and six sources at HRM-3 (Table 4.2). According to the source apportionment model results, the major sources contributing to the organic carbon in $PM_{2.5}$ are gasoline vehicles (16-23%), diesel vehicles (21-29%), wood combustion (9-11%), and meat cooking (4-9%). Contributions of gasoline and diesel vehicles to organic carbon mass in Table 4.2 are roughly equivalent at Aldine, while the contribution of diesel-powered vehicles is considerably higher than gasoline vehicles at HRM-3 and La Porte.

Excess organic carbon mass is the difference between the measured organic mass by carbon (OMC) and the sum of the contributions of the primary OC sources identified by the mass balance. OMC is usually calculated as 1.4 times the OC mass (Watson et al., 1988). This excess OC mass may originate either from secondary organic aerosol formation or from sources not included in the model calculations, therefore this excess mass will be called "other organics" in the rest of this work.

The sum of other organics and secondary ammonium sulfate concentrations plus the apportioned mass concentrations represented 94% of $PM_{2.5}$ mass at HRM-3 and was overestimated by 8% at La Porte and 11% at Aldine. The lower percentage of the $PM_{2.5}$ mass at HRM-3 that could be explained by the mass balance is probably because HRM-3

is located in a highly industrialized area, and there may be other sources such as refineries and petrochemical plants contributing to fine particle levels that were not included in the mass balance model. In addition to the important primary sources of $PM_{2.5}$, secondary sources were important contributors to fine particle mass with secondary sulfate contributing 31%, 31%, and 49%, and other organics contributing 20%, 18%, and 19% of the fine particle mass at Aldine, HRM-3 and La Porte, respectively.

Source apportionment on wood smoke episode days

The contribution of the same sources was calculated separately for the wood smoke episode when regional haze episode attributed to forest fires in Eastern Texas influenced particulate matter concentrations in Houston [*Junquera et al.*, 2005]. Table 4.3 shows the source contribution estimates at three sites on these two days and the contribution of each source to organic carbon levels. Calculations of secondary sulfate and other organics were done as described above. $PM_{2.5}$ mass was dominated by the same sources as in the first case, including secondary sulfate, other organics, diesel vehicles, gasoline vehicles, wood combustion and vegetative detritus. The contribution of the road dust and meat cooking sources (as evidenced by the considerable decrease in octadecenoic acid levels during the episode) were not statistically different than zero at the three sites, and therefore these sources were not included in the model. The contribution of the wood combustion source to the $PM_{2.5}$ mass was approximately two times higher at each site than the contributions in the previous case, as expected. This result was consistent with, and primarily driven by, the concentration measurements of levoglucosan, which showed an increase of 173% during the wood smoke episode at all

three sites [*Yue and Fraser,* 2004a,b]. The results for the two cases (non-wood smoke and wood smoke) were compared graphically in Figures 4.4 and 4.5 with Figure 4.4 showing the contribution of primary sources, secondary sulfate and other organics to $PM_{2.5}$ mass and Figure 4.5 showing the contribution of primary sources and other organics to $PM_{2.5}$ OC mass.

Table 4.3. Source contributions at three sites to ambient $PM_{2.5}$ mass and organic carbon (OC) concentrations (in micrograms per cubic meter) for the days during the wood smoke episode. Organic carbon masses have not been scaled to represent mass of organic compounds.

Source Categories	Aldine		HRM-3		La Porte	
	$PM_{2.5}$ Mass	$PM_{2.5}$ OC	$PM_{2.5}$ Mass	$PM_{2.5}$ OC	$PM_{2.5}$ Mass	$PM_{2.5}$ OC
Gasoline Vehicles	1.68± 0.59	0.74 ± 0.26	3.18± 0.99	1.40 ± 0.43	1.56 ± 0.47	0.69 ± 0.18
Diesel Vehicles	3.48± 0.43	1.11 ± 0.14	3.63± 0.48	1.16 ± 0.15	2.91 ± 0.35	0.93 ±0.09
Vegetative Detritus	0.72± 0.09	0.23 ± 0.03	0.67± 0.09	0.21 ± 0.03	0.54 ± 0.07	0.17 ± 0.01
Meat Cooking	n.i.	n.i.	0.05± 0.01	0.02 ± 0.00	n.i.	n.i.
Wood Combustion	2.02± 0.27	1.13 ± 0.15	2.32± 0.37	1.30 ± 0.21	1.54 ± 0.21	0.86 ± 0.12
Sum of Apportioned $PM_{2.5}$ Mass	7.90± 0.78		9.85± 1.16		6.55± 0.63	
Sum of Apportioned OC		3.21± 0.33		4.09± 0.51		2.65± 0.26
Measured OC		14.17		11.15		11.38
Other Organics		10.95		7.06		8.73
Secondary Sulfate	8.80		9.45		8.68	
Sum of $PM_{2.5}$ mass apportioned to primary sources, other organics and secondary sulfate	27.65		26.36		23.96	
Measured $PM_{2.5}$ mass	28.45		25.30		26.85	
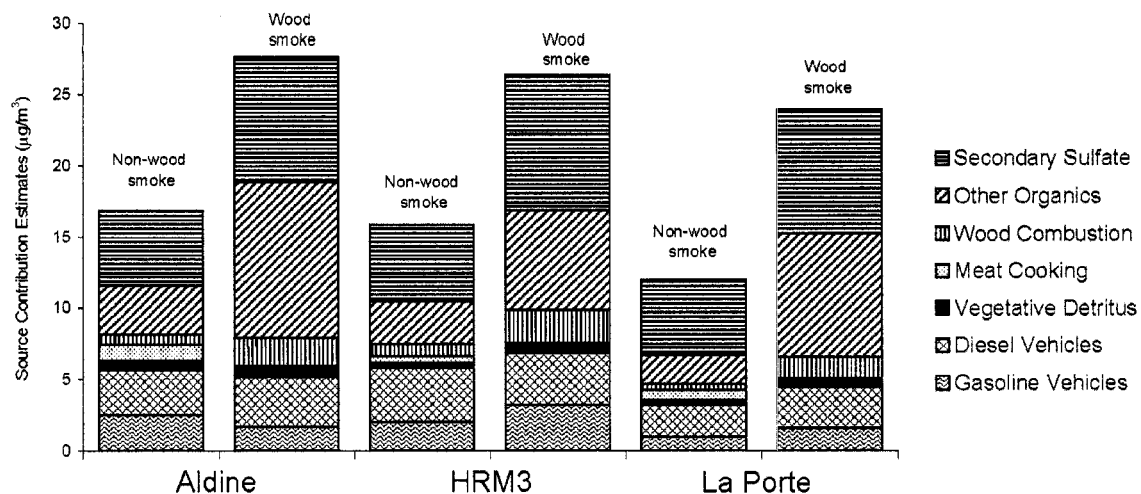
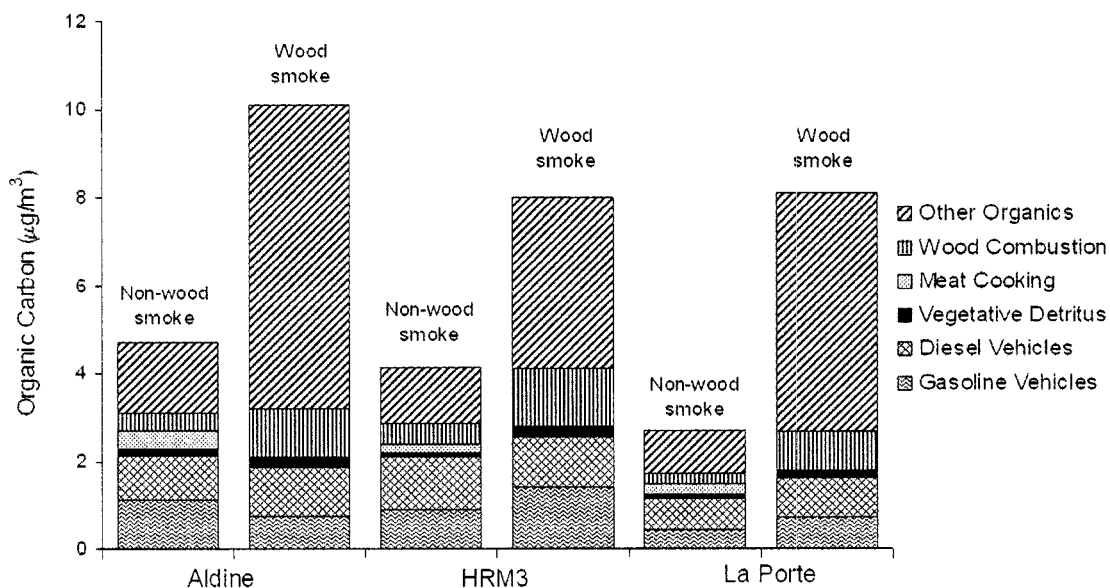**Figure 4.4.** Comparison of the source contributions to PM$_{2.5}$ mass in two cases.

Figure 4.5. Comparison of the source contributions to OC in PM$_{2.5}$ in two cases.

The apportionment of organic carbon in PM$_{2.5}$ for the wood smoke case showed

that the sum of the contributions of the primary sources to organic carbon concentrations

is only slightly higher during the wood smoke episode (3-35% increase), therefore most

of the increase in measured OC mass is attributable to the other organics (137-328%

increase) for the wood smoke episode (Figure 4.4). From Figure 4.5, one can observe

slight changes in the contributions of gasoline vehicles, diesel vehicles, vegetative

detritus, whereas a significant increase can be observed in wood combustion source

contribution to organic carbon (173%, 176% and 250% at Aldine, HRM-3, and La Porte,

respectively) which lead to an increase in the total mass attributed to primary sources

(Table 4.2 and 4.3).

Although the sum of the mass attributed to all primary sources during the wood

smoke episode showed some increase due to the increase in the contribution of wood

combustion, the dramatic increase in total $PM_{2.5}$ mass during the wood smoke episode

can be attributed to other organics (including secondary formation) and secondary

ammonium sulfate (Figure 4.4). The contribution of other organics to total $PM_{2.5}$ mass

showed an increase of 137-328%, secondary sulfate increased 64-75% at each site in the

wood smoke episode case. Possible reasons for the increase in the contribution of

secondary sulfate and other organics are presented in Section 4.1.4.2.

4.1.4.2. Secondary Aerosol Formation

The source apportionment analysis performed on wood smoke episode days and

non-wood smoke episode days shows that secondary sulfate and other organics increased

significantly during the wood smoke episode. Sulfate contributions averaged 5.3 and 9.0

$\mu g/m^3$ and contributions of other organics averaged 2.8 and 8.9 $\mu g/m^3$ on non-wood

smoke episode days and during wood smoke episode, respectively.

The increased mass of other organics during the wood smoke episode could be due to inaccurate source profiles, increased partitioning of organic semi-volatile species to the particle phase or heterogeneous reactions on the wood smoke particles producing additional condensed material. Inaccuracy in source profiles, specifically a low value of the OC/levoglucosan ratio used in the CMB calculations, may be a reason for the increase in other organics during the wood smoke episode. The OC/levoglucosan ratio used in this work was based on the data of *Schauer et al* [2001]. Recent data have shown wide variability in this ratio depending on combustion conditions [*Fine et al.*, 2002; *Sanders et al.*, 2003; *Shafizadeh, et al.*, 2003] and the ratio may be influenced by atmospheric reactions of levoglucosan.

A second potential cause of the increase in other organics during the wood smoke episode is increased partitioning of semi-volatile species into the particle phase. The increased wood smoke concentration, of approximately 1.5 $\mu g/m^3$, will cause some additional semi-volatile species to partition into the particle phase. However, since primary OC concentrations in the wood smoke episode increase by a much smaller percentage than do the other organics concentrations, it seems unlikely that this phenomenon would explain all of the observed increase in other organics.

Finally, heterogeneous reactions may explain the increase in other organics during the wood smoke episode. *Jang et al.* [2003] found that indigenous sulfuric acid produced from combustion of fossil fuels (e.g. wood smoke) could initiate the acid-catalyzed heterogeneous reactions on the particle phase. *Jang et al.* [2002] observed these heterogeneous reactions for a system involving ozone reaction with α-pinene, which

Russell and Allen [2005] found was the dominant secondary organic aerosol precursor in southeast Texas.

Possible reasons for the increased concentrations of sulfate on wood smoke episode days are direct emission of sulfate from the forest fires, displacement of chloride in the fire emissions by sulfate, and secondary aerosol formation through chemical reactions, possibly heterogeneous reactions. Source characterization for wood combustion has shown that sulfate is present in only trace levels from wood combustion [*Hays et al.*, 2002; *Schauer et al.*, 2001; *Cachier et al.*, 1996; *Robinson et al.*, 2004]. As a result, the source apportionment calculations show that direct primary emissions of sulfate from wood combustion did not play a role in creating high sulfate concentrations in ambient particulate matter. Particulate matter from fires is emitted at high temperatures, and at these temperatures, many inorganic elements such as KCl volatize and condense back onto particle surfaces. Chloride displacement occurs when SO_2 and the atmospheric O_2 react with KCl forming particulate phase K_2SO_4. Some chloride displacement may occur, but typical chloride concentrations in oak and pine wood smoke [up to a few percent, *Hays et al.*, 2002; *Schauer et al.*, 2001; *Cachier et al.*, 1996; *Robinson et al.*, 2004] are not sufficient to account for the observed sulfate enhancements; so direct emissions from fires matter containing chloride, followed by chloride displacement, are also not the cause of the high sulfate concentrations observed during the fire events.

If direct emissions of sulfate and chloride displacement do not explain the entire observed sulfate, then it is likely that chemical reactions transforming SO_2 to sulfate are the dominant source. Chemical pathways for SO_2 oxidation to sulfate include (1) the

homogeneous oxidation of SO_2 by OH• in the gas phase, (2) the condensed-phase

reactions of SO_2 with active oxidants such as peroxides and ozone, and (3) the

heterogeneous reactions of SO_2 on non-aqueous carbonaceous particles.

(1) In the gas phase, SO_2 reacts with OH radical to form H_2SO_4 and H_2SO_4

condenses on available particles. This homogeneous reaction can produce very high

sulfate concentrations if the atmosphere has significant SO_2 and OH• mixing ratios.

Buzcu et al. (2006) provided some evidence of elevated SO_2 concentrations on days with

and without intense fire activity. Their data suggested that SO_2 and OH• concentrations

were not particularly elevated during days of intense fire activity, so gas phase reactions

do not explain the enhanced sulfate formation during the wood smoke episode.

(2) Hydration of wood smoke particles leads to increased aqueous phase volumes

and aqueous phase reactions. Wood smoke particles are initially emitted as dry and

relatively hydrophobic materials; these hydrophobic particles can then undergo

atmospheric reactions, making them hydrophilic and able to take up water. The volume

of water taken up by the particles will depend not only on the particle mass available, but

also on the size distribution of the particles. *Buzcu et al.* (2006) made an upper bound

estimate of the volume of aqueous-phase condensed onto wood smoke particles (roughly

50 $\mu g/m^3$) by applying a growth factor of 1.4 (*Gasparini et al.*, 2004) to particle size

distributions measured on 6 September at the La Porte site. This volume of water together

with upper bound estimates of the aqueous concentration of SO_2 (based on the maximum

observed gas phase SO_2 concentration of 66 ppbv) and the aqueous oxidation rate [500%

h^{-1}, *Seinfeld and Pandis*, 1998] lead to a sulfate formation rate of only 2×10^{-13} g $m^{-3} h^{-1}$.

This upper bound suggests that the increase in the volume of aqueous phase in the

atmosphere due to wood smoke, with no new chemistry due to the wood smoke, is not likely to explain the high sulfate concentrations during the wood smoke episode (*Buzcu et al.*, 2006).

(3) Thus, only gas-particle-phase surface reactions are left as a possible explanation for the sulfate formation observed in the wood smoke episode. Conversion of SO_2 gas into sulfate aerosol has been observed on the surface of carbonaceous particles [*Novakov et al.*, 1974; *Brodzinsky et al.*, 1980; *Mamane and Gottlieb*, 1989]. In addition to directly forming sulfate, these reactions of SO_2 with carbonaceous particles can convert hydrophobic particle surfaces into hydrophilic surfaces. A variety of mechanisms for SO_2 oxidation reactions on carbonaceous surfaces have been proposed, involving a variety of oxidizing species [*Novakov et al.*, 1974; *Liberti et al.*, 1978; *Tartarelli et al.*, 1978; *Britton and Clarke*, 1980; *Baldwin*, 1982]. *Buzcu et al.* (2006) demonstrated that rates of heterogeneous reactions could be sufficiently high to explain the observed sulfate enhancements during the wood smoke episode. They examined the increase in the contributions of secondary sulfate aerosols during the wood smoke episode using a 3-D photochemical grid model. The simulations, together with ambient data, indicated that the increase in sulfate concentrations observed during this wood smoke episode were consistent with heterogeneous/surface reactions on wood smoke particles.

The next section reports the results of the preliminary laboratory investigations to quantify the impact of heterogeneous chemistry of the formation of sulfate aerosols on mineral surfaces.

4.2. Secondary sulfate formation on mineral surfaces

4.2.1. Introduction

Gas-phase sulfur dioxide can react with mineral aerosol to form particulate sulfate. Atmospheric modeling studies have shown that mineral particles have a potentially important role in the chemistry of troposphere, by interacting with trace atmospheric gases such as SO_2 (*Dentener et al.*; 1996; *Luria and Sievering*, 1991). *Cheng et al.* (1971) suggested that many heavy metal compounds, which are known to be present in atmospheric aerosols, have an important catalytic effect on SO_2 oxidation, especially at high relative humidity.

Several researchers have detailed the chemistry of the heterogeneous oxidation of SO_2 on mineral surfaces, including mineral dusts (*Goodman et al.*, 2000; *Goodman et al.*, 2001; *Underwood et al.*, 2001; *Ullerstam et al.*, 2002; *Ullerstam et al.*, 2003), calcium carbonate (*Lei et al.*, 2004) and fly ash material (*Mamane and Pueschel*, 1979) to understand the impact that these reactions may have on the chemistry of the atmosphere. Others have shown that SO_2 could be oxidized to sulfate in aqueous aerosol by ozone and hydrogen peroxide (*Seinfeld and Pandis*, 1998, *Krischke et al.*, 2000; *Keene et al.*, 1998). *Usher et al.* (2002) found that SO_2 irreversibly adsorbs as sulfite (SO_3^{2-}) and /or bisulfite (HSO_3^-) on all particle surfaces with the exception of SiO_2. The adsorbed species can be oxidized to sulfate (SO_4^{2-}) and/or bisulfate (HSO_4^-) upon exposure to ozone.

In Section 4.1, secondary formation of particulate matter has been shown to be a major source of ambient fine particles in Texas. Specifically, it has been shown that the sum of secondary organic mass and secondary sulfate mass could exceed the mass of

primary particles during regional haze episodes. As mentioned in Section 4.1.4.2, *Buzcu et al.* (2006) have shown that existing routes of secondary sulfate formation from the oxidation of gaseous SO_2 cannot explain observed ambient secondary sulfate levels during severe wood smoke episodes. *Buzcu et al.* (2006) demonstrated that rates of heterogeneous reactions could be high enough to explain the observed sulfate enrichment during the wood smoke episodes.

Based on the results of these previous studies, the extensive field study, TexAQS II, aims to improve the scientific understanding of secondary particle formation and transport in regional haze episodes. One goal of this study is to investigate the role of metal and mineral content of ambient $PM_{2.5}$ on the heterogeneous chemistry of secondary fine particle formations. For this purpose, the $PM_{2.5}$ samples that will be collected during the TexAQS II study at rural monitoring sites in Texas will be quantified for the metal and mineral content by ICP-MS. The metal content of the equivalent samples will be augmented by resuspending material from known mineral sources such as road dust, coal fly-ash, refinery catalyst material with a quantifiable amount of material. The role of the mineral material in heterogeneous sulfate formation will be investigated by passing SO_2 over $PM_{2.5}$ samples and by quantifying the sulfate formation using chromatographic methods.

Before the collection and the augmentation of the ambient $PM_{2.5}$ samples, preliminary laboratory investigations were performed to quantify the impact of mineral material only on the heterogeneous formation of secondary sulfate. To investigate the role of different minerals in sulfate formation, road dust samples collected near a sampling site and samples of fly ash from a local coal-fired power plant were

resuspended on the blank filters. Dilute SO_2 gas was then passed over the filters and analyzed for the sulfate formation. In this section, we will report the results of these preliminary laboratory investigations. The results of the measurement of the formation of sulfate from the oxidation of gaseous SO_2 will be used to understand if the exposure of mineral materials to SO_2 in the atmosphere leads to the formation of particulate sulfate.

These investigations will improve our understanding of the role of metals in heterogeneous sulfate formation, identify which metals can contribute to the formation of elevated $PM_{2.5}$ sulfate levels during regional haze episodes, and will serve as the basics of the further research.

4.2.2. Methodology

4.2.2.1. Resuspension of Primary Source Samples on the Filters

Gelman Teflon membrane filters (47-mm diameter) were chosen for their low tare weight and mass stability. New filters were augmented with a quantified amount of primary particle material from a specific source. The primary particle material used in these experiments includes known sources of $PM_{2.5}$ that are rich in metal content, such as local road dust and coal combustion fly ash. Road dust samples were collected near a local air quality monitoring site (HRM-3) located in the industrial Houston Ship Channel area. Coal-combustion fly ash was obtained from the pollution control equipment installed at a local power plant (Parish Power Plant). Prior to the resuspension, each filter was weighed using a Cahn C-35 microbalance to determine the original weight of the filter. Prior to the weighing, filters were kept in a humidity and temperature controlled

environmental chamber for a 48-hour equilibration at 40% relative humidity and 24°C temperature.

The filters were installed in aluminum filter holders downstream of an environmental chamber used to resuspend primary particle material. The resuspension chamber draws air in through a HEPA filter to remove any particles from the resuspension supply air. The air stream is pulled through a size-selective cyclone separator to remove particles larger than 2.5 microns. The sample stream is split and divided into three streams passing through parallel filter holders to allow coating of primary material onto the filters. Flow across the parallel filter holders were controlled with critical flow orifice plates.

After resuspending the mineral material onto the filter, the filters were reweighed to determine the amount of material coated and transferred to a petridish for storage until analysis. The coated filters will be analyzed by ICP-MS in University of Houston to determine the chemical composition of the mineral material.

4.2.2.2. Sulfate Formation Experiments

The first experimental set-up passed dilute 100ppm SO_2 in air over the blank filters and filters of mineral material for 30 minutes. The airflow was controlled by placing critical orifices at each filter holder to provide a constant flow of 5 L/min to each filter.
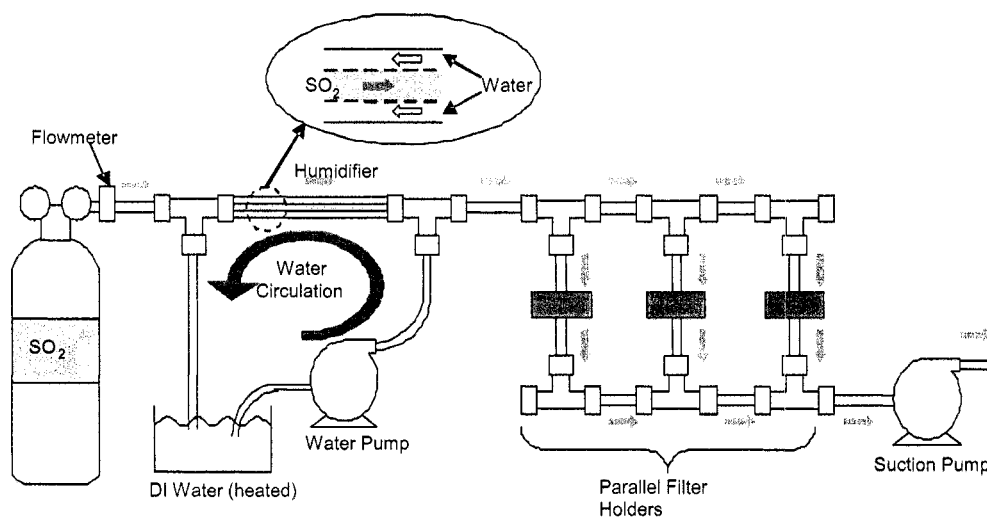
Figure 4.6 Schematic diagram of the experimental set-up.

The experiment was repeated by passing the dilute SO_2 through a Nafion

humidifier (Perma Pure Inc. MH-Series Humidifier) to increase the relative humidity of

the air stream. The humidifier is a tube-in-shell semi-permeable membrane that allows

the transfer of water vapor between a liquid water supply and the gas stream. Heated DI

water supply was circulated using a water pump through the humidifier, and humidity

was adjusted by regulating the water temperature of the humidifier, or by controlling the

flow rate of water to the humidifier. The SO_2 gas was routed inside the tubing and the

heated water was circulated outside the shell (Figure 4.6).

Dust particles deposited on the filter were exposed to SO_2 for 30 minutes.

Immediately after the exposure, the filters were removed from the filter holders and

submerged in 10 ml deionized water in a glass beaker, and the beakers were placed in

ultrasonic agitator for 2 hours. Each filter was analyzed for sulfate formation by ion

chromatography to determine if the mineral augmentation increased the SO_2 oxidation rate. Analytical and laboratory blanks were used to subtract sulfate present in filter media.

A second experimental set up used different amounts of road dust and coal fly ash uniformly placed over the bottom of a Pyrex flask. These samples were exposed to a continuous flow (1-4 l/min) of 100 ppm diluted SO_2 in air. The sample was deposited into 10 ml DI water, agitated for 2 hours, and after being filtered, was analyzed for sulfate by ion chromatography.

For all the experiments, the amount of sulfate on the samples was quantified by ion chromatography using a Dionex IC 20 system, equipped with an AS-50 autosampler, and an IonPac AS14/AG14 analytical/guard column. The quantity of sulfate measured was used to calculate the sulfate formation rate $d[SO_4^{2-}]/dt$. The anion eluent used was the 3.5mM Na_2CO_3 + 1.0mM $NaHCO_3$. The eluent flow rate was set to 1.20 ml/min and the injection volume was 25μl.

4.2.3. Results and Discussion

4.2.3.1. Analysis of Filter Samples

An unexposed dust sample was used to obtain the original sulfate concentration for all materials studied. By subtracting sulfate concentration on the augmented filters, which are exposed to dry and humidified SO_2 gas, from the sulfate concentration measured on the unexposed augmented filters, and then by normalizing the concentrations by the mass of mineral dust collected on the filters, the amount of sulfate

formed per mass of mineral dust was determined. Ion chromatographic analysis of the samples obtained immediately after the mineral dust was exposed to dry SO_2 showed the higher concentration of sulfate ions compared to unexposed samples only in one of the three experiments (Experiment 4 in Table 4.4). In the other experiments, the measured sulfate concentrations on SO_2-exposed filters were not significantly higher than the unexposed ones. In two of the three experiments run by passing humidified SO_2 (Experiments 1 and 2 in Table 4.4), the measured sulfate formation capacity (per mg of dust) was the same, whereas in the Experiment 3, only half of this amount was formed per mg of road dust material on the filter.

Table 4.4. Sulfate formation on mineral particles on filters.

Exp. No.	Exposure Time (min)	RH (%)	Filter Loading (mg)	Sulfate Formation (μg)	Sulfate (μg) Formed per mg dust	SO_2 converted to sulfate on the surface (μg) per mg dust	Fraction of Conversion (%)
1	30	95	7.253	26.80	3.70	2.47	0.08
2	30	95	15.202	59.29	3.90	2.60	0.17
3	40	95	3.354	5.97	1.78	1.19	0.01
4	60	Dry	9.390	34.29	3.65	2.43	0.03

Assuming that all of the SO_2 was removed from the gas stream and converted to sulfate, the fraction of conversion, which is the ratio of mass of SO_2 removed by the dust material to the amount of SO_2 introduced to the filters was calculated and reported in Table 4.4.

SO_2 removal and sulfate formation was proportional to the particle mass on the filters (Figure 4.7). This shows that not only the outer layer of road dust particles were effective in SO_2 removal, but the whole particle mass. For the loadings ranging from 3 –

15 mg mineral mass, the sulfate formation was proportional to the mineral mass. In higher loadings, SO_2 may not encounter all the available mineral particles and thus sulfate may not be proportional to the mineral mass.

The chart shows Sulfate Formation (ug) on the y-axis ranging from 0 to 70, and Filter Loading (mg) on the x-axis ranging from 0 to 20, with the trend line equation:
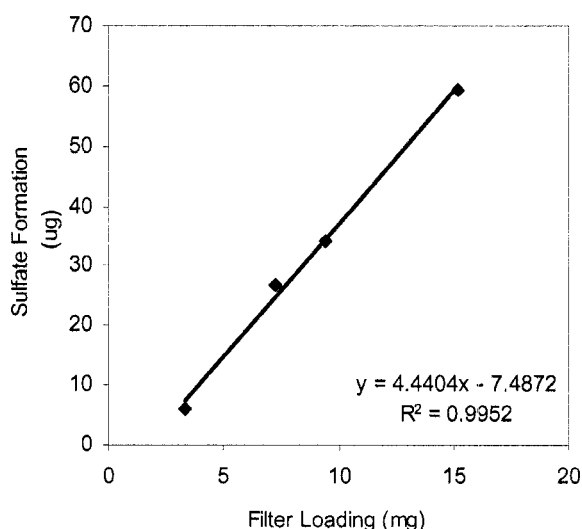
$$y = 4.4404x - 7.4872$$
$$R^2 = 0.9952$$

Figure 4.7. Sulfate formation (µg) on road dust particles as a function of the dust mass on the filters (mg).

Unfortunately, the filter augmentation experiments were not successful for coal fly ash samples. Since the coal fly ash particles were much smaller in size than the road dust particles, a stable resuspension on the filters could not be achieved. Once in contact with the SO_2 gas, most of the fly ash mass on the filter was lost due to the flow of the gas through the filters. For this reason, the sulfate formation on coal fly ash particles along with road dust particles was investigated using a bulk sample as explained in the next section.

4.2.3.2. Bulk Analysis

Twelve experiments on bulk mineral materials were conducted under different relative humidities and mineral loadings for samples: road dust and coal combustion fly ash. Different flow rates of SO_2 into the system were tried but no significant effect on sulfate formation was observed (Table 4.5). *Cheng et al.* (1971) also conducted experiments with the same SO_2 concentration and different critical orifices to regulate the flow rate of the gas mixture and concluded that gas phase diffusional resistance did not influence the overall rate of conversion of SO_2 to SO_4^{2-}.

First, 500 mg of mineral material was exposed to dry SO_2 for 30 minutes. After the SO_2 exposure is completed, 50 mg of the exposed mineral material was sonicated in 10 ml DI water. These conditions allowed the formation of sulfate on the surfaces of mineral particles and higher sulfate formation was observed on coal fly-ash sample than on the road dust sample (experiments 1 and 7 in Table 4.5). However, the sulfate formed per mg of mineral was lower than the values observed during the filter flow experiments.

The experiments were repeated for humidified air by passing the dilute SO_2 through a Nafion humidifier to increase the relative humidity of the air stream. Humidity was adjusted by regulating the water temperature of the humidifier. The flow rate of water to the humidifier was kept low at 1 l/min to increase the performance of the humidifier, and the water was heated to temperatures of 30°C, 50°C and 70°C.

Table 4.5. Sulfate formation on road dust and coal fly ash particles.

Exp. No.	Mineral	RH (%)	SO$_2$ flow rate (l/min)	Amount of mineral (mg)	Sulfate Formation (µg)	Sulfate (µg) Formed per mg dust	SO$_2$ converted to sulfate on the surface (µg) per mg dust	Fraction of Conversion (%)
1	Dust	0	1	50	19.78	0.40	0.26	0.17
2	Dust	100	1	50	389.00	7.78	5.19	3.38
3	Dust	0	2	100	135.67	1.36	0.91	0.59
4	Dust	80	2	10	96.97	9.70	6.46	0.42
5	Dust	80	2	20	85.13	4.26	2.84	0.37
6	Dust	80	2	30	44.69	1.49	0.99	0.19
7	Coal	0	1	50	84.81	1.70	1.13	0.74
8	Coal	100	1	50	264.00	5.28	3.52	2.29
9	Coal	0	2	100	196.77	1.97	1.31	0.85
10	Coal	80	2	10	15.85	1.58	1.06	0.07
11	Coal	80	2	20	31.94	1.60	1.06	0.14
12	Coal	80	2	30	33.36	1.11	0.74	0.14

At all these temperatures however, the water temperature rapidly reached the dew point and liquid droplets formed over the mineral material. Subsequent analysis of these samples showed much higher sulfate formation rates (Table 4.5, experiments 2 and 8), suggesting that the higher the humidity, the higher the amount of SO$_2$ converted to sulfate on the mineral particle surfaces. This result is consistent with the results of previous studies (*Cheng et al*, 1971), and although these conditions might represent actual environmental conditions, the research objective to study heterogeneous chemistry promulgated control of the humidity to prevent the formation of the water droplets. Therefore, for the next set of experiments, which will be described later in this section, the water temperature was kept at room temperature, 24°C, which maintained the relative humidity of the system at 80%.

The lower sulfate formation rates for both mineral samples exposed to dry SO_2 might be due to the insufficient contact of SO_2 with mineral surfaces when high amounts of minerals were used (500 mg in this case). Therefore, a new set of experiments were performed where lower amounts of mineral particles were exposed to SO_2. The mineral samples were then directly sonicated in 10 ml of DI water. In Table 4.5, experiments 3 and 9 represent these trials for 100 mg road dust and coal fly ash samples. The data show that the sulfate formed per mg mineral mass was higher for both samples than the previous higher mass experiments. The capacity of sulfate formation was calculated as 1.36 and 1.97 μg sulfate per mg mineral for road dust and coal fly ash, respectively, from the 100 mg exposure experiment.

The fraction of conversion of SO_2 to sulfate was higher for the bulk analysis than for the filter samples, although SO_2 converted to sulfate on the surface per mass was lower. Since SO_2 flow rates were 1 l/min and 2 l/min in these experiments, total SO_2 amount introduced to the system was lower leading to the higher fractions of conversion of SO_2.

Finally, another set of experiments were run using still lower amounts of mineral material (10, 20, and 30 mg) to see if the capacity of sulfate formation will further increase, as substrate mass decreased. Also these experiments will test if the capacity for sulfate formation is proportional to mass of the mineral material. For experiments 4-6 in Table 4.5, higher sulfate formation capacity was observed on road dust particles compared to the previous results with 100 mg mineral mass. In these experiments, the sulfate formation capacity was found to be inversely proportional to the mass of the mineral material. This directly shows a lower sulfate capacity wen experiments are

performed with smaller mineral mass. On the other hand, the sulfate formation capacity was little changed for coal fly ash samples (Experiments 10- 12 in Table 4.5). In fact, for 10 mg and 20 mg samples, exposed to SO_2, the same amount of sulfate formed on the mineral surfaces per mg mass, whereas the sulfate formation capacity decreased for higher sample mass (30 mg). Moreover, the sulfate formation capacity was not higher for these samples than for 50 and 100 mg fly ash samples as observed for road dust mineral.

As a result of these experiments, the sulfate formation capacities were lower than the ones reported in some of the previous studies. Among the possible reasons are the differences between the substances used, and variations in surface area, particle size, the composition and reactivity of the particles, lower gas flow rates (lower than 1 l/min) compared to other studies, and the fact that oxidants were used in the other studies such as O_3, NO_2 (*Dlugi*, 1981; *Mamane and Gottlieb*, 1989). *Ullerstam et al.* (2002) stated that only a small amount of SO_2 can be oxidized by the active sites on the mineral material and use of an oxidant results in a more efficient oxidation. The importance of the composition of the particles on the SO_2 oxidation rates is addressed by *Usher et al.* (2002), who showed that the initial uptake of SO_2 on China loess was $3x10^{-5}$, which is substantially lower than the uptake for other mineral powders such as MgO, Fe_2O_3, and Al_2O_3. SiO_2 was found to have an initial uptake coefficient of less than $1x10^{-7}$ thus showing no reactivity toward SO_2 gas. The reason of the low reactivity of China loess toward SO_2 gas was that 48% China loess was silicon, likely as SiO_2. *Judeikis et al.* (1978) investigated SO_2 reactivity with fly ash materials and encountered with very low SO_2 removal rates, indicating the possibility of the exposure of these materials to near saturation levels of SO_2 either before or during collection. Subsequent analysis of the fly

ash sample indicated a strong sulfate signal. Therefore, the researchers washed the fly ash material with distilled water to remove soluble sulfates, and observed substantial increases in the fly ash reactivity against SO_2. *Judeikis et al.* (1978) also pointed out the possible effects of organics on rates and capacities for SO_2 removal. Urban aerosols contain an organic fraction that may be less reactive toward SO_2 removal (*Friedlander,* 1973).

The SO_2 conversion capacities were comparable to the results of *Judeikis et al.* (1982), who calculated 4.0 µg SO_2 per mg MgO at 0% relative humidity (RH), 1.4 µg SO_2 per mg fly ash at 95% RH, and 17.0 µg SO_2 per mg Al_2O_3 at 95% RH. *Liberti et al.* (1978) reported 0.06 µg sulfate formed per mg fly ash from coal-fired power plant, and 0.75-1.5 µg sulfate formed per mg atmospheric dust.

4.3. Conclusions

A chemical mass balance (CMB) model was used to estimate the contributions of primary and secondary sources of $PM_{2.5}$ during a regional haze episode in Houston, Texas. The analysis consisted of apportionment calculations on data collected during the wood smoke episode and separately on data collected on other days not affected by the wood smoke episode. Analysis of the data collected on non-wood smoke-episode days indicated that the major contributors to $PM_{2.5}$ mass were secondary sulfate, diesel and gasoline powered vehicles, other organics, and wood combustion. Secondary sulfate represented almost all of the sulfate measured whereas primary sources were found to account for the majority (64-69%) of the measured organic carbon at three sites. The

contribution of the wood combustion source showed a doubling at all sites during the wood smoke episode whereas the contributions of other primary sources did not increase significantly. This result is consistent with the increase in the concentrations of levoglucosan during the wood smoke episode at each site, while the concentrations of marker species for other sources were not dramatically higher on the wood smoke episode days. $PM_{2.5}$ mass almost doubled on the wood smoke episode days, and the contributions of the secondary sources, namely secondary sulfate and other organics increased 68% and 228% at each site, respectively. The apportioned mass together with the secondary aerosol contributions accounted for 97% and 89% of $PM_{2.5}$ mass at Aldine and La Porte, respectively and was overestimated by 4% at HRM-3.

In order to provide direct evidence of sulfate formation on mineral particles through heterogeneous reactions, a series of laboratory investigations was performed. This is preliminary work a set of experiments to study heterogeneous sulfate formation on augmented ambient fine particulate matter samples. The analysis of the fly ash indicated a strong sulfate signal, decreasing the reactivity of fly ash particles to SO_2 exposure, and resulted in a low sulfate formation rate on fly ash particles. In general, the relative humidity increased the sulfate formation capacity of the mineral particles. Larger amounts of sulfate formed as a result of heterogeneous reactions on smaller amounts of road dust particles, whereas the sulfate formation capacities were about the same for various amounts of coal fly ash particles.

CHAPTER 5

Conclusions

5.1 Summary

Methods for the application of a multivariate receptor modeling technique have been developed. The analysis of the data collected at three sites in Houston during the summer of 2003 resulted in isolating and evaluating 3 or 4 major source factors of 54 VOCs for each weekly period in the Houston Ship Channel region. The most important isolated factors affecting these three sites were found to be consistent with profiles of refining, petrochemical production, gasoline and natural gas/accumulation emissions, which indicated the importance of the reactive compounds that have high ozone formation potential, as well as less reactive VOCs that have longer lifetimes in the atmosphere. Other sources, which have minor contributions to VOC concentrations, included aromatics emissions, industrial emissions (only at HRM-3 and Lynchburg sites), biogenic and mobile source/transient industrial (only at the Wallisville site). A nighttime data analysis performed at two sites found higher contributions of each source factor to total NMHC mass, since loss of VOCs due to the photochemical reactions was minimum.

After performing the source apportionment calculations, an analysis was performed on ozone standard exceedance days that found that very high contributions of the dominant sources of VOCs such as petrochemical facilities and refineries during times that are favorable to ozone formation led to peak ozone concentrations and exceedances of 1-hour ozone standard at each site. It has also been determined that

exceedingly high contributions of sources emitting low carbon number alkanes can lead to ozone formation as well as sources emitting highly reactive olefinic VOCs.

Next, the relative contributions of the important sources of VOCs calculated by PMF were compared with the emission inventories of VOCs in Houston. In general, the composition and the location of the sources developed from the source apportionment results were consistent with the reported industrial emissions despite some disagreements. Reported emissions and source apportionment calculations established that the contribution of petrochemical facilities to VOC levels at one of the sites were higher than the inventoried emissions. For this reason, inventoried emissions used as inputs to photochemical models are unlikely to reproduce ozone concentrations accurately. Compared to the PMF results, the inventory underestimated the refining and gasoline emissions at all sites. The fractional contribution from natural gas emissions was 100 times the inventoried emissions on average at all sites. This shows that natural gas emissions from the industrial facilities in the region were significantly underestimated in the inventory or other sources, such as area sources are important for the emissions of low carbon number alkanes.

In several recent studies, the failure of previous modeling efforts to reproduce the observed extreme levels of ozone was traced to a large underestimate of alkene emissions, specifically, ethylene and propylene, from the petrochemical facilities in the highly industrialized Houston Ship Channel region. This work, however, found that emissions of volatile organic compounds from other important industrial applications emitting refining gases, natural gas, gasoline vapor and aromatics were also underestimated in the emission inventories. Especially, emissions of ethane and propane

from natural gas sources were found to be largely underreported in the inventories, however, the modeling efforts proved that these compounds were actually co-emitted in large amounts representing the natural gas emissions.

Almost all recent studies focus only on the highly reactive volatile organic compounds, mainly ethylene and propylene, when investigating the reason of high ozone concentrations in Houston. This work brings a new perspective to the reasons of high ozone levels in Houston showing the importance of other emissions sources of VOCs besides petrochemical production emissions while not underestimating the importance of petrochemical emissions.

Finally, in Chapter 3, the event emissions of ethylene and propylene from the industrial complexes have been examined and their effects on the calculated source contributions have been studied. Of these event emissions, 42% did not reach any of the study sites because of the direction of the wind. The event plume passed over the study sites in 40% of all the events. For 63% of the event emissions that reached the study sites, the modeled concentrations of ethylene or propylene at the sites were so low that they did not have any additional influence on the source contributions calculated at those sites. For 3-5% of the events, the modeled emissions and the source contributions could not be compared due to the lack of the ambient concentration data. The influence of the modeled event emissions on the calculated source contributions could be detected for 26% of the events reaching the Wallisville site. This ratio was much lower for HRM-3 and Lynchburg sites. The recent concern regarding the event emissions was first addressed by David Allen's group in University of Texas, Austin. In *Allen et al.* (2004) and *Murphy and Allen* (2005), they statistically analyzed event emissions from the industrial facilities

in Houston in detail. This work is the first attempt looking at the event emissions from a different perspective and assessing their significance from source apportionment point of view.

In Chapter 4, a chemical mass balance (CMB) model was used to estimate the contributions of primary and secondary sources of $PM_{2.5}$ in Houston, Texas. The analysis consisted of running the model on data collected during a regional wood smoke episode and separately on data collected on other days not affected by the wood smoke episode. Analysis of the data collected on non-wood smoke-episode days indicated that the major contributors to $PM_{2.5}$ mass were secondary sulfate, diesel and gasoline powered vehicles, other organics, and wood combustion. Secondary sulfate represented almost 100% of the sulfate measured whereas primary sources were found to account for the majority of the measured organic carbon at three sites. The contribution of the wood combustion source showed an increase by an average of 200% at all sites whereas the contributions of other primary sources did not increase significantly during the wood smoke episode. $PM_{2.5}$ mass almost doubled on the wood smoke episode days, and the contributions of the secondary sources, namely secondary sulfate and other organics increased 68% and 228% at each site, respectively. The second part of Chapter 4 reported the evidence of heterogeneous formation of sulfate particles on mineral surfaces exposed to dilute SO_2 in air.

5.2 Recommendations for Future Research

Heterogeneous Sulfate Formation on the Ambient Particulate Matter Samples

As a continuation of the laboratory investigations performed in Chapter 4, fine particle sampling equipment will be set up at three different rural monitoring sites across Texas (San Saba in the Hill Country, San Augustine in East Texas, and Clarksville in Northeast Texas) in coordination with the TexAQS II field study and multiple equivalent samples of ambient $PM_{2.5}$ will be collected in accordance with EPA established protocols on Teflon membrane filters. One set of the samples will be analyzed for native metal content, and one of the other two sets will be augmented with known metal rich primary fine particle source material, and used to determine the impact of primary emissions of metals on secondary sulfate formation. The results will indicate if the augmentation of ambient PM samples with mineral material enhances the rate of sulfate formation. The methods used in the preliminary laboratory investigations will be improved to effectively perform the sulfate formation experiments on the Teflon membrane filters. The formation of sulfate due to the exposure of different minerals other than road dust and coal fly ash such as crustal material, refinery catalyst material, hematite and calcium carbonate to SO_2 in air will be investigated. The sulfate formation due to the exposure of ambient particulate matter to SO_2 in the absence of photooxidants such as ozone, hydrogen peroxide, or nitrogen oxide will also be studied. The effects of ultraviolet variation on the rate of sulfate formation will be assessed.

Analysis of $PM_{2.5}$ from Motor Vehicles in a Tunnel Vehicle exhaust particles contain a great variety of organic compounds. Among these compounds may be relatively stable molecules that could be used to trace and quantify the presence of vehicle exhaust in

urban atmospheres. If unique tracer compounds characteristic of exhaust from gasoline and diesel vehicles could be identified and these compounds can also be measured in ambient air, then the fractions of the ambient aerosol derived from gasoline and diesel vehicles could be accurately determined.

Petroleum compounds such as hopanes and steranes present in the gasoline-vehicle exhaust can be used as molecular tracers of $PM_{2.5}$ emitted from gasoline-powered motor vehicles (*Schauer et al.*, 1996). *Schauer et al.* (2002) have shown that the isoprenoids and tricyclic terpanes are distinctive compounds of gasoline and therefore can be used as tracers for gasoline vehicle exhaust emissions.

Although the number of light-duty diesel vehicles is much less than gasoline vehicles, the emission rates of particulate matter from diesels are higher than those of gasoline-vehicles, and their contribution to $PM_{2.5}$ concentrations cannot be ignored (*Cadle et al.* 1999). PAH profiles may help in separating gasoline from diesel emissions. PAH emission rates for diesel vehicles are usually much higher than those for gasoline vehicles (*Rogge et al.*, 1993). Moreover, OC percentages for diesel vehicles are found to be much lower than those for gasoline vehicles, thus OC/EC ratio can also be used to separate gasoline and diesel emissions (*Cadle et al.* 1999).

Although particulate matter emissions from motor vehicle exhaust are composed mostly of carbonaceous material, the emissions also comprise various elements including some trace metals certain of which possess toxic properties and commonly present in excess of natural levels (*Sternbeck et al.*, 2002). Emission rates of trace elements such as Pb, Br, Zn, Cu, Si, Ca, and P for diesel exhaust are found to be higher than those for gasoline (*Cadle et al.*, 1999). Since zinc dithiophosphate is a standard anti-wear and anti-

oxidant additive in lubricating oils, zinc and phosphorus are present in the motor vehicle exhaust (*Cadle et al.*, 1999). Similarly, calcium and magnesium are found in motor oil as detergent additives and copper as an antioxidant, and therefore these species are also present in vehicle exhaust (*Cadle et al.*, 1999).

Many air quality models that account for the ambient concentrations due to primary emissions from motor vehicles use atmospheric transport calculations, which rely on measurements made while the vehicles are operated on a chassis dynamometer (*Fraser et al.*, 1999). However, extrapolating from dynamometer tests to real world conditions is complicated by differences between laboratory and on-road vehicle conditions (type, maintenance, operating range), exhaust dilution ratios and driving behavior. Therefore, emission measurements in conventional dynamometric tests alone are not sufficient to fully address this problem. In order to do so, studies need to be performed under realistic driving conditions in environments where the contribution from other emission sources is eliminated. As an alternative, the contribution of primary emissions from motor vehicles to $PM_{2.5}$ concentrations can be estimated based on emission measurements made as the vehicle fleet is operated in a roadway tunnel. These measurements can be related to ambient air quality via organic molecular tracer techniques and receptor modeling techniques. Measurements in traffic tunnels have been used successfully for quantifying emissions of a large number of particulate pollutants by several researchers (*Fraser et al.*, 1999; *Sternbeck et al.*, 2002; *McGaughey et al.*, 2004).

We were planning to perform a tunnel sampling and analysis study in a roadway tunnel in Houston, TX as part of this thesis, however were unable to get the permission of access to the tunnel due to the construction projects going on in the tunnel. When the

construction is completed in the tunnel and the permission is given by the City of Houston, this project might be started. This study will report a comprehensive characterization of the individual organic species and metals emitted from motor vehicles in particle phase and to determine the detailed source signatures of vehicular emissions. Air samples will be collected in the Washburn Tunnel, which runs under the Houston Ship Channel and is the only vehicle tunnel currently in operation in the state of Texas. Samples will be analyzed for organics and metal content of PM2.5 to get more detailed and accurate chemical composition profiles for vehicle emissions. Chemical composition profiles will be a valuable data source to perform receptor modeling in order to quantify contributions of different types of vehicle emissions, e.g. diesel and gasoline exhaust emissions. The particle number and the chemically speciated, size-segregated, particle distributions can also be measured.

Secondary Organic Aerosols

Source apportionment methods can be extended to understand and quantify the relative contribution of biogenic and anthropogenic components to the secondary aerosols using photochemical air quality models. Since the dependence of secondary organic aerosol (SOA) on other reactive species, reactive organic gases and NOx levels, and the speciated SOA compositions are not well understood, such data may significantly improve the accuracy of model predictions of fine particulate matter. Eulerian photochemical grid models are usually well suited to modeling secondary pollutants because they account for chemical interactions between sources.

Appendix A

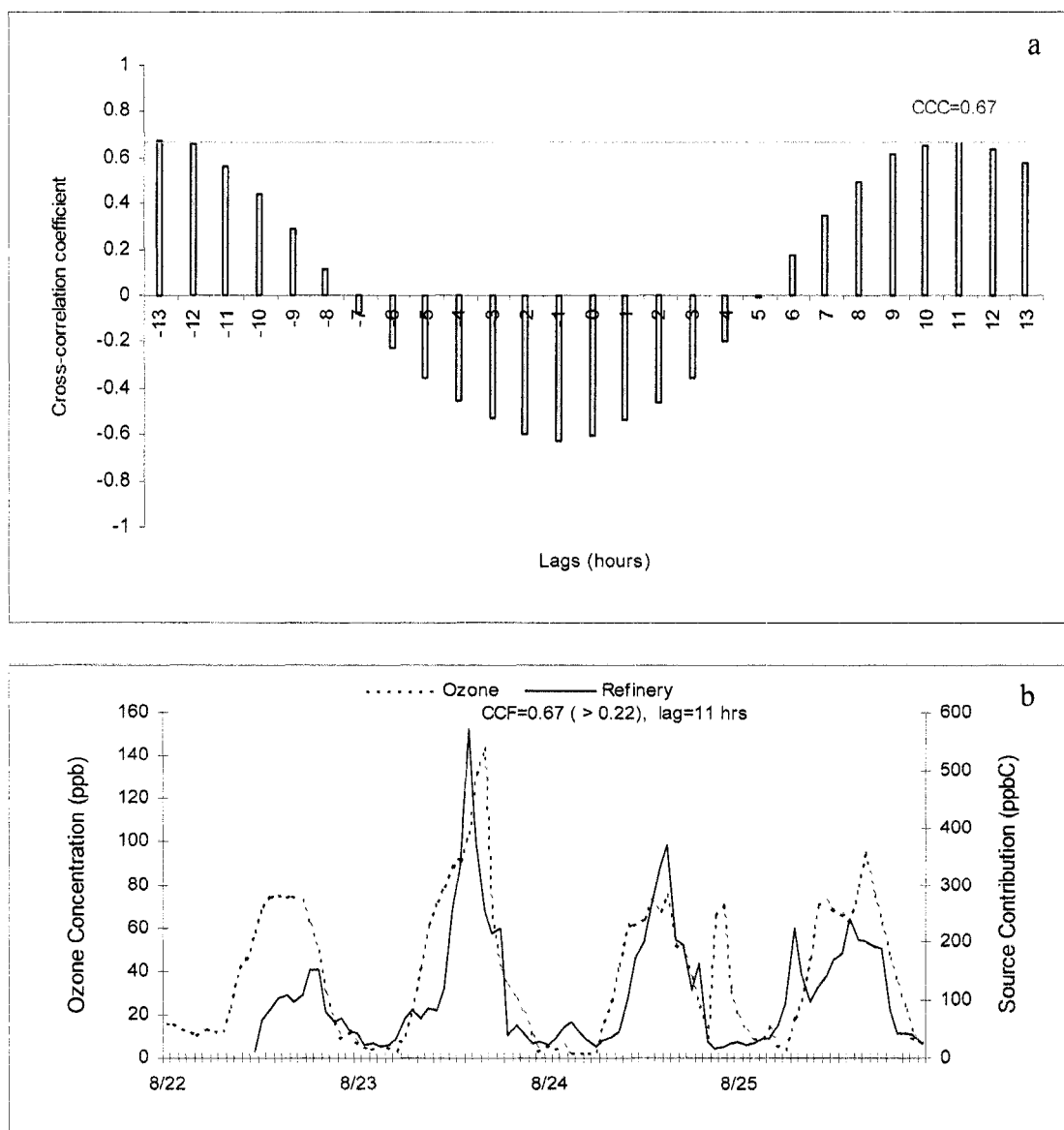## Additional Results of the Ozone Time Series Analysis

Figure A.1. Cross correlation function between ozone and refinery emissions time series for the same period at Wallisville (a), and 1-hour ozone time series and lagged contributions of refinery emissions source at Wallisville (b).
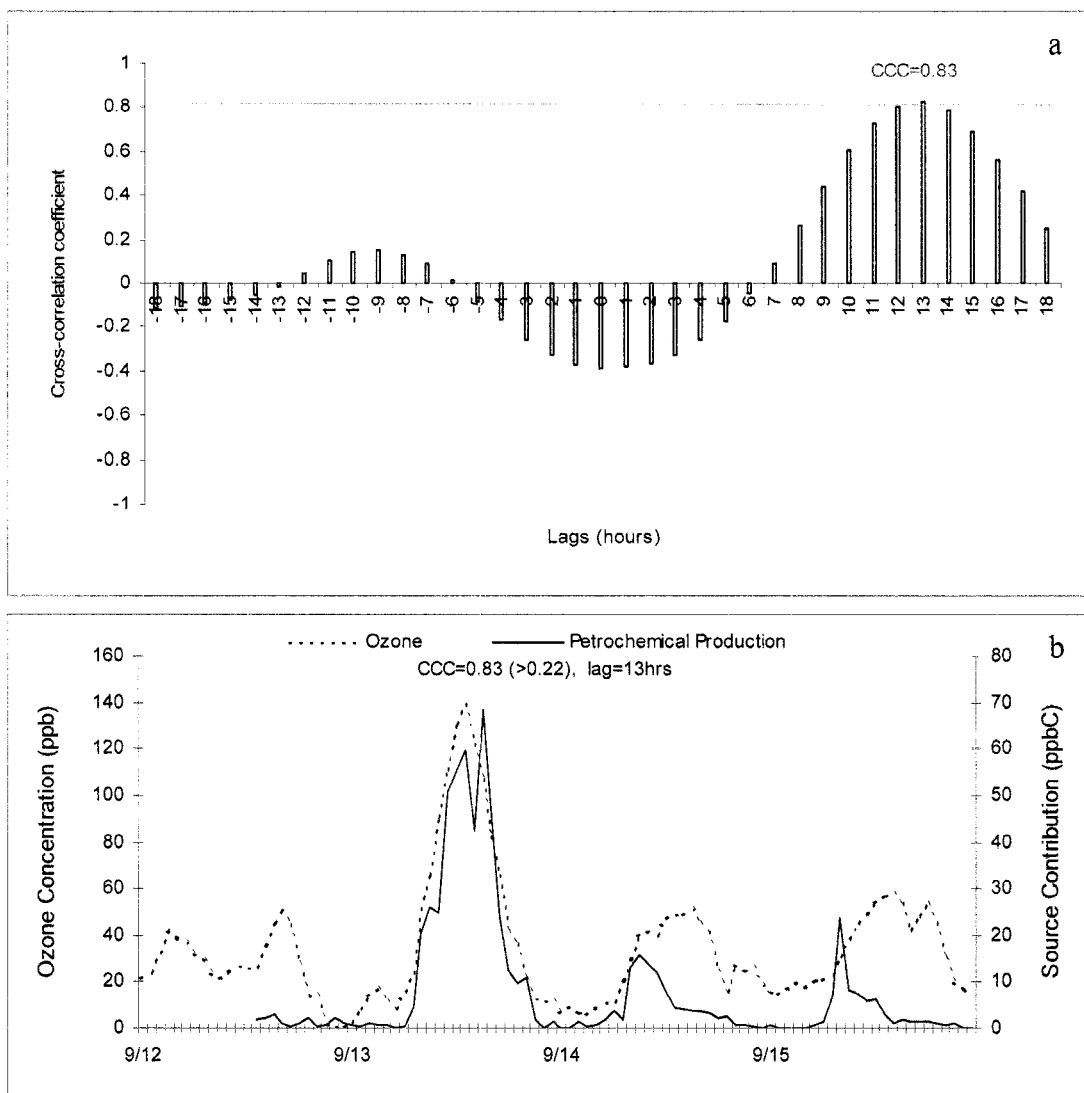
Figure A.2. Cross correlation function between ozone and petrochemical production time series for the same period at Wallisville (a), and 1-hour ozone time series and lagged contributions of petrochemical production source at Wallisville (b).
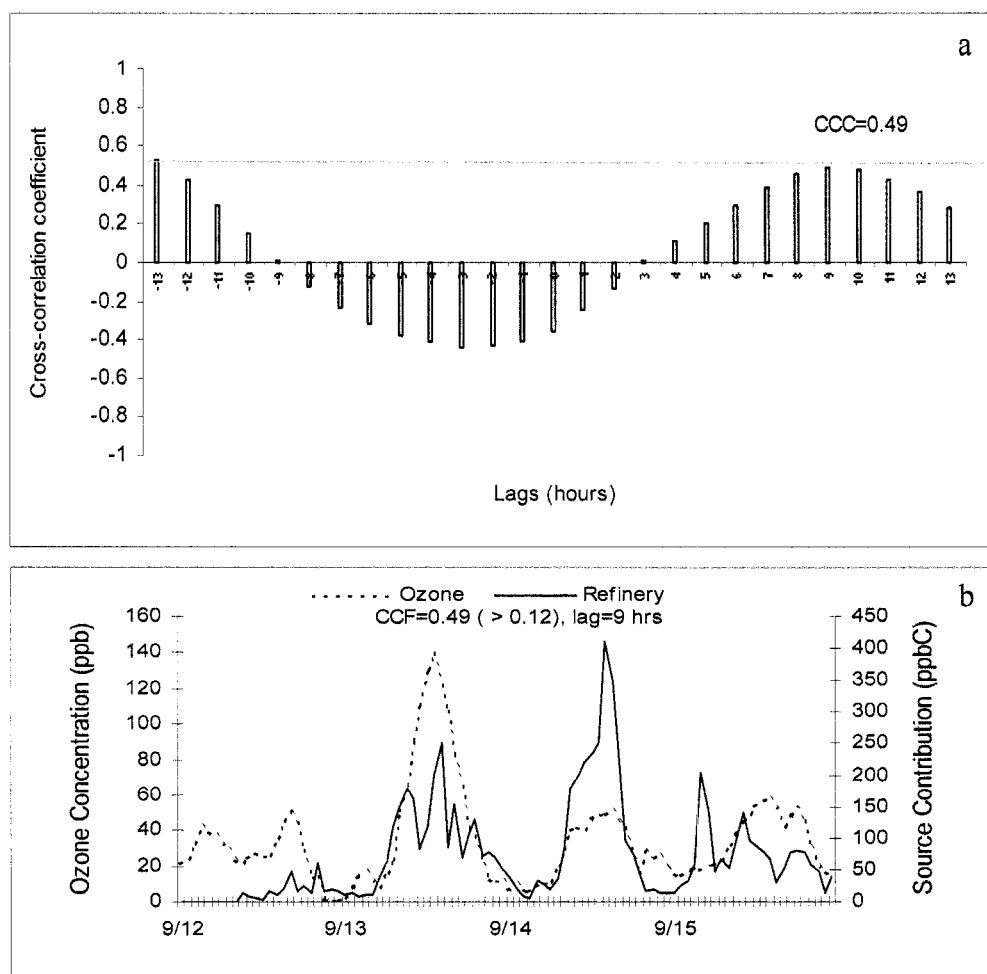
Figure A.3. Cross correlation function between ozone and refinery emissions time series for the same period at Wallisville (a), and 1-hour ozone time series and lagged contributions of refinery emissions source at Wallisville (b).
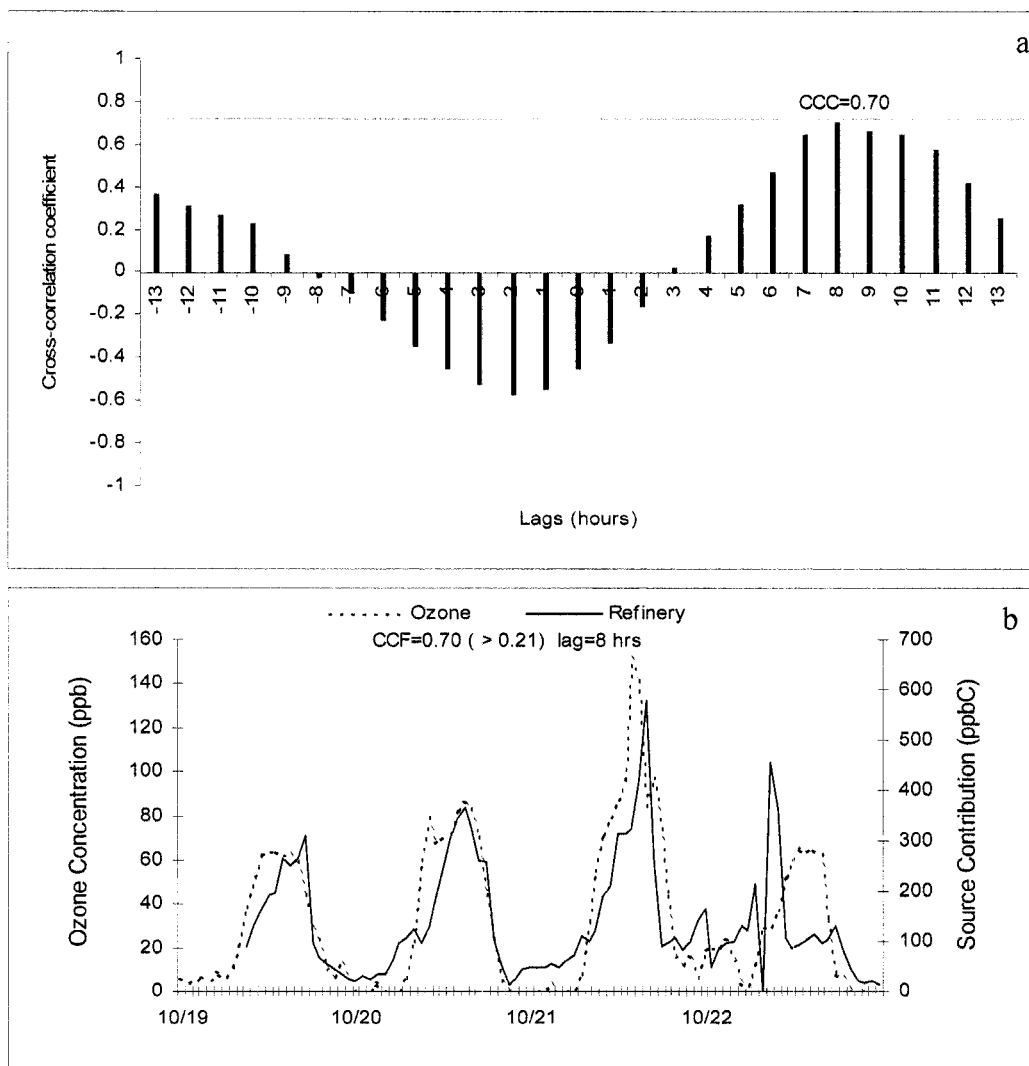
Figure A.4. Cross correlation function between ozone and refinery emissions time series for the same period at Wallisville (a), and 1-hour ozone time series and lagged contributions of refinery emissions source at Wallisville (b).
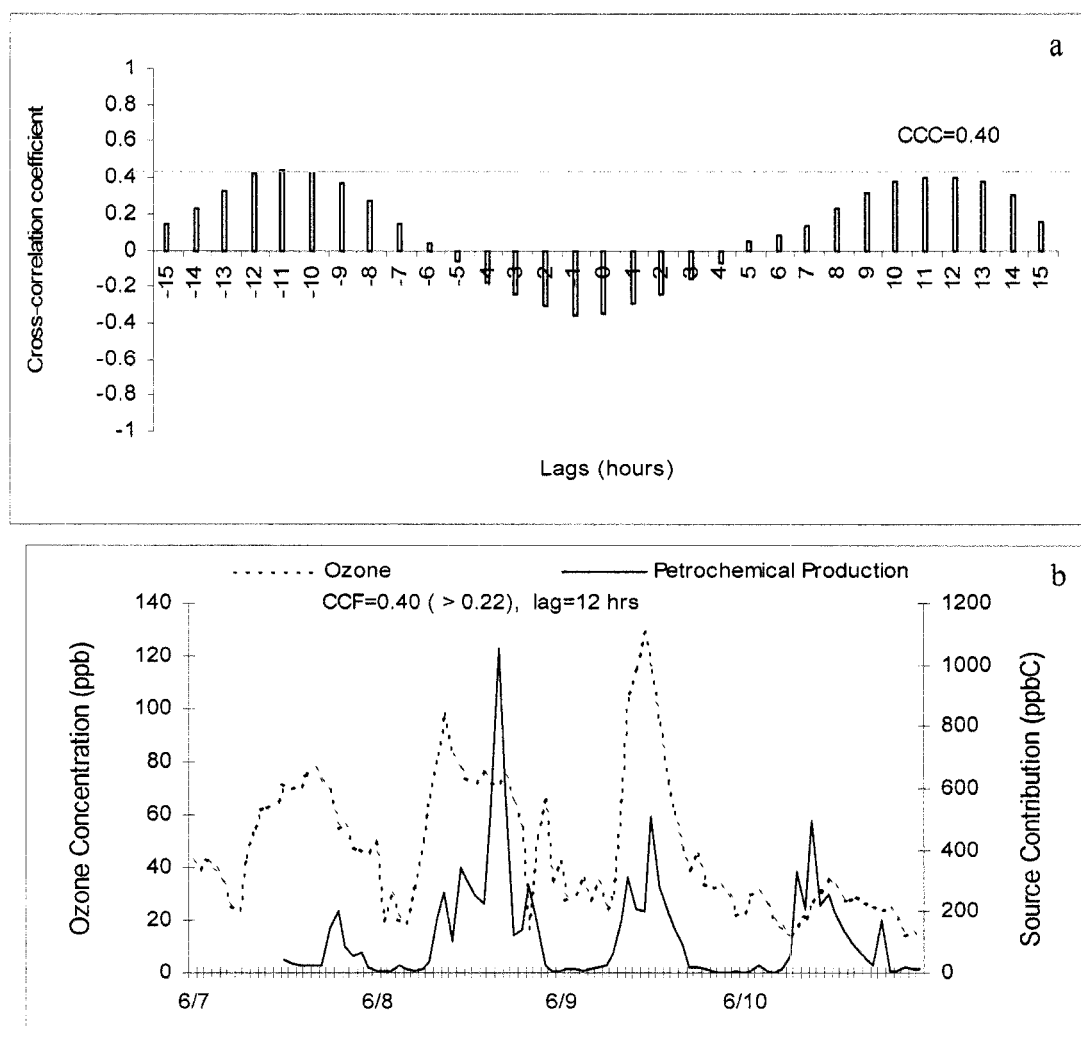
Figure A.5. Cross correlation function between ozone and petrochemical production time series for the same period at Lynchburg (a), and 1-hour ozone time series and lagged contributions of petrochemical production source at Lynchburg (b).
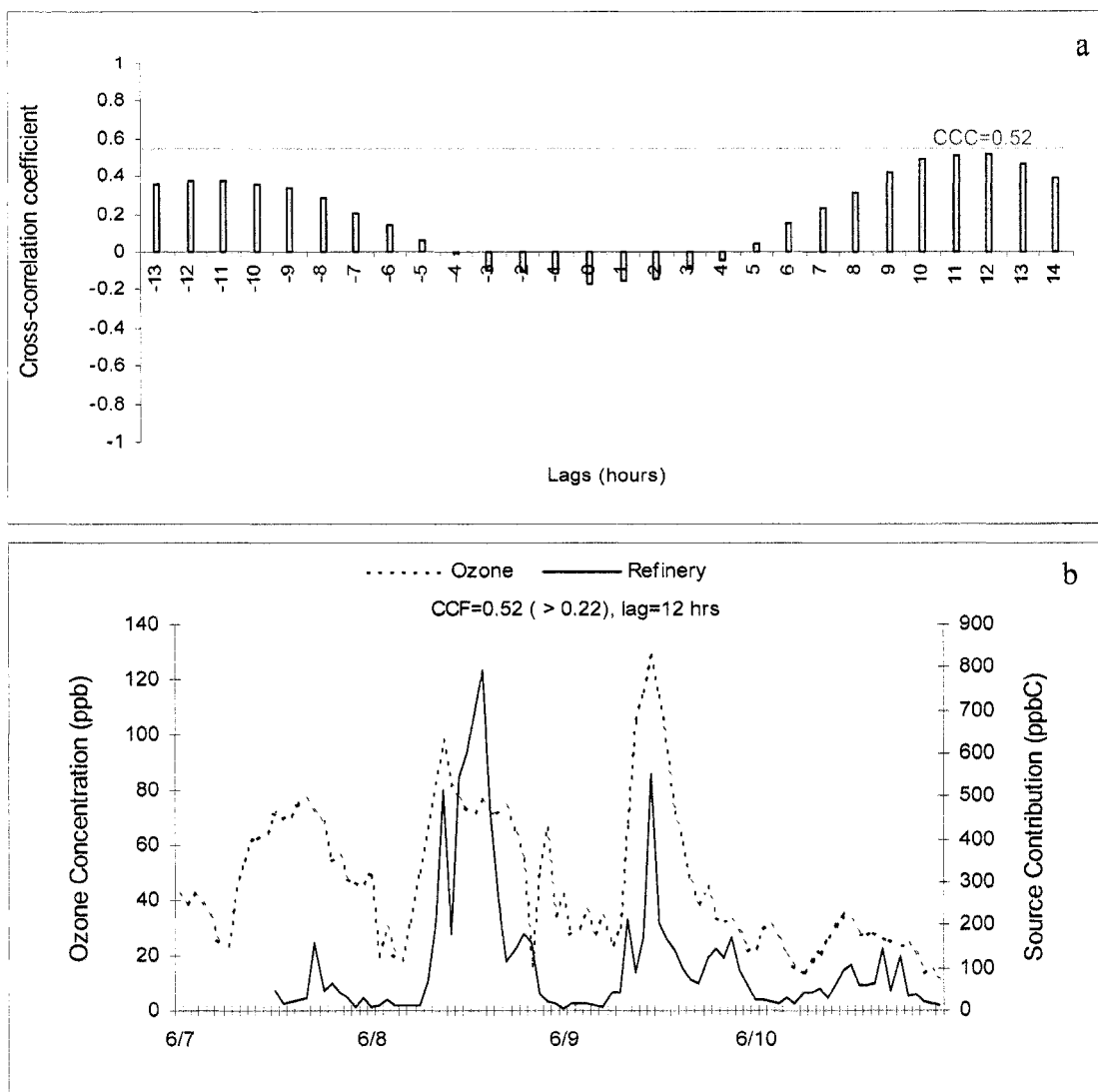
Figure A.6. Cross correlation function between ozone and refinery emissions time series for the same period at Lynchburg (a), and 1-hour ozone time series and lagged contributions of refinery emissions source at Lynchburg (b).

Figure A.7. Cross correlation function between ozone and gasoline emissions time series for the same period at Lynchburg (a), and 1-hour ozone time series and lagged contributions of gasoline emissions source at Lynchburg (b).

Figure A.8. Cross correlation function between ozone and refinery emissions time series for the same period at Lynchburg (a), and 1-hour ozone time series and lagged contributions of refinery emissions source at Lynchburg (b).
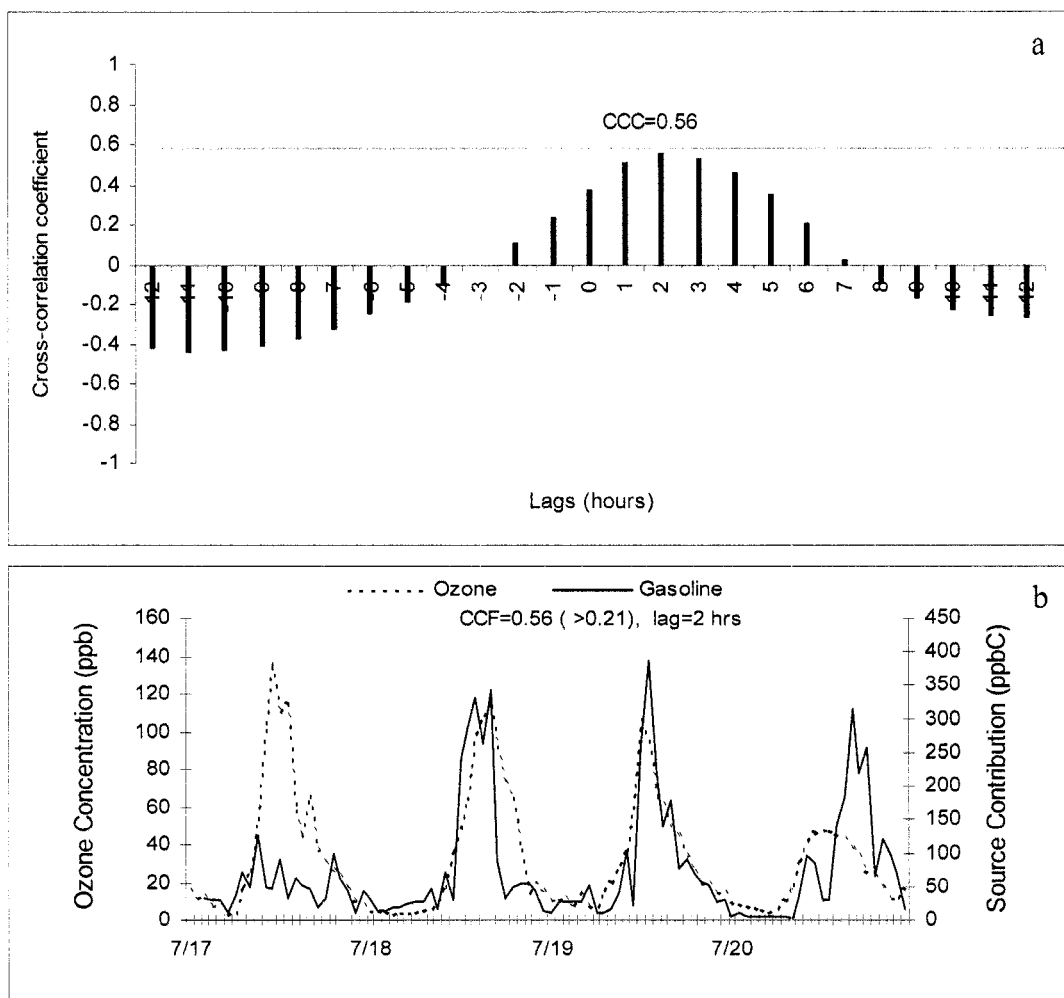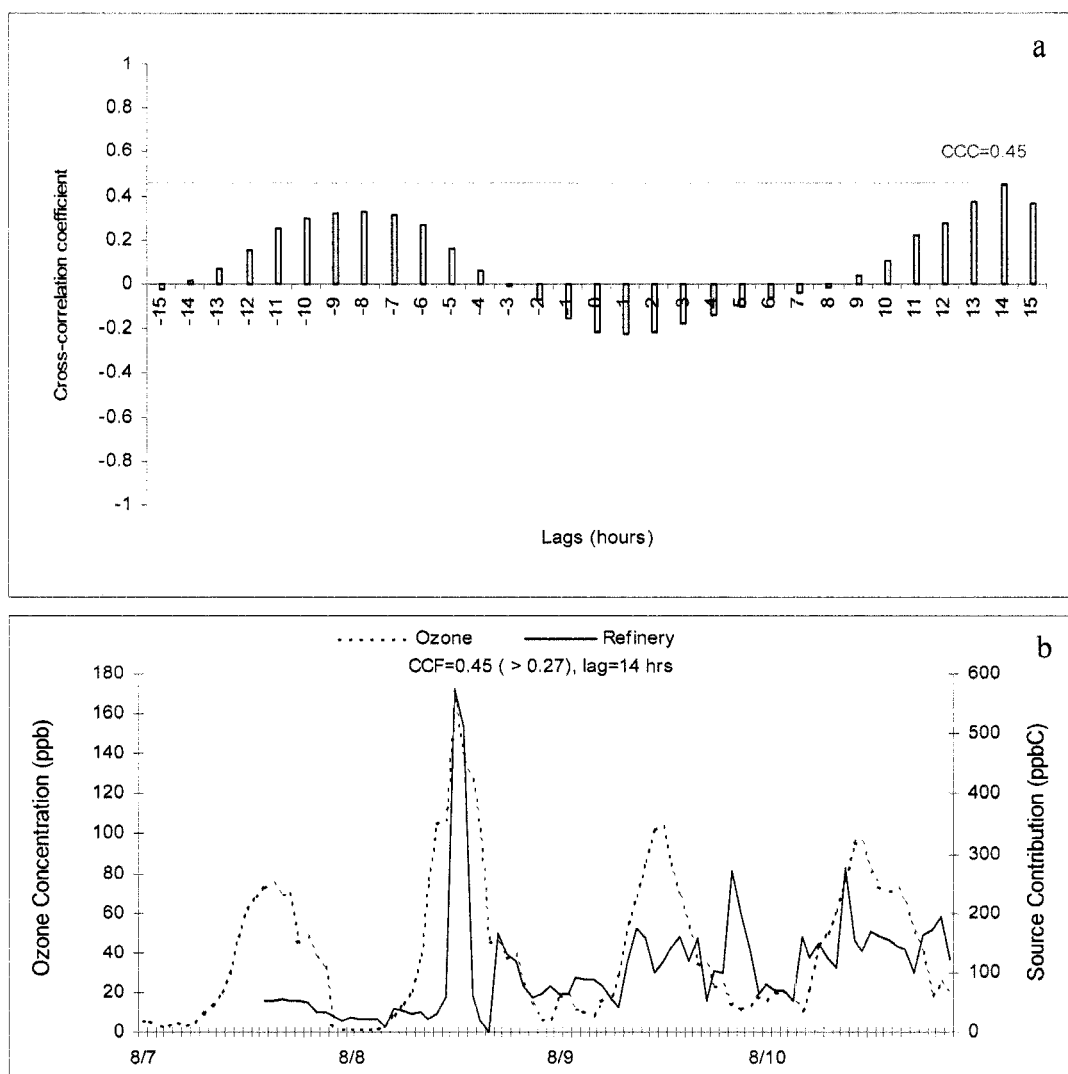
Figure A.9. Cross correlation function between ozone and refinery emissions time series for the same period at Lynchburg (a), and 1-hour ozone time series and lagged contributions of refinery emissions source at Lynchburg (b).
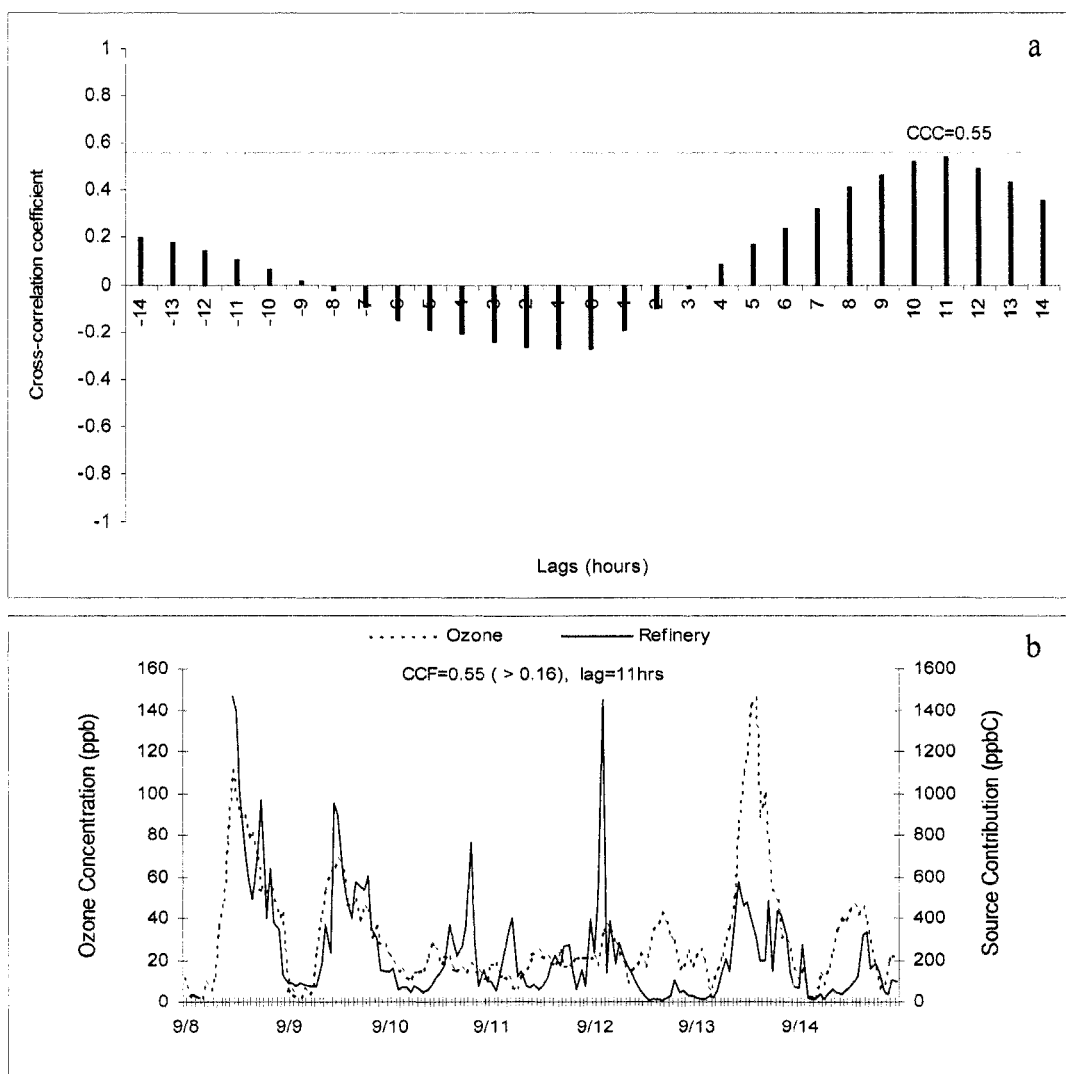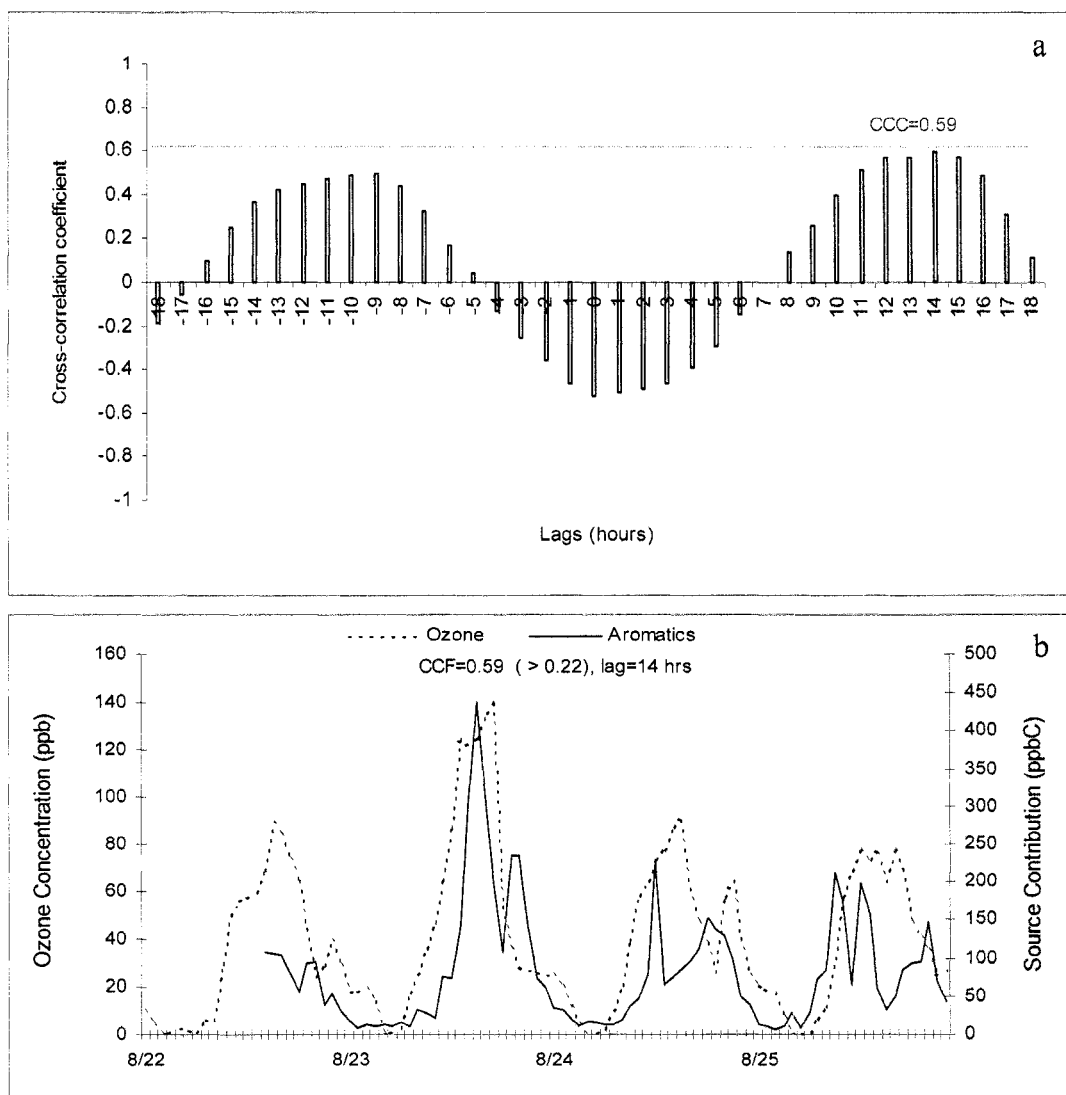
Figure A.10. Cross correlation function between ozone and aromatics emissions time series for the same period at HRM-3 (a), and 1-hour ozone time series and lagged contributions of aromatics emissions source at HRM-3 (b).

References

Allen, D., Murphy, C., Kimura, Y., Vizuete, W., Edgar, T., Jeffries, H., Kim, B-K., Webster, M., Symons, M. Variable industrial VOC emissions and their impact on ozone formation in the Houston Galveston area. Final Report, Texas Environmental Research Consortium Project H-13, 2004. www.harc.edu/harc/Projects/AirQuality/Projects/Status/H13.aspx

Anderson, M.J., Miller, S.L., Milford, J.B. Source apportionment of exposure to toxic volatile organic compounds using positive matrix factorization. *J. Exp. Anal. .Environ. Epidemiology,* 1, 295-307, 2001.

Andreae, M.O. Soot carbon and excess fine potassium: Long-range transport of combustion-derived aerosols, *Science,* 220, 1148-1151, 1983.

Antilla, P., Paatero, P., Tapper, U., Jarvinen, O. Source Identification of bulk wet deposition in Finland by Positive Matrix Factorization. *Atmos. Environ.,* 29, 1705-1718, 1995.

Ashbaugh, L.L., Malm, W.C., Sadeh, W.Z. A Residence time probability analysis of sulfur concentrations at Grand Canyon National Park. *Atmos. Environ,* 19, 1263-1270, 1985.

Baldwin, A.C. Heterogeneous reactions of sulfur dioxide with carbonaceous particles, *Int. J. Chem. Kinetics,* 14, 269-277, 1982.

Begum, B.A., Kim, E., Biswas, S.K., Hopke, P.K. Investigation of sources of atmospheric aerosol at urban and semi-urban areas in Bangladesh. *Atmos. Environ.* 38, 3025-3038, 2004.

Begum, B.A., Kim, E., Jeong, C.H., Lee, D.W., Hopke, P.K. Evaluation of the potential source contribution function using the 2002 Quebec forest fire episode. *Atmos. Environ.* 39, 3719-3724, 2005.

Berkowitz, C.M., Jobson, T., Jiang, G.F., Spicer, C.W., Doskey, P.V. Chemical and meteorological characteristics associated with rapid increases of O_3 in Houston, Texas *J. Geophys. Res.-Atmos.*, 109 (D10) Art. No. D10307, 2004.

Blake, N.J., Blake, N.R., Chen, T-Y., Collins Jr., J.E., Sachse, G.W., Anderson, B.E., Rowland, F.S. Distribution and seasonality of selected hydrocarbons and halocarbons over the western Pacific basin during PEM-West A and PEM-West B, *J. Geophys. Res.*, 102, 28315-28331, 1997.

Britton, L.G., Clarke, A.G. Heterogeneous reactions of sulfur-dioxide and SO_2-NO_2 mixtures with a carbon soot aerosol. *Atmos. Environ.*, 14, 829-839, 1980.

Brodzinsky, R., Chang, S.G., Markowitz, S.S., Novakov, T. Kinetics and mechanism for the catalytic-oxidation of sulfur-dioxide on carbon in aqueous suspensions, *J. Phys. Chem.*, 84, 3354-3358, 1980.

Brown, S.G., Reid, S.B., Roberts, P.T., Buhr, M.P., Funk, T.H. Reconciliation of the VOC and NOx Emission Inventory with ambient data in the Houston, Texas region. 13th Annual Emission Inventory Conference "Working for Clean Air in Clearwater, Clearwater, FL, 2004.

Brown, S.G.; Hafner, H.R. Source apportionment of VOCs in the Houston, TX area.

NARSTO Emission Inventory Workshop, Austin, TX, 2003.

ftp://ftp.cgenv.com/pub/downloads/emissionsworkshop/workshop2003/air.html

Buzcu, B., Fraser, M.P., Kulkarni P., Chellam S. Source identification and apportionment

of fine particulate matter in Houston, TX using positive matrix factorization.

Environ. Eng. Sci. 20, 533-545, 2003.

Buzcu B., Fraser, M.P. Source identification and apportionment of volatile organic

compounds in Houston, TX. *Atmos. Environ.*, in press, 2006

Buzcu, B., Yue, Z.W., Fraser, M.P., Nopmongcol, U., Allen, D.T. Secondary Particle

Formation and Evidence of Heterogeneous Chemistry During A Wood Smoke

Episode in Texas. *J. Geophys. Res –Atmos.*, *in press,* 2006.

Cachier H.L.C., Pertuisot, M.H., Gaudichet, A., Echalar, F., Lacaux, J.P. African fire

particulate emissions and atmospheric influence, *Biomass Burning and Global

Change*, 1, 428-440, 1996.

Cadle, S.H., Mulawa, P.A., Hunsanger, E.C., Nelson, K., Ragazzi, R.A., Barrett, R.,

Gallagher, G.L., Lawson, D.R., Knapp, K.T., Snow, R. Composition of light-duty

motor vehicle exhaust particulate matter in the Denver, Colorado area. *Environ.

Sci. Technol.*, 33, 2328-2339, 1999.

Cardelino, C., Chang, W., Chang, M. E. Comparison of emissions inventory estimates

and ambient concentrations of ozone precursors in Atlanta, Georgia. In *The

Emissions Inventory: Applications and Improvement, Proceedings of an*

International Specialty Conference; Raleigh, NC, 1994; *VIP45*, Air & Waste Management Association: Pittsburgh, PA, 1995; pp 195-206.

Carter W.P.L. Development of ozone reactivity scales for volatile organic compounds. Report prepared for the U.S. Environmental Protection Agency, Research Triangle Park, NC, EPA-600/3-91-050, 1991.

Carter W.P.L. Development of ozone reactivity scales for volatile organic compounds. *J. Air & Waste Manage. Assoc.*, 44, 881-899, 1994.

Chang, C.C. Infrared studies of SO_2 on gamma-alumina. *J. Catal.* 53, 374-385, 1978.

Cheng, R.T., Corn, M., Frohliger, J.O. Contributions to the reaction kinetics of water soluble aerosols and SO_2 in air at ppm concentrations. *Atmos. Environ.*, 5, 987-1008, 1971.

Chinkin, L.R., Korc, M.E., Janssen, M. Comparison of emissions inventory and ambient concentration ratios of NMOC, NOx , and CO in the Lake Michigan Air Quality Region. In *The Emissions Inventory: Applications and Improvement, Proceedings of an International Specialty Conference,* Raleigh, NC, 1994; *VIP-45*, Air & Waste Management Association: Pittsburgh, PA, 1995; pp 238-249.

Chun, K.C., Quon, J.E. Capacity of ferric oxide particles to oxidize sulfur dioxide in air. *Environ. Sci. Technol.*, 7, 532-538, 1973.

Crutzen, P.J., Andreae M.O. Biomass burning in the tropics: Impact on atmospheric chemistry and biogeochemical cycles, *Science*, 250, 1669-1678, 1990.

Dennis, A., Fraser, M.P., Anderson, S., Allen, D.T. Air pollutant emissions associated with forest, grassland, and agricultural burning in Texas, *Atmos. Environ.*, 36, 3779-3792, 2002.

Dentener, F.J., Carmichael, G.R., Zhang, Y., Lelieveld, J., Crutzen, P.J. Role of mineral aerosol as a reactive surface in the global troposphere. *J. Geophys. Res.*, 101, 22869-22889, 1996.

Dlugi, R. SO_2 oxidation in aerosol particles and droplets. *J. Aerosol Sci.*, 14, 292-297, 1983.

Draxler, R.R., Rolph, G.D. HYSPLIT (HYbrid Single-Particle Lagrangian Integrated Trajectory) Model access via NOAA ARL READY Website (http://www.arl.noaa.gov/ready/hysplit4.html). NOAA Air Resources Laboratory, Silver Spring, MD, 2003.

Estes, M., Smith, J., Price, J., Cantu, G., Boyer, D., Fang, Z., Neece, J. Preliminary emission adjustment factors using automated gas chromatography data. Attachment 7, Technical Support Document of the Texas Commision on Environmental Quality, 2002.

ftp://ftp.tnrcc.state.tx.us/pub/OEPAA/TAD/Modeling/HGAQSE/Modeling/Doc/TSD_PH ASE1/attachment7-agc_ei_adjustment.pdf

Fine, P.M., Cass, G.R., Simoneit, B.R.T. Organic compounds in biomass smoke from residential wood combustion: Emissions characterization at a continental scale, *J. Geophys. Res.*, 107, Art. No. 8346, 2002.

Fraser, M.P., Cass, G.R. Simoneit, B.R.T. Particulate organic compounds emitted from motor vehicle exhaust and in the urban atmosphere. *Atmos. Environ.*, 33, 2715-2724, 1999.

Fraser, M.P., Lakshmanan, K. Using levoglucosan as a molecular marker for the long-range transport of biomass combustion aerosols. *Environ. Sci. Technol.*, 34, 4560-4564, 2002.

Fraser, M.P., Lakshmanan, K., Fritz, S.G., Ubanwa, B. Variation in composition of fine particulate emissions from heavy-duty diesel vehicles, *J. Geophys. Res.*, 107, Art. No. 8346, 2002.

Friedlander, S.K. Chemical element balances and identification of air pollution sources. *Environ. Sci. Technol..*, 7, 235-273, 1973.

Fujita, E.M., Crooes, B.E., Bennett, C.L., Lawson, D.R., Lurmann, F., Main, H.H. Comparison of emission inventory and ambient concentration ratios of CO, NMOG, and NOx in California's South Coast Air Basin. *J. Air & Waste Manag. Assoc.*, 42, 264-276, 1992.

Fujita, E.M., Watson, J.G., Chow, J.C., Lu, Z. Validation of the chemical mass balance receptor model applied to hydrocarbon source apportionment in the Southern California Air Quality Study. *Environ. Sci. Technol.*, 28, 1633-1649, 1994.

Fujita, E.M., Lu, Z., Robinson, N.F., Watson, J.G. VOC source apportionment for the coastal oxidant assessment for Southeast Texas. Draft Final Report prepared for the Texas Natural Conservation Commission by Desert Research Institute, 1995.

Fujita, E.M. Hydrocarbon source apportionment for the 1996 Paso del Norte ozone study. *Sci. Total Environ.* 276, 171-184, 2001.

Fujita, E.M., Campbell, D.E., Zielinska, B., Sagebiel, J.C., Bowen, J.L., Goliff, W.S., Stockwell, W.R., Lawson, D.R. Diurnal and weekday variations in the source contributions of ozone precursors in California's South Coast Air Basin. *J. Air & Waste Manage. Assoc.*, 53, 844-863, 2003.

Gao, N., Cheng, M-D., Hopke, P. Potential source contribution function analysis and source apportionment of sulphur species measured at Rubidoux, CA during the Southern Califirnia Air Quality Study, 1987. *Anal. Chimica Acta*, 277, 369-380, 1993.

Gasparini, R., Li, R.J., Collins, D.R. Integration of size distributions and size-resolved hygroscopicity measured during the Houston Supersite for compositional categorization of the aerosol, *Atmos. Environ.*, 38, 3285-3303, 2004.

Goodman, A.L., Underwood, G.M., Grassian, V.H. A laboratory study of the heterogeneous reaction of nitric acid on calcium carbonate particles. *J. Geophys. Res. –Atmos.*, 105, 29053-29064, 2000.

Goodman, A.L., Li, P., Usher, C.R., Grassian, V.H. Heterogeneous uptake of sulfur dioxide on aluminum and magnesium oxide particles. *J. Phys. Chem. A.*, 105, 6109-6120, 2001.

Gouw, J.A., Middlebrook, A.M., Weineke, C., Goldan, P.D., Kuster, W.C., Roberts, J.M., Fehsenfeld, F.C., Worsnop, D.R., Canagaratna, M.R., Pszenny, A.A.P, Keene, W.C., Marchewka, M., Bertman, S.B., Bates, T.S. Budget of organic

carbon in a polluted atmosphere: Results from the New England Air Quality Study in 2002. *J. Geophys. Res. – Atmos.*, 110, Art. No. D16305, 2005.

Hagerman, L.M., Aneja, V.P., Lonneman, W.A. Characterization of non-methane hydrocarbons in the rural southeast United States. *Atmos. Environ.*, 31, 4017-4038, 1997.

Harley R.A., Hannigan M.P., Cass G.R. Respeciation of organic gas Emissions and the detection of excess unburned gasoline in the atmosphere. *Environ. Sci. Technol.*, 26, 2395-2408, 1992.

Harley, R.A., Cass, G.R. Modeling the atmospheric concentrations of individual volatile organic compounds. *Atmos. Environ.*, 29, 905-922, 1995.

Harley, R.A., Sawyer, R.F., Milford, J.B. Updated photochemical modeling for California's South Coast Air Basin: Comparison of chemical mechanisms and motor vehicle emission inventories. *Environ. Sci. Technol.*, 31, 2829-2839, 1997.

Haste, T.L., Chinkin, L.R., Kumar, N., Lurmann, F.W., Hurwitt, S.B. Use of ambient data collected during IMS95 to evaluate a regional emission inventory for the San Joaquin Valley. STI-997211-1800-FR, Final report prepared for the San Joaquin Valleywide Air Pollution Study Agency, c/o the California Air Resources Board, Sacramento, CA, by Sonoma Technology, Inc., Santa Rosa, CA, 1998.

Hays, M.D., Geron, C.D., Linna, K.J., Smith, N.D., Schauer, J.J. Speciation of gas-phase and fine particle emissions from burning of foliar fuels, *Environ. Sci. Technol.*, 36, 2281-2295, 2002.

Henry, R.C. Dealing with near colinearity in Chemical Mass Balance receptor models. *Atmos. Environ.,* 26A, 933-938, 1992.

Henry, R.C., Speigelman, C.C., Collins, J.F., Park, E-S. Reported emissions of volatile organic compounds are not consistent with observations. *Proc. Natl. Acad. Sci.* 94, 6596-6599, 1997.

Hildeman, L.M., Markowski, G.R., Cass, G.R. Chemical composition of emissions from urban sources of fine organic aerosol, *Environ. Sci. Technol.,* 25, 744-759, 1991.

Jang, M., Czoschke, N.M., Lee, S., Kamens, R.M. Heterogeneous atmospheric aerosol production by acid-catalyzed particle-phase reactions, *Science,* 298, 814-817, 2002.

Jang, M., Carroll, B., Chandramouli, B., Kamens, R.M. Particle growth by acid-catalyzed heterogeneous reactions of organic carbonyls on pre-existing aerosols. *Environ. Sci. Technol.,* 37, 3828-3837, 2003.

Javitz, H.S., Watson, J.G., Robinson, N.F. Performance of Chemical Mass Balance model with simulated local-scale aerosols. *Atmos. Environ.,* 22, 2309-2322, 1988.

Jiang, W., Singleton, D.L., Hedley, M., McLaren, R., Dann, T., Wang, D. Comparison of organic compound compositions in the emissions inventory and ambient data for the Lower Fraser Valley *J. Air & Waste Manage. Assoc.* 47, 851-860, 1997.

Jobson, B.T., Berkowitz, C.M., Kuster, W.C., Goldan, P.D., Williams, E.J., Fesenfeld, F.C., Apel, E.C., Karl, T., Lonneman, W.A., Riener, D. Hydrocarbon source signatures in Houston, TX: Influence of the petrochemical industry. *J. Geophys. Res. – Atmos.,* 109, Art. No. D24305, 2004.

Jolly, J.R., Mercado, F.I., Sullivan, D.W. A comparison of ambient and emission VOC to NOx ratios at two monitors in Houston, TX. 13th Annual Emission Inventory Conference "Working for Clean Air in Clearwater, Clearwater, FL, 2004.

Jorquera, H., Rappengluck, B. Receptor modeling of ambient VOCs at Santiago, Chile. *Atmos. Environ.*, 38, 4243-4263, 2004.

Judeikis, H.S., Stewart, T.B., Wren, A.G. Laboratory studies of heterogeneous reactions of SO_2. *Atmos. Environ.*, 12, 1633-1641, 1978.

Junquera, V., Russell, M.M., Vizuete, W., Kimura, Y. Allen, D.T. Wildfires in eastern Texas in August and September 2000: Emissions, aircraft measurements and impact on photochemistry, *Atmos. Environ.*, 39, 4983-4996, 2005.

Juntto, S., Paatero, P. Analysis of daily precipitation data by positive matrix factorization, *Environmetrics*, 5,127-144, 1994.

Kahl, J. A cautionary note on the use of air trajectories in interpreting atmospheric chemistry measurements. *Atmos. Environ.*, 27A, 3037-3038, 1993.

Karge, H.G., Dalla Lana, I.G. Infrared studies of SO_2 adsorption on a claus catalyst by selective poisoning of sites. *J. Phys. Chem.*, 88, 1538-1543, 1984.

Katzenstein, A.S., Doezema, L.A., Simpson, I.J., Blake, D.R., Sherwood Rowland, F. Extensive regional atmospheric hydrocarbon pollution in the southwestern United States. *Proc. Natl. Acad. Sci.*, 100, 11975-11979, 2003.

Keene, W.C., Sander, R., Pszenny, A.A.P. Aerosol pH in the marine boundary layer: A review and model evaluation. *J. Aerosol. Sci.*, 29, 339-356, 1998.

Kim, E., Hopke, P.K., Edgerton, E. Source identification of Atlanta aerosol by positive matrix factorization. . *J. Air & Waste Manage. Assoc.*, 53, 731-739, 2003.

Kim, E., Hopke, P.K. Source apportionment of fine particles at Washington, DC utilizing temperature resolved carbon fractions. *J. Air & Waste Manage. Assoc.*, 54, 773-785, 2004.

Kleinman, L.I., Daum, P.H., Imre, D., Lee, Y.-N., Nunnermacker, L.J., Springston, S.R., Weinstein-Lloyd, J., Rudolph, J. Ozone production rate and hydrocarbon reactivity in 5 urban areas: A cause of high ozone concentration in Houston. *Geophys. Res. Lett.*, Art. No. 1467, 2002.

Korc, M.E., Jones, C.M., Chinkin, L.R., Main, H.H., Roberts, P.T., Blachard, C. Use of PAMS data to evaluate the Texas coast emission inventory. Work assignment 2-95, EPA Contract No. 68D30020, STI-94520-1558-FR, Final report prepared for U.S. Environmental Protection Agency, Research Triangle Park, NC, by Sonoma Technology, Inc., Santa Rosa, CA, 1995.

Krischke, U., Staubes, R., Brauers, T., Gautrois, M., Burkert, J., Stobener, D., Jaeschke, W. Removal of SO_2 from marine boundary layer over the Atlantic Ocean: A case study on the kinetics of the heterogeneous S(IV) oxidation on marine aerosols. *J. Geophys. Res.*, 105, 14412-14422, 2000.

Lei, L., Chen, Z., Ding, J., Zhu, T., Zhang, Y. A DRIFTS study of SO_2 oxidation on the surface of $CaCO_3$ particles. *Spectros. Spec. Anal.*, 24, 1556-1559, 2004.

Liberti, A., Brocco, D., Possanzini, M. Adsorption and oxidation of sulfur-dioxide on particles, *Atmos. Environ.*, 12, 255-261, 1978.

Luria, M., Sievering, H. Heterogeneous and homogeneous oxidation of SO2 in the remote marine atmosphere. *Atmos. Environ.*, 25, 1489-1496, 1991.

Mamane, Y., Gottlieb, J. The study of heterogeneous reactions of carbonaceous particles with sulfur and nitrogen oxides using a single particle approach, *J. Aerosol Sci.*, 20, 575-584, 1989.

Mamane, Y.; Pueschel, R F. Oxidation of SO_2 on the surface of fly ash particles under low relative humidity conditions. *Geophys. Res. Let.*, 6, 109-112, 1979.

Martin, M.A., Childers, J.W., Palmer, R.A .Fourier-transform infrared photoacoustic-spectroscopy characterization of sulfur-oxygen species resulting from the reaction of SO_2 with CaO and $CaCO_3$. *Applied Spectroscopy*, 41, 120-126, 1987.

Mazurek, M.A., Cass, G.R., Simoneit, B.R.T. Biological input to visibility-reducing aerosol particles in the remote arid southwestern United States, *Environ. Sci. Technol.*, 25, 684-694, 1991.

McGaughey, G.R., Desai, N.R., Allen, D.T., Seila, R.L., Lonneman, W.A., Fraser, M.P., Harley, R.A., Pollack, A.K., Ivy, J.M., Price, J.H. Analysis of motor vehicle emissions in a Houston tunnel during the Texas Air Quality Study 2000. *Atmos. Environ.*, 38, 3363-3372, 2004.

Miller, S.L., Anderson, M.J., Daly, E.P., Milford, J.B. Source apportionment of exposures to volatile organic compounds. I. Evaluation of receptor models using simulated exposure data. *Atmos. Environ.*, 36, 3629-3641, 2002.

Murphy, C.F., Allen, D.T. Hydrocarbon emissions from industrial release events in the

Houston-Galveston area and their impact on ozone formation. *Atmos. Environ.*,

39, 3785-3798, 2005.

Na, K., Kim, Y.P. Seasonal characteristics of ambient volatile organic compounds in

Seoul, Korea. *Atmos. Environ.*, 35, 2603-2614, 2001.

Na, K., Kim, Y.P., Moon, K.C., Moon, I., Fung, K. Concentrations of volatile organic

compounds in an industrial area of Korea. *Atmos. Environ.*, 35, 2747-2756, 2001.

Na, K., Kim, Y.P., Moon, K.C. Diurnal characteristics of volatile organic compounds in

the Seoul atmosphere. *Atmos. Environ.*, 37, 733-742, 2003.

Novakov, T., Chang, S.G., Harker, A.B. Sulfates as pollution particulates: catalytic

formation on carbon (soot) particles, *Science*, 186, 259-261, 1974.

Paatero, P. Least squares formulation of robust nonnegative factor analysis. *Chemom.

Intel. Lab. Sys.*, 37, 23-35, 1997.

Paatero, P. User's guide for positive matrix factorization programs PMF2 and PMF3,

2000. ftp://rock.helsinki.fi/pub/misc/pmf.

Paatero, P., Tapper, U. Analysis of Different Modes of Factor Analysis as Least Squares

Fit Problems. *Chemom. Intell. Lab. Syst.*, 18, 183-194, 1993.

Paatero, P., Tapper, U. Analysis of positive matrix factorization: A nonnegative factor

model with optimal utilization of error estimates of data values. *Environmetrics*

5, 111-126, 1994.

Poirot, R.L., Wishinski, P.R., Hopke, P.K., Polissar, A.V. Comparative Application of Multiple Receptor Methods to Identify Aerosol Sources in Northern Vermont. *Environ. Sci. Technol.*, 35, 4622-4636, 2001.

Ramadan, Z., Song, X-H, Hopke, P.K. Identification of sources of Phoenix aerosol by positive matrix factorization. *J. Air & Waste Manage. Assoc.*, 50, 1308-1320, 2000.

Robinson, M.S., Chavez, J., Velazquez, S., Jayanty, R.K.M. Chemical speciation of $PM_{2.5}$ fires of the coconino national collected during prescribed forest near Flagstaff, Arizona, *JA&WMA*, 54, 1112-1123, 2004.

Rogge, W.F., Hildemann, L.M., Mazurek, M.A., Cass, G.R., Simoneit, B.R.T. Sources of fine organic aerosol 4. Particulate abrasion products from leaf surfaces of urban plants, *Environ. Sci. Technol.*, 27, 2700-2711, 1993a.

Rogge, W.F., Hildemann, L.M., Mazurek, M.A., Cass, G.R., Simoneit, B.R.T. Sources of fine organic aerosol 3. Road dusts, tire debris and organometallic brake lining dust: Roads as sources and sinks, *Environ. Sci. Technol.*, 27, 1892-1904, 1993b.

Rogge, W.F., Hildemann, L.M., Mazurek, M.A., Cass, G.R. Sources of organic aerosol. 2. Noncatalyst and catalyst equipped automobiles and heavy-duty diesel trucks. *Atmos. Environ.*, 27, 636-651, 1993c.

Russell, M. M., Allen, D. T., Collins, D. R., Fraser, M. P. Daily, seasonal, and spatial trends in PM2.5 mass and composition in Southeast Texas, *Aerosol Sci. Tech.*, 38(S1), 14-26, 2004

Russell, M.M., Allen, D.T. Predicting Secondary Organic Aerosol Formation Rates in Southeast Texas, *J. Geophys. Res. – Atmos.*, in press, 2005.

Ryerson T.B., Trainer, M., Angevine, W.M., Brock, C.A., Dissly, R.W., Fehsenfeld F.C., Frost, G.J., Goldan, P.D., Holloway, J.S., Hubler, G., Jakoubek, R.O., Kuster, W.C., Neuman, J.A., Nicks, D.K., Parrish, D.D., Roberts, J.M., Sueper, D.T. Effect of petrochemical industrial emissions of reactive alkenes and Nox on tropospheric ozone formation in Houston, Texas. *J. Geophys. Res. – Atmos* 108 (D8), Art. No. 4249, 2003.

Salvador, P., Artinano, B., Alonso, D.G., Querol, X., Alastuey, A. Identification and characterization of sources of PM10 in Madrid (Spain) by statistical methods. *Atmos. Environ.*, 38, 435-447, 2004.

Sanders, E.B., Goldsmith, A.I., Seeman, J.I. A model that distinguishes the pyrolysis of D-glucose, D-fructose, and sucrose from that of cellulose. Application to the understandng of cigarette smoke formation. *J. Anal. App. Pyrolysis*, 66, 29-50, 2003.

Schauer J.J., Rogge, W.F., Hildemann, L.M., Mazurek, M.A., Cass, G.R. Source apportionment of airborne particulate matter using organic compounds as tracers. *Atmos. Environ.*, 30, 3837-3855, 1996.

Schauer, J.J., Kleeman, M.J., Cass, G.R., Simoneit, B.R.T. Measurement of emissions from air pollution sources. 1. C_1 through C_{29} organic compounds from meat charbroiling. *Environ. Sci. Technol.*, 33, 1566-1577, 1999.

Schauer, J.J., Kleeman, M.J., Cass, G.R., Simoneit, B.R.T. Measurement of emissions from air pollution sources. 3. C_1-C_{29} organic compounds from fireplace combustion of wood. *Environ. Sci. Technol.,* 35, 1716–1728, 2001.

Schauer, J.J., Kleeman, M.J., Cass, G.R., Simoneit, B.R.T. Measurement of emissions from air pollution sources. 5. C_1-C_{32} organic compounds from gasoline-powered motor vehicles. *Environ. Sci. Technol.,* 36, 1169–1180, 2002.

Schauer J.J., Fraser M.P., Cass G.R., Simoneit B.R.T. Source reconciliation of atmospheric gas-phase and particle-phase pollutants during a severe photochemical smog episode. *Environ. Sci. Technol.,* 36, 3806-3814, 2002.

Scheff, P.A., Wadden, R.A. Receptor modeling of volatile organic compounds. 1. Emission Inventory and Validation. *Environ. Sci. Tech.,* 27, 617-625, 1993.

Seinfeld, J.H., Pandis, S.N. Atmospheric Chemistry and Physics, Wiley Interscience, New York, 1998.

Shafizadeh, F., Furneaux, R.H., Cochran, T.G., Scholl, J.P., Sakai, Y. Production of levoglucosan and glucose from pyrolysis of cellulosic materials, *J. Appl. Polymer Sci.,* 23, 3525-3539, 2003.

Sillman, S. The relation between ozone, NOx and hydrocarbons in urban and polluted rural environments. *Atmos. Environ.,* 33, 1821-1845, 1999.

Song, X-H., Polissar, A.V., Hopke, P.K., 2001. Sources of fine particle composition in the northeastern US. *Atmos. Environ.* 35, 5277-5286.

Sternbeck, J., Sjodin, A., Andreasson, K. Metal emissions from road traffic and the influence of resuspension – results from two tunnel studies, *Atmos. Environ.*, 36, 4735-4744, 2002.

Stoeckenius, T., Jimenez, M. Reconciliation of an emission inventory with PAMS ambient monitoring data in the Mid-Atlantic region. Revised Final Report, prepared for Mid-Atlantic Regional Air Management Association by ENVIRON International Corporation, Novato, CA, 2000.

Stohl, A. Computation, accuracy and applications of trajectories – a review and bibliography. *Atmos. Environ.*, 32, 947-966, 1998.

Tartarelli, R., Davini, P., Morelli, F., Corsi, P. Interactions between SO_2 and Carbonaceous Particulates, *Atmos. Environ.*, 12, 289-293, 1978.

Tran, C., Yarwood, G., Pollack, A.K., Koo, B., Chandraker, P., Tana, C. Effect of hotsoak and diurnal emissions spatial allocation methodology on predicted ozone levels. Final Report, HARC Project H-8B, 2003. http://www.harc.edu/harc/Projects/AirQuality/Projects/ShowDocument.aspx?documentID=69

Texas Commission on Environmental Quality (TCEQ) Ambient air quality monitoring sites. 2005. http://www.tceq.state.tx.us/cgi-bin/compliance/monops/select_summary?region12.gif.

Texas Commision on Environmental Quality (TCEQ). Air emissions event report database. 2004. Accessed April 2006 at http://www2.tnrcc.state.tx.us/eer/main/index.cfm?fuseaction=searchForm.

Ullerstam, M., Vogt, R., Langer, S., Ljungstrom, E. The kinetics and mechanism of SO_2 oxidation by O_3 on mineral dust, *Physical Chemistry Chemical Physics*, 4, 4694-4699, 2002.

Ullerstam, M., Johnson, M.S., Vogt, R., Ljungstrom, E. DRIFTS and Knudsen cell study of the heterogeneous reactivity of SO_2 and NO_2 on mineral dust, *Atmos. Chem. Phys.*, 3, 2043-2051, 2003.

Underwood, G.M., Li, P., Grassian, V.H. A Knudsen cell study of the heterogeneous reactivity of nitric acid on oxide and mineral dust particles. *J. Phys. Chem. A.*, 105, 6609-6620, 2001.

Usher, C.R., Al-Hosney, H., Carlos-Cuellar, S., Grassian, V.H. A laboratory study of the heterogeneous uptake and oxidation of sulfur dioxide on mineral dust particles. *J. Geophys. Res.*, 107, No. D23, 4713, 2002.

U.S. Environmental Protection Agency. EPA 400-F-92-007, 1994.

U.S. Environmental Protection Agency. Enhanced Ozone Monitoring (PAMS). http://www.epa.gov/air/oaqps/pams/, 1999.

U.S. Environmental Protection Agency. National Air Quality and Emissions Trends Report 1998 EPA 454/R-00-003, U.S. EPA, Washington, D.C., 2000.

Vivanco, M.G., Andrade, M. de F. Validation of the emission inventory in the Sao Paulo Metropolitan Area of Brazil, based on ambient concentrations ratios of CO, NMOG and NOx and on a photochemical model. *Atmos. Environ.* 40, 1189-1198, 2006.

Walsh, M.P. Mobile sources and air toxics. In: Patrick, D.R. (Ed.) Toxic Air Pollution Handbook. Van Nostrand Reinhold, New York, 1994, pp. 483.

Watson, J.G. Overview of receptor model principals. *J. Air Poll. Cont. Assoc.* 34, 619-623, 1984.

Watson, J.G., Chow, J.C., Pritchett, L.C., Pierson, W.R., Frazier, C.A., Purcell, R.G. Olmez, I., The 1987-88 Metro Denver brown cloud study, Desert Research Institute, Doc 8810 1F2, Desert Research Institute, Reno, NV, 1988.

Watson, J.G., Robinson, N.F., Chow, J.C., Henry, R.C., Kim, B.M., Pace, T.G., Meyer, E.I., Nyugen, Q. The USEPA/DRI chemical mass balance receptor model, CMB 7.0, *Environmental Software*, 5, 38-49, 1990.

Watson, J.G., Robinson, N.F., Fujita, E.M., Chow, J.C., Pace, T.G., Lewis, C., Coulter, T. CMB8 applications and validation protocol for $PM_{2.5}$ and VOCs, Desert Research Institute Document No. 1808.2D1, Desert Research Institute, Reno, NV, 1998.

Watson, J.G., Chow, J.C.; Fujita, E.M. Review of volatile organic compound source apportionment by chemical mass balance. *Atmos. Environ.* 35, 1564-1584, 2001.

Wiedinmyer, C., Guenther, A., Estes, M., Yarwood, G., Allen, D.T. A land use database and examples of biogenic isoprene emission estimates for the State of Texas, USA, *Atmos. Environ.,* 35, 6465-6477, 2001.

Wiens, D., Florence, L.Z., and Hiltz, M. Robust Estimation of Chemical Profiles of Airborne Particulate Matter. *Environmetrics.* 12: 25-40, 2000.

Wiswanath, R.S. Characteristics of oil-field emissions in the vicinity of Tulsa, Oklahoma. *J. Air & Waste Manage. Assoc.* 44, 989-994, 1994.

Yue, Z.W., Fraser, M.P. Characterization of nonpolar organic fine particulate matter in

Houston, Texas, *Aerosol Sci. Technol.*, 38, S1, 60-67, 2004a.

Yue, Z.W., Fraser, M.P. Polar organic compounds measured in fine particulate matter

during TexAQS 2000, *Atmos. Environ.*, 38, 3253-3261, 2004b.

Zhao, W., Hopke, P.K., Karl, T. Source identification of volatile organic compounds in

Houston, Texas. *Environ. Sci. Technol.* 38, 1338-1347, 2004.